GSK-3 IN HYPERGLYCEMIA-INDUCED ATHEROSCLEROSIS

INVESTIGATION INTO THE ROLE OF GLYCOGEN SYNTHASE KINASE-3 IN HYPERGLYCEMIA-INDUCED ATHEROSCLEROSIS

By

ANNA JEAN-JOO BOWES, B.Sc. (Hons.)

A Thesis

Submitted to the School of Graduate Studies

In Partial Fulfillment of the Requirements

For the Degree

Doctor of Philosophy

McMaster University

DOCTOR OF PHILOSOPHY (2009) McMaster University

(Biochemistry and Biomedical Sciences) Hamilton, Ontario

TITLE: Investigation into the role of glycogen synthase kinase-3 in hyperglycemia-induced atherosclerosis

AUTHOR: Anna Jean-Joo Bowes, B.Sc. (Hons.) (McMaster University)

SUPERVISOR: Geoff H. Werstuck, Ph.D.

NUMBER OF PAGES: xxiv, 183

ABSTRACT

Diabetes mellitus is a major independent risk factor for cardiovascular disease and stroke. However, the molecular and cellular mechanisms by which diabetes contributes to the development of vascular disease are not fully understood. We have shown that conditions of hyperglycemia are associated with accumulation of intracellular glucosamine, a downstream metabolite of glucose. Our findings indicate that elevated levels of intracellular glucosamine can promote inflammation and lipid accumulation – the hallmark features of atherosclerosis – in vascular cells and HepG2 cells.

Here I demonstrate that exposure of HepG2 cells to the branched chain fatty acid, valproic acid, increases cellular resistance to glucosamine-induced lipid accumulation and nuclear factor-κB activation. *In vivo* I show that hyperglycemic apolipoprotein E-deficient ($ApoE^{-/-}$) mice fed a diet supplemented with 625 mg/kg valproic acid have significantly reduced lesion volumes relative to non-supplemented controls. Valproate supplementation has no apparent effect on the plasma levels of glucose, or lipids, nor does it affect the expression of ER chaperones. Significant reductions were observed in total hepatic lipids (> 50.4%) and hepatic glycogen synthase kinases (GSK)-3β activity (> 55.8%) in mice fed the valproate supplemented diet.

In vitro I demonstrate that valproic acid directly inhibits GSK-3α/β. Also pretreatment with novel GSK-3 inhibitors protects primary mouse hepatocytes from glucosamine-induced unesterified cholesterol accumulation. I further establish the role of GSK-3 by showing that GSK-3-deficient mouse embryonic fibroblasts do not accumulate

unesterified cholesterol after glucosamine treatment. Dietary supplementation with 2-ethylbutyric acid, a novel and potent GSK-3 inhibitor *in vitro*, did not reduce lesion development in hyperglycemic ApoE$^{-/-}$ mice and significantly increased atherosclerosis in normoglycemic mice. This may be a side effect attributed to multiple cellular pathways controlled by GSK-3.

In conclusion, I have identified a pathway involving glucosamine-induced cellular dysfunction that leads to accelerated hyperglycemia-associated atherosclerosis. This pathway involves GSK-3, which regulates glucosamine-induced unesterified cholesterol accumulation.

ACKNOWLEDGEMENT

Six years ago when I almost gave up pursuing science, I met two most wonderful people who changed the course of my life. The first one is Dr. Geoff Werstuck who took me in as his very first graduate student. I will always pride myself on having had known a wonderful person and a scientist like Geoff, who was always the first one to give me encouragement, guidance, and a new perspective. The second person is Tim Bowes, my husband, who has supported and held me strong everyday by pouring overwhelming amount of love, kindness, appreciation, and encouragement.

My project would not have been successfully carried out without the day to day training and patience provided by Peter Shi and Dr. Mohammad Khan. Whenever things were tough, I was still hopeful and excited to come to the lab because I knew they were going to make things better. My committee members Dr. Stephen Shaughnessy, Dr. Bernardo Trigatti, and Dr. Bradley Doble have always given me more than what they were needed to make me become a better scientist. I would like to give sincerely thanks Drs. Richard Epand, Gerry Wright, and David Andrews for opening a door to a graduate career and encouraging me to press on. Some of the most unforgettable memories here at Henderson Research Centre were created with Lindsie Robertson who together persevered through everything from failing experiments and parking patrol to mid-day B&Titus. My stay here was made more enjoyable because of the support I got from all the HRC members including Linda May, Dr. Ji Zhou, Dr. Sudesh Sood, Colin Yee, Steve Colgan, Jennifer Caldwell, Andrew Sage, Chloe Milsom, and Melec Zeadin. Lastly, I would like to thank my parents Jin-Young and Yun-Sook Kim and my brother Josh for their continual prayers, support, and sacrificial love poured over me for the past 30 years.

TABLE OF CONTENTS

LIST OF FIGURES

LIST OF TABLES

LIST OF ABBREVIATIONS

AcH3 lys9	acetylated lysine 9 on histone H3
ADP	adenosine diphosphate
AGE	advanced glycation end-product
ANOVA	analysis of variance
$ApoE^{-/-}$	apolipoprotein E-deficient
AP-1	activator protein 1
APC	adenomatous polyposis coli
AR	aldose reductase
AS160	Akt substrate 160
ATP	adenosine triphosphate
cAMP	cyclic adenosine monophosphate
CBP	CREB-binding protein
CCD	charge coupled device
CD36	cluster of differentiation 36
CD68	cluster of differentiation 68
cDNA	complementary deoxyribonucleic acid
CHOP	C/EBP homologous protein
CK II	casein kinase II

CREB	cAMP response element binding
CVD	cardiovascular disease
DAG	diacylglycerol
DM	diabetes mellitus
DMEM	Dulbecco's Modified Eagle's Medium
DMSO	dimethyl sulfoxide
DNA	deoxyribonucleic acid
DTT	dithiothreitol
DVL	dishevelled
EBA	2-ethylbutyric acid
EC	endothelial cell
EDTA	ethylenediaminetetraacetic acid
EGTA	ethylene glycol tetraacetic acid
eIF2B	eukaryotic initiation factor 2B
eNOS	endothelial nitric oxide synthase
ER	endoplasmic reticulum
E-selectin	endothelial-leukocyte adhesion molecule-1
FACS	fluorescence-activated cell sorting
FAS	fatty acid synthase
FBS	fetal bovine serum

FoxO1	forkhead box O1
FRAT	frequently rearranged in advanced T-cell lymphomas
G6Pase	glucose-6-phosphatase
GADD	growth arrest and DNA damage
GAPDH	glyceraldehyde-3-phosphate dehydrogenase
GFAT	glucosamine-fructose-6-phosphate amidotransferase
GlcN	glucosamine
GlcNAc	N-acetylglucosamine
GLUT	glucose transporter
GRP78/BiP	glucose responsive protein 78
GS	glycogen synthase
GSK-3 Inh II	glycogen synthase kinase-3 inhibitor II
GSK-3α	glycogen synthase kinase-3 alpha
GSK-3β	glycogen synthase kinase-3 beta
GSK-$3^{-/-}$	glycogen synthase kinase-3 knock out
GSK-3KO	glycogen synthase kinase-3 knock out
HAT	histone acetyltransferase
HDAC	histone deacetylase
HDL	high density lipoprotein

HEPES	4-(2-hydroxyethyl)-1-piperazineethanesulfonic acid
HepG2	human hepatocarcinoma
HG	hyperglycemic or hyperglycemia
HMG-CoA	3-hydroxy-3-methyl-glutaryl-CoA
HMG-CoAR	3-hydroxy-3-methyl-glutaryl-CoA reductase
HPLC	high-performance liquid chromatography
HRP	horseradish peroxidase
HSP	heat shock protein
ICAM-1	intercellular adhesion molecule-1
IkBα	inhibitor kappaB alpha
IKK-2	IkB kinase-2
IKK-A	IkB kinase-A
IL	interleukin
IR	insulin receptor
IRS	insulin receptor substrate
KDEL	lysine-aspartic acid-glutamic acid-leucine
LDL	low density lipoprotein
Li	Lithium
LXR	Liver X receptor

MEF	mouse embryonic fibroblast
mLDL	modified low density lipoprotein
MMP	matrix metalloproteinase
MOPS	3-(N-morpholino)propanesulfonic acid
mTOR	mammalian target of rapamycin
NAD^+ or NADH	nicotinamide adenine dinucleotide
NADPH	nicotinamide adenine dinucleotide phosphate
NFAT	nuclear factor of activated T-cells
NF-κB	nuclear factor-kappaB
NG	normoglycemic or normoglycemia
NOD	non-obese diabetic
O-GlcNAc	O-linked N-acetylglucosamine
OGT	O-GlcNAc transferase
OGTT	oral glucose tolerance test
oxLDL	oxidized low density lipoprotein
PAI-1	Plasminogen activator inhibitor-1
PBS	phosphate-buffered saline
PCR	polymerase chain reaction
PDI	protein disulfide isomerase
PDK1	3-phosphoinositide-dependent protein kinase-1

PEPCK	phosphoenolpyruvate carboxykinase
PERK	ER-resident PKR-ER-related kinase
PI3K	phosphatidylinositol 3-kinase
PKAc	protein kinase A catalytic subunit
PKB/Akt	protein kinase B/Akt
PKC	protein kinase C
PS	penicillin/streptomycin
PSA	polysialic acid
PtdIns(3,4,5)P3	phosphatidylinositol (3,4,5) trisphosphate
PtdIns(4,5)P2	phosphatidylinositol (4,5) bisphosphate
PUGNAc	O-(2-acetamido-2-deoxy-d-glucopyranosylidene)amino-N-phenylcarbamate
qPCR	quantitative polymerase chain reaction
RAGE	receptor for advanced glycation endproduct
recGSK-3	recombinant GSK-3
RIPA	Radioimmunoprecipitation assay buffer
RNA	ribonucleic acid
ROS	reactive oxygen species
s.d.	standard deviation
SDS	sodium dodecyl sulfate

SDS-PAGE	sodium dodecyl sulfate-polyacrylamide gel electrophoresis
s.e.m.	standard error of means
Ser	serine
SMC	smooth muscle cell
SP1	specificity protein 1
SR-A	scavenger receptor-A
SREBP	sterol regulatory element binding protein
SRF	serum response factor
STZ	streptozotocin
T1DM	type I diabetes mellitus
T2DM	type II diabetes mellitus
TBST	tris-buffered saline tween-20
TCF	T-cell factor
TGF-β	transforming growth factor-beta
Thr	threonine
Tm	tunicamycin
TNF-α	tumor necrosis factor-alpha
TSA	Trichostatin A
Tyr	tyrosine

UDP-GlcNAc	uridine diphosphate-N-acetylglucosamine
UPR	unfolded protein response
UV	ultraviolet
VCAM-1	vascular cell adhesion molecule-1
VLDL	very low density lipoprotein
VPA	valproic acid
WCIF	Wright Cell Imaging Facility
WT	wild-type

1 INTRODUCTION – PART I

1.1 ATHEROSCLEROSIS

Atherosclerosis is an inflammatory disease characterized by lipid accumulation in the walls of large arteries (Glass and Witztum 2001; Kher and Marsh 2004; Lusis 2000). It is the underlying cause of cerebro- and cardiovascular disease (CVD) that together account for nearly half the annual mortality in the Western society (Ross 1999; Glass and Witztum 2001). Researchers have identified several risk factors for CVD including type 1 and type 2 diabetes mellitus, high cholesterol, stress, hypertension, smoking, obesity, lack of exercise, and high risk diet (Anand et al. 2008).

1.1.1 Overview of disease progression

Arteries are blood vessels that carry blood from the heart to the peripheral regions of the body. The large arteries have a thick wall comprised of three layers, the intima, the media, and the adventitia, that allows them to endure considerable pressure (Lusis 2000). The luminal side of the inner most layer, the intima, consists of a single layer of endothelial cells (ECs) covering extracellular connective tissue, mostly consisting of proteoglycans and collagen, and the internal elastic lamina (Glass and Witztum 2001; Lusis 2000). The media is composed of vascular smooth muscle cells (SMCs), which give the artery structure and support. The adventitia is made of connective tissues with fibroblasts and SMCs (Lusis 2000). The development of atherosclerosis is initiated by dysfunction of ECs in response to injury. Insult to the endothelial layer, caused by sheer

stress or interaction with various substances including elevated concentrations of low density lipoproteins (LDLs), stimulates ECs to express and display vascular cell adhesion molecule-1 (VCAM-1), endothelial-leukocyte adhesion molecule-1 (E-selectin), and intercellular adhesion molecule-1 (ICAM-1) that bind to circulating monocytes and T cells. Chemokines secreted by ECs promote monocytes to migrate into the intima where they differentiate and mature into macrophages. Macrophages express scavenger receptors including SR-A, CD36 and CD68 that bind to and facilitate the uptake of oxidized LDLs (oxLDLs). Macrophages that become filled with fatty droplets of cholesterol esters are called "foam cells", which are found in early lesions known as fatty streaks as well as mature atherosclerotic plaques. The cytokines secreted by macrophage/foam cells and lymphocytes reinforce the inflammatory process and induce vascular SMCs to proliferate and migrate into the intima. SMCs secrete collagen, glycoprotein, and elastin that collectively form extracellular matrix, giving rise to a fibrous cap that is thought to stabilize the lesion. However, SMCs also secrete proteases (collagenases, gelatinases, stromolysin, and cathepsins) which degrade extracellular matrix proteins. Concurrently, other inflammatory cells including macrophages, T cells and mast cells, release pro-inflammatory cytokines that reduce the production of collagen by SMCs, contributing to the destabilization of the fibrous cap (Hansson and Libby. 2006). Together, these effects can lead to the thinning of the fibrous cap, which promotes lesion rupture (Lusis, 2000; Glass and Witztum. 2001; Libby, 2008). When lesion rupture occurs, lipids and tissue factors of the necrotic core come in contact with blood components, initiating platelet adherence and thrombosis (Glass and Witztum. 2001,

Lusis, 2000). The thrombus, or blood clot, can occlude the artery and block blood flow near the site of the rupture, causing myocardial infarction or travel to the brain and cause a stroke.

Figure 1. Initiation of early atherosclerosis

When there is an excess amount of circulating low density lipoproteins (LDLs) in the blood, LDL particles penetrate into the artery wall where they undergo chemical alterations to become modified (mLDL) or oxidized LDLs (oxLDL). The mLDL stimulates endothelial cells to express adhesion molecules to attract monocytes and T cells from the blood. Monocytes migrate into the intimal layer and mature into active macrophages which ingest mLDL and oxLDL, becoming filled with fatty droplets. These macrophage-derived foam cells secrete cytokines to promote migration of smooth muscle cells from the media to the intima where they secrete collagen, glycoprotein and elastin to produce fibrous cap over the developing plaque.

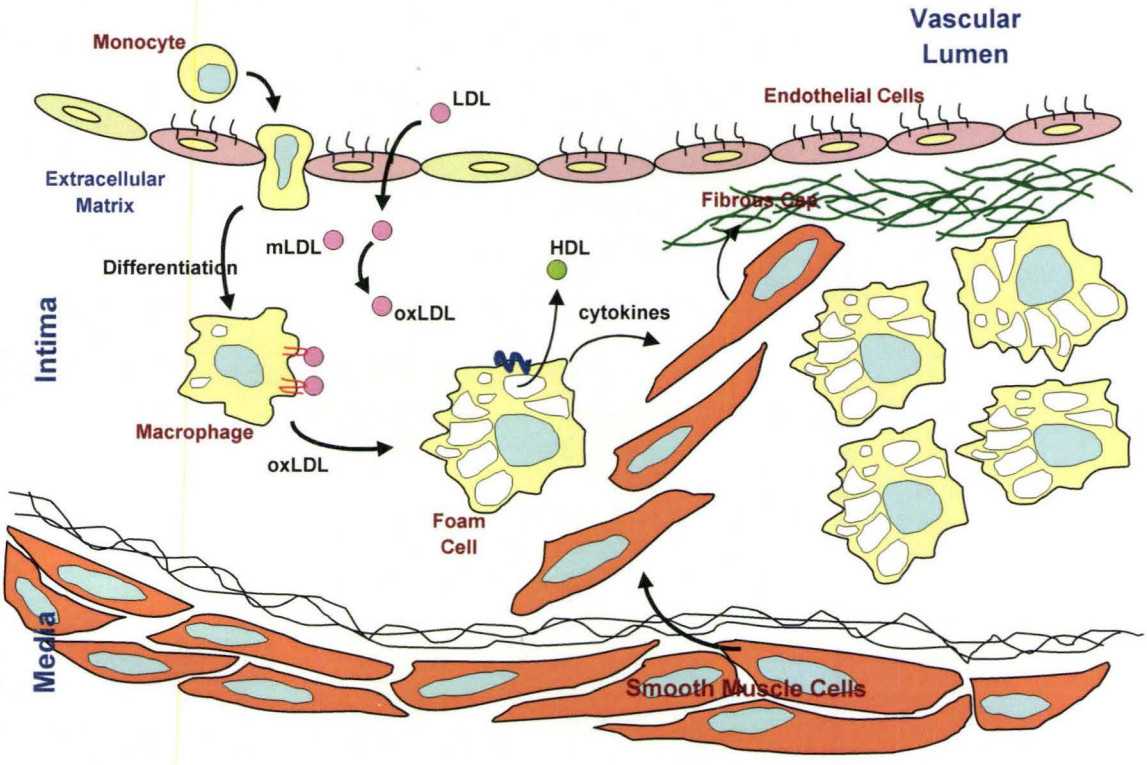

Adapted from Glass and Witztum. Cell 2001

Figure 2. Advanced atherosclerotic lesion

In advanced lesions, foam cells undergo necrosis, depositing cholesterol and lipids into the growing plaque. Inflammatory molecules and proteases secreted by foam cells and smooth muscle cells destabilize the fibrous cap, ultimately leading to plaque rupture. Tissue factor and lipids in the necrotic core of the plaque then come in contact with blood components and initiate the coagulation cascade, creating a clot or thrombus. The thrombus can block blood flow near the site of rupture causing myocardial infarction or travel to the brain and cause a stroke.

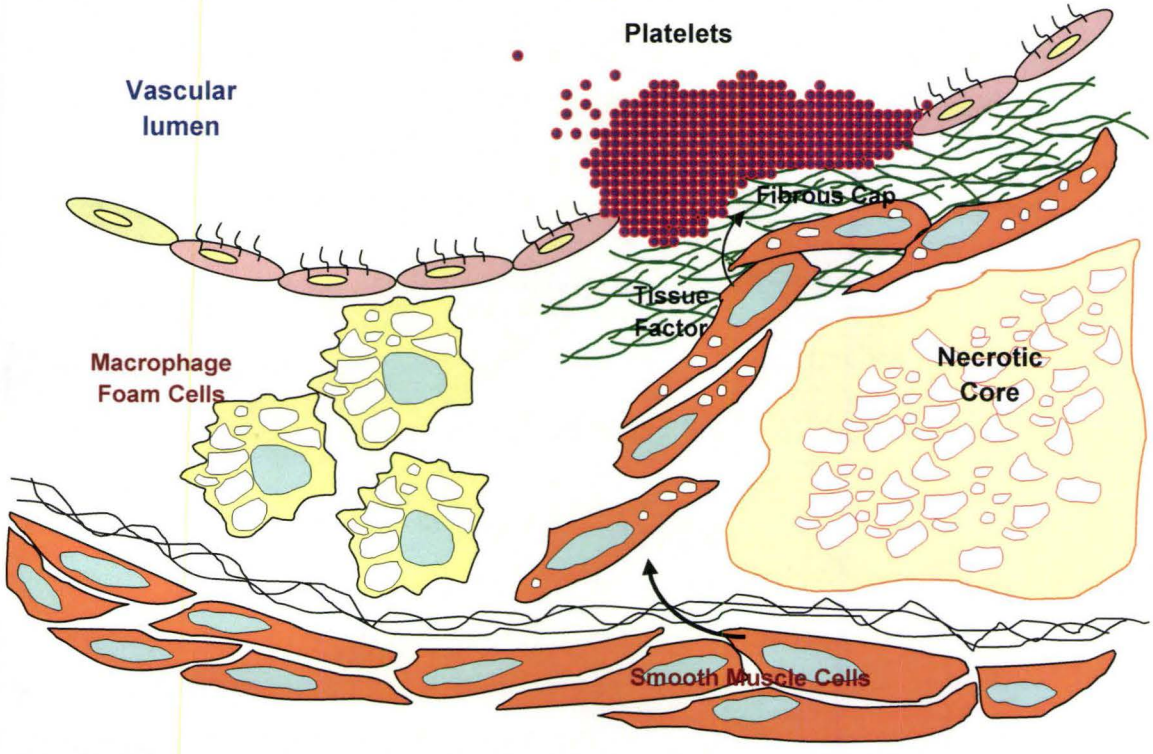

Adapted from Glass and Witztum. Cell 2001

1.1.2 Role of inflammation and lipid accumulation in atherogenesis

In recent years, atherosclerosis has been recognized as a chronic inflammatory disease characterized by severe immunological activity initiated by accumulation of lipids in the artery wall (Ross 1999; Hansson and Libby 2006). During the early events of atherogenesis, the immune responses to the mounting lipids and lipoprotein particles in the intima promote the expression of adhesion molecules and chemo-attracting proteins that recruit monocytes, T-cells and leukocytes (Hansson 2005). The presence of sub-endothelial mLDLs and oxLDLs and increased amount of unesterified cholesterol within macrophages promote the expression and secretion of tumour necrosis factor (TNF)-α, interferon (IFN)-γ, matrix metalloproteinases (MMPs), and interleukin (IL)-1 and 6 (Ross 1999; Alam et al. 2004).

Nuclear factor-kappa B (NF-κB) is a transcription factor responsible for activation of numerous genes involved in the inflammatory response which makes it a key player in the body's proper immune function (Li and Verma 2002). NF-κB is found to be highly activated in vessel walls of animal models of atherosclerosis and in the cells that make up human atherosclerotic lesions (Hajra et al. 2000; Wilson et al. 2000; Brand et al. 1996; Monaco et al. 2004).

NF-κB is comprised of relA (p65), relB, c-Rel, p105/p50, and p100/p52, which all share a structurally conserved N-terminal region that allows dimerization, nuclear-localization, and DNA-binding (Li and Verma. 2002). When inflammatory mediators, such as TNF-α, bind to their receptors on the cell surface, IκB kinase (IKK)-2

phosphorylates IκBα, which leads to its ubiquitylation and proteosomic degradation, releasing the p50/p65 dimer of NF-κB (Xanthoulea et al. 2005). Phosphorylation of p65 by kinases, such as protein kinase A catalytic subunit (PKAc), casein kinase (CK) II, glycogen synthase kinase (GSK)-3β, and IKK-1/2, is essential for its binding to cAMP response element binding (CREB)-binding protein (CBP) in the nucleus and the activation of target gene transcription (Li and Verma. 2002).

During the early stage of foam cell formation, most of the internalized cholesterols in macrophages are stored as esterified cholesterol. However, as the lesion advances, there is an increase in unesterified cholesterol content and a decrease in esterified cholesterol (Small et al. 1984; Kruth and Fry. 1984). Accumulation of unesterified cholesterol can lead to apoptosis in foam cells, an event that contributes to the growth of necrotic core and plaque rupture (Tabas. 2000; Li et al. 2005). In addition, high levels of unesterified cholesterol in macrophages have been shown to induce secretion of TNF-α and IL-6 through the activation of NF-κB (Li et al. 2005). The accumulation of unesterified cholesterol in the endoplasmic reticulum (ER) leads to abnormal stiffening of the ER membrane, activating the ER stress pathway, which can lead to cellular dysfunction, further accelerating atherogenesis (Li et al. 2004)

1.2 DIABETES MELLITUS

Diabetes mellitus (DM) is a group of diseases characterized by elevated blood glucose levels or hyperglycaemia (Brownlee. 2001; Bell and Polonsky. 2001).

Individuals with fasting blood glucose levels consistently greater than 7 mM or having blood glucose levels at or above 11.1 mM, 2 hours after the oral glucose tolerance test (OGTT) are diagnosed with DM. Fasting blood glucose levels between 7.0 - 11.1 mM or glucose levels of 7.8 mM to 11.1 mM 2 hours after OGTT are considered pre-diabetic (Melchionda et al. 2002).

Hyperglycemia usually results from deficiency of insulin action. Deficiency in the production of insulin, generally due to autoimmunological destruction of pancreatic β-cells, is referred to as type 1 or insulin-dependent diabetes mellitus (T1DM). In type 2 or non-insulin-dependent diabetes mellitus (T2DM), skeletal muscle cells and adipocytes do not respond appropriately to the circulating insulin (Freidenberg et al. 1987). In T2DM, the β-cells initially produce more insulin to maintain glucose levels, a condition known as hyperinsulinemia. However, this can eventually lead to β-cell death or apoptosis. (Pick et al. 1998).

1.2.1 Glucose-induced insulin secretion

Under normal conditions, levels of insulin are responsive to the plasma levels of glucose (Bell and Polonsky. 2001). After a large caloric intake, glucose in the blood stream is transported into pancreatic β-cells via glucose transporter 2 (GLUT2) where it is converted into glucose-6-phosphate and shunted into the glycolytic pathway and Kreb cycle to generate ATP. Increases in ATP:ADP ratio lead to closure of the ATP sensitive K^+ channels on the plasma membrane, resulting in depolarization and influx of extracellular calcium coupled with a release of calcium from the intracellular storage.

These events induce insulin-containing secretory granules to fuse with the plasma membrane resulting in release of insulin into the circulation (Bell and Polonsky. 2001).

1.2.2 Insulin signalling

Insulin signalling in peripheral tissues is initiated by the binding of insulin to insulin receptors (IRs) that are found on skeletal muscle, adipose tissues, and many other cell types. Insulin binding to its receptor promotes activation of intrinsic receptor protein tyrosine kinase activity which results in its autophosphorylation (Kasuga et al. 1983) (Figure 3). Activated residues in the cytoplasmic face of IR interact with insulin receptor substrate proteins (IRS1 and IRS2) to phosphorylate them on specific tyrosine sites. Phosphorylated IRS1/2, in turn, recruits the p85 subunit of phosphatidylinositol 3- kinase (PI3K) to the plasma membrane where the p110 subunit of PI3K converts phosphatidylinositol (4,5) bisphosphate (PtdIns(4,5)P_2) to the lipid second messenger phsphatidylinositol (3,4,5) triphosphate (PtdIns(3,4,5)P_3) (Frojdo et al. 2009). PtdIns(3,4,5)P3 then recruits 3-phosphoinositide-dependent protein kinase-1 (PDK1) and protein kinase B (PKB/Akt) to the plasma membrane so that PDK1 can activate PKB/Akt. PKB has many substrates including Akt substrate 160 (AS160), endothelial nitric oxide synthase (eNOS), IκB kinase (IKK)-α, mammalian target of rapamycin (mTOR) and GSK-3α/β (Lawlor and Alessi. 2001). PKB phosphorylation on Ser21/9 inactivates GSK-3α/β, thereby relieving inhibition of glycogen synthase (GS) and eukaryotic initiation factor 2B (eIF2B), allowing insulin-induced glycogen and protein synthesis (Figure 3) (Hurel et al. 1996; Welsh et al. 1996). Insulin-stimulated activation of PKB also aids the

uptake of plasma glucose into the skeletal muscle cells and adipocytes through the inhibition of AS160, which triggers translocation of glucose transporter GLUT4 to the plasma membrane (Huang and Czech. 2007; Cohen. 2006). Studies done in human muscle and adipose tissues from insulin resistant, obese and T2DM individuals show defects in one or more steps of insulin signalling (Krook et al. 2000; Cozzone et al. 2008; Nikoulina et al. 2000).

Insulin also plays an important role in various functions carried out by the liver. Insulin-activated phosphorylation of forkhead box O1 (FoxO1) by PI3K prevents FoxO1 from entering the nucleus. This prevents transcriptional activation of phosphoenolpyruvate carboxykinase (PEPCK) and glucose 6-phosphatase (G6Pase), the genes involved in gluconeogenesis, thereby decreasing glucose output from the liver (Matsumoto et al. 2006). Insulin increases transcription of SREBP-1c through liver X receptor (LXR) and specificity protein 1 (Sp1) and activates SREBP-1c by inducing its translocation into the nucleus to enhance transcription of genes involved in the biosynthesis of fatty acid and triglyceride (Deng et al. 2007; Brown and Goldstein. 1997;). This further aids in the clearing of excess glucose from circulation and its storage as lipids.

Figure 3. Outline of the signalling pathway by which insulin initiates glycogen, protein, and lipid synthesis

Binding of insulin to the insulin receptor (IR) initiates autophosphorylation of the cytoplasmic domain of IR which phosphorylates insulin receptor substrates (IRS1/2). Phosphorylated IRS1/2 recruits phosphatidylinositol 3- kinase (PI3K) to the plasma membrane where it converts phosphatidylinositol (4,5) bisphosphate (PtdIns(4,5)P_2) to PtdIns(3,4,5)P_3. This allows 3-phosphoinositide-dependent protein kinase-1 (PDK1) to activate protein kinase B (PKB/Akt) by phosphorylation. PKB/Akt then inactivates glycogen synthase kinase (GSK)-3 by phosphorylating it at Ser21/9. This relieves glycogen synthase (GS) and eukaryotic initiation factor 2B (eIF2B) inhibition and initiates insulin-induced glycogen and protein synthesis in muscle and adipose tissue. Additionally, PKB/Akt phosphorylation of AS160 induces glucose uptake by triggering glucose transporter GLUT4 translocation to the plasma membrane in these tissues. In the liver, insulin inhibits gluconeogenesis and stimulates lipogenesis via activation of SREBP-1c through specificity protein 1 (Sp1) and liver X receptor (LXR).

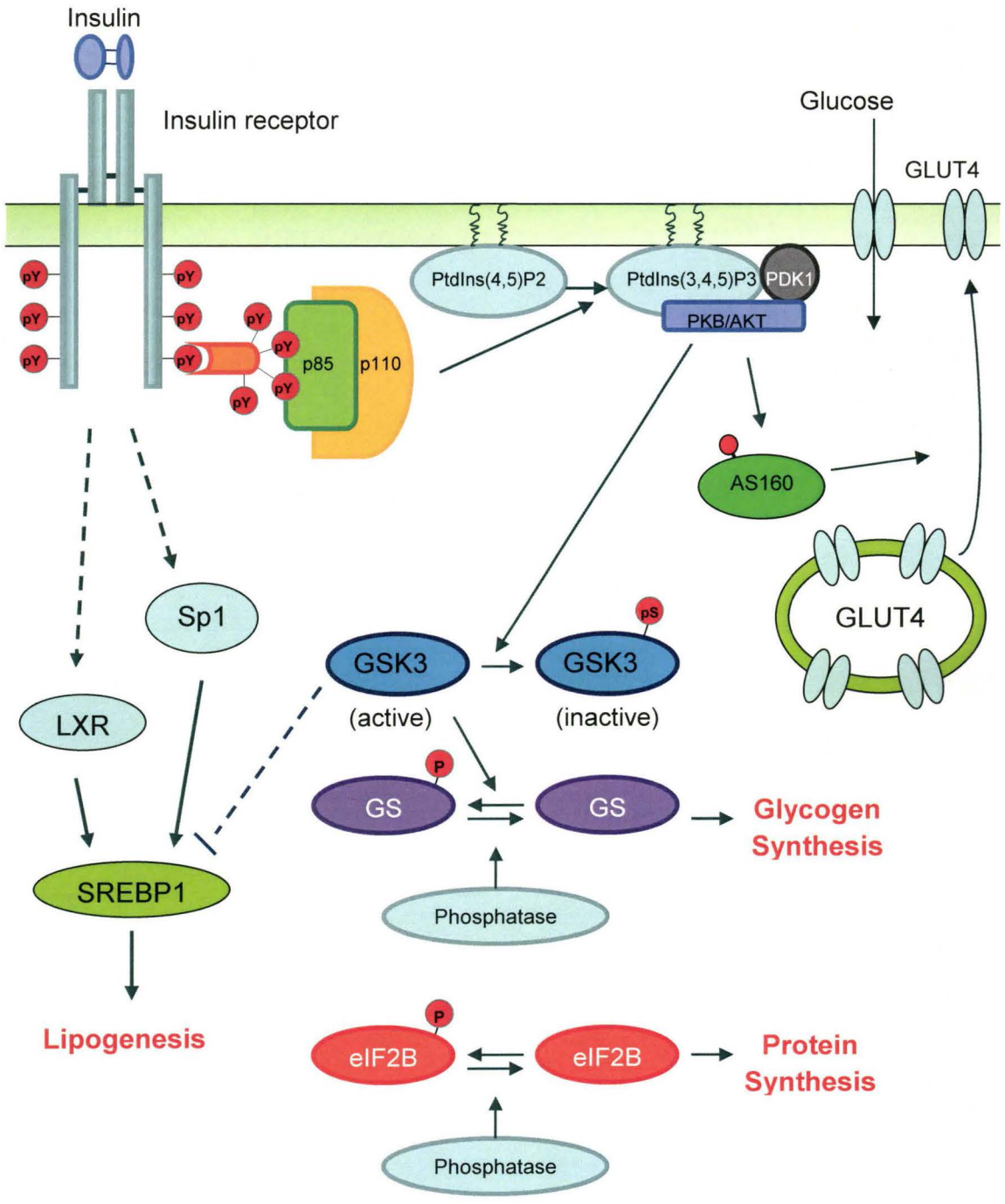

Adapted from Cohen and Frame. Nature Reviews 2001

1.3 POTENTIAL MECHANISMS LINKING DIABETES TO ATHEROSCLEROSIS

Both Type I and Type II DM are potent independent risk factors for atherosclerosis, and individuals with DM have a 2-4 fold increased risk of developing CVD with reduced life expectancies (Haffner et al. 1998). Chronic hyperglycemia, a key aspect common to both types of diabetes, is believed to be the major causative factor of accelerated atherosclerosis. Several mechanisms have been proposed to explain the pro-atherogenic effects of hyperglycemia. These include increased flux to the polyol pathway and hexosamine pathway, the formation of advanced glycation end-products (AGE), and activation of protein kinase C (PKC), all of which lead to increased oxidative stress and activation of pro-inflammatory pathways in vascular cells (Brownlee 2005; Goldberg 2004). Elevated intracellular production of glucosamine can also lead to increased endoplasmic reticulum (ER) stress which has been identified in several independently compiled lists of cardiovascular risk factors (Robertson et al. 2006; Zhou et al. 2004; Ozcan et al. 2004; Li et al. 2005; Werstuck et al. 2006).

1.3.1 Oxidative stress

Hyperglycemia-associated oxidative stress is the most extensively studied potential mechanism through which diabetes may induce accelerated macro- and microvascular diseases. Over-production of superoxide by the mitochondrial electron

transport system, triggered by hyperglycemia-induced cellular pathways, has been proposed as the unifying mechanism (Brownlee. 2005; Moreno and Fuster. 2004).

Aldose reductase (AR), the first and rate-limiting enzyme in the polyol pathway, catalyzes the reduction of a variety of carbonyl compounds. Under normoglycemic conditions, AR does not significantly contribute to the metabolism of glucose due to its low affinity to the molecule (Srivastava et al. 1999). However, under conditions of hyperglycemia, the reduction of glucose to polyalcohol sorbitol by AR increases, resulting in depletion of NADPH. This leads to limited regeneration of glutathione and leaves the cell vulnerable to damage by reactive oxygen species (ROS) (Kaneko et al. 2005; Chung et al. 2003). Moreover, sorbitol can be further oxidized to fructose by the NAD^+-dependent enzyme sorbitol dehydrogenase causing increased intracellular NADH levels, thereby inhibiting the activity of glyceraldehyde-3-phosphate dehydrogenase (GAPDH). This results in increased production of AGE and diacylglycerol (DAG) which activates PKC (Kaneko et al. 2005). Fructose can also enter the hexosamine pathway to contribute to cellular dysfunction, as discussed below.

Elevated intracellular glucose levels lead to the generation of dicarbonyls which react with the amino groups of proteins through a non-enzymatic process to form AGE (Degenhardt et al. 1999; Wells-Knecht et al. 1995). The rate of this reaction is directly proportional to the concentration of glucose. Enhanced levels of AGE may alter the function of the protein by cross-linking molecules of the extracellular matrix and/or by interaction with the receptor for AGE (RAGE) on macrophages, vascular ECs and SMCs (Li et al. 1996; Neeper et al. 1992). The AGE-RAGE interaction triggers a signal

transduction cascade producing intracellular ROS that initiate inflammatory responses through NF-κB activation (Hofmann et al 2001; Lander et al. 1997). This leads to increased transcription of adhesion molecules and pro-inflammatory factors including ICAM-1, VCAM-1, E-selectin, tissue factor, TNF-α, interleukin (IL)-1α and IL-6 (Gleissner et al. 2007). AGE has also been shown to induce endothelial permeability allowing monocytes to pass through the vascular endothelial layer into the intima of a damaged arterial wall *in vivo* (Goldin et al. 2006).

Hyperglycemia increases *de novo* synthesis of DAG, an activator of the majority of PKC isoforms, in cultured vascular cells and in diabetic animals (Koya and King. 1998). PKC may also be indirectly activated by the AGE-RAGE signalling pathway and has been shown to have increased activity when the polyol pathway is activated by elevating the levels of ROS in vascular cells (Thallas-Bonke et al. 2004). Activation of PKC, in turn, decreases production of nitric oxide in smooth muscle cells and inhibits insulin-stimulated expression of eNOS in cultured endothelial cells (Kuboki et al. 2000). PKC-α increases endothelial permeability whereas the β and δ isoforms induce capillary and vascular occlusion, activation of NF-κB, and increased ROS formation, all of which contribute to accelerated atherosclerosis (Brownlee. 2001).

There is also an increased flux of glucose into the hexosamine pathway during hyperglycemic episodes. Normally, only 1-3% of intracellular glucose enters in the hexosamine pathway to produce N-acetylglucosamine (GlcNAc). GlcNAc is used for the glycosylation of newly synthesized proteins to aid in proper folding and function

(Marshall et al. 1991). However, increased levels of GlcNAc compete with phosphorylation of transcription factors, such as Sp1. This can lead to over production of plasminogen activator inhibitor 1 (PAI-1) and transforming growth factor-β (TGF-β) and cause occlusion of micro-vessels by accumulation of matrix protein (Goldberg et al. 2000; Brownlee. 2001).

Common to all of these pathways is the over-production of superoxide by the mitochondrial electron transport chain (Brownlee. 2005). Consequently, oxidative stress has been suggested as the unifying mechanism of hyperglycemia-induced cellular dysfunction and researchers were hopeful that the atherogenic complications of diabetes could be prevented by anti-oxidant treatment. Nonetheless, in all major clinical trials, treatment of diabetic patients with anti-oxidant supplements have had little success in the prevention of cardiovascular outcomes (Yusuf et al. 2000; Lonn et al. 2002; McQuillan et al. 2001; Thomson et al. 2007), suggesting that other pathways may also play causative roles in disease progression.

1.3.2 Glucosamine-induced cellular dysfunction

The first step of the hexosamine pathway involves the conversion of fructose-6-phosphate to glucosamine-6-phosphate by the rate-limiting enzyme glutamine:fructose-6-phosphate amidotransferase (GFAT) (McKnight et al. 1992). The glucosamine-6-phosphate is then further metabolized to UDP-N-acetylglucosamine which can be used as a substrate for O-linked glycosylation by O-GlcNAc transferase (OGT). O-linked

glycosylation can be removed from a protein by the nucleocytoplasmic enzyme O-GlcNAcase (Bouche et al. 2004; Dong and Hart. 1994). The involvement of the hexosamine pathway has been studied mainly using over-expression of GFAT and administration of glucosamine to cultured cells or animals. This strategy bypasses GFAT and provides a direct substrate for UDP-GlcNAc, thereby accelerating the effect of hyperglycemia. Increased flux of glucose into the hexosamine pathway has been associated with insulin resistance in adipocytes and enhanced apoptosis in pancreatic β-cells (Vosseller et al. 2002; D'Alessandris et al. 2004). When cultured cells were treated with high glucose or glucosamine, there was an increase in O-glycosylation of proteins involved in insulin signalling, such as IR and IRS1/2, resulting in reduced activation of PKB/Akt and inhibition GSK-3 (Vosseller et al. 2002; D'Alessandris et al. 2004). In mouse skeletal muscle and adipose tissue, over-expression of GFAT led to a decrease in insulin-stimulated glucose uptake and translocation of GLUT4 to the plasma membrane, whereas GFAT over-expression in mouse liver showed increased glycogen storage, hyperlipidemia, obesity, insulin resistance, and glucose intolerance (Cooksey et al. 1999; Veerababu et al. 2000). In humans acute glucosamine infusion mimicked some metabolic features of diabetes such as an increase in fasting glucose levels (Monauni et al. 2000). However, there is also evidence suggesting that insulin resistance caused by hyperglycemia and glucosamine may occur through pathways independent of proteins involved in insulin signalling (Arias et al. 2004).

In addition to inhibition of eNOS by O-linked N-acetylglucosamine (O-GlcNAc) in hyperglycemic conditions, increased flux into the hexosamine pathway and

glucosamine production has been shown to induce pro-inflammatory responses and lipid accumulation in cultured cells (Du et al. 2001; James et al. 2002; Kim et al. 2005). Both glucose and glucosamine dose-dependently enhanced VCAM-1 promoter activity via NF-κB *in vitro*, and glucosamine supplementation to LDL receptor-deficient mice, fed the Western diet, enhanced early atherosclerosis (James et al. 2002; Tannock et al. 2006). Our lab has also shown that elevated levels of intracellular glucosamine in cell types relevant to atherogenesis, can promote cellular dysfunction characteristic to atherosclerosis. Treatment with 5mM glucosamine for 18-24 h significantly induced accumulation of unesterified-cholesterol and NF-κB activity in human hepatocarcinoma (HepG2) cells (Figure 4) (Kim et al. 2005; Werstuck et al. 2006). This may occur through a mechanism involving GSK-3 activation, an enzyme shown to be activated by glucosamine (Vosseller et al. 2002; D'Alessandris et al. 2004). GSK-3 was shown to be an enzyme required for activation of NF-κB, the transcription factor that regulates pro-inflammatory genes (Hoeflich et al. 2000). Moreover, glucosamine is a potent inducer of ER stress, a cellular state caused by accumulation of unfolded or misfolded proteins in the ER, which can trigger apoptosis through activation of GSK-3 (Song et al. 2002; Srinivasan et al. 2005; Brewster et al. 2006; Takadera et al. 2007). Therefore, examining the role of GSK-3 in the effects of elevated intracellular glucosamine levels is a critical step in elucidating the mechanism of diabetic atherosclerosis. Currently, very little is known about the involvement of GSK-3 in lipid metabolism and atherogenesis. Therefore, the use of small molecule inhibitors and genetic manipulation of GSK-3 can

serve as useful tools in delineating the involvement of GSK-3 in hyperglycemia-induced atherosclerosis.

Figure 4. Glucosamine increases unesterified-cholesterol content and NF-κB signalling in HepG2 cells.

A. Filipin staining of HepG2 cells exposed to 0 or 5 mM glucosamine (GlcN) as indicated. After 24 hours, cells were washed, fixed in paraformaldehyde and stained with filipin. Intracellular filipin-cholesterol complexes were visualized by fluorescence microscopy and images were captured with a digital camera. Representative images are shown. **B**. HepG2 cells were transfected with a reporter plasmid containing a luciferase gene driven by promoters containing NF-κB or serum response factor (SRF)-binding elements. After 24 h, cells were treated with glucosamine (5 mM) or tunicamycin (2 μg/ml) for an additional 8 h. Cell extracts were prepared and luciferase activity was quantified. The data represent the averages ± SD of three experiments, each performed in triplicate. *$P<0.05$ relative to untreated controls.

A.

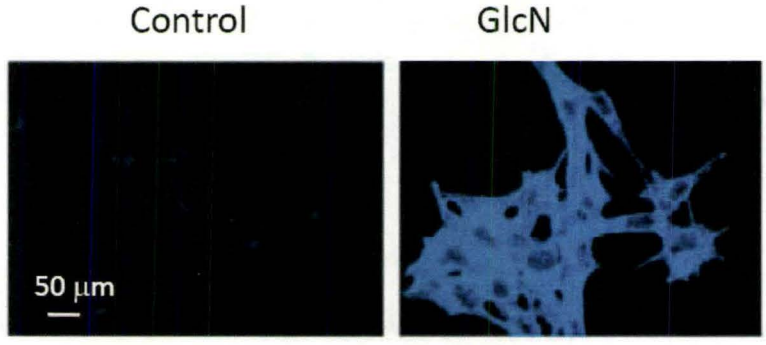

Kim *et al.* JCI 2005

B.

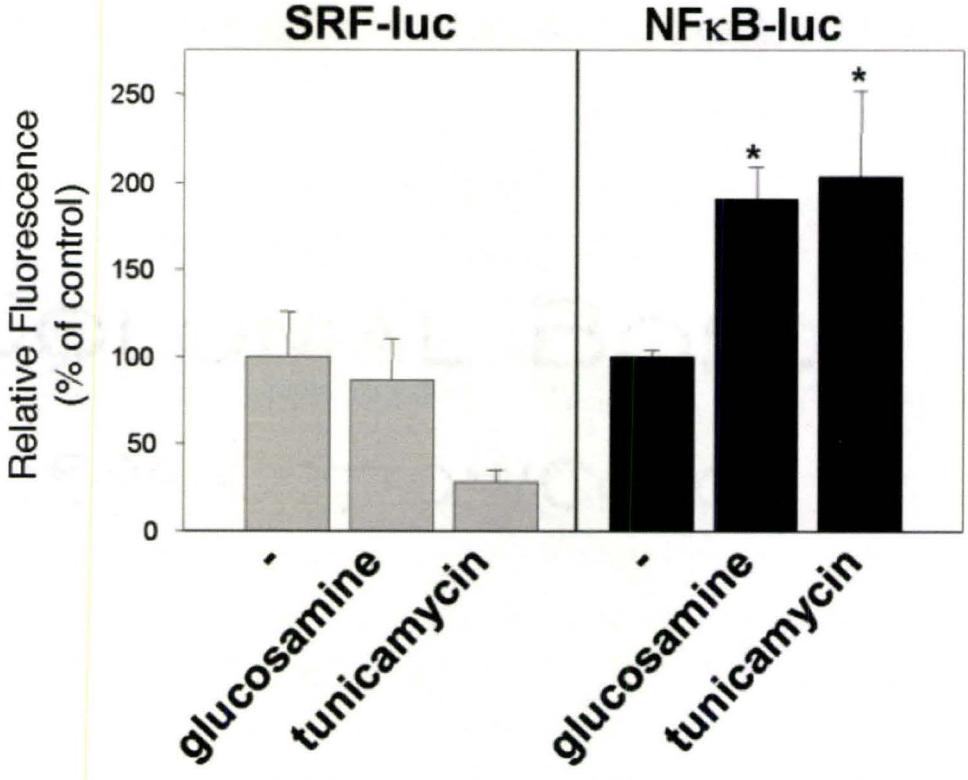

Werstuck *et al.* Diabetes 2006

1.4 VALPROIC ACID

Valproic acid (VPA), or 2-propylpentanoic acid, is a small branched-chain fatty acid and a potent and widely prescribed drug that acts both as an anti-convulsant in the treatment of epilepsy and as a mood-stabilizer to control bipolar disorder (Bowden et al. 1994; Penry and Dean 1989). Despite its wide use, the specific molecular mechanisms responsible for its clinical efficacy are not clear. Exposure to millimolar concentrations of VPA can induce a variety of cellular responses that may be responsible for its clinical efficacy (MacDonald and Bergey. 1979; Phiel et al. 2003; Wang et al. 1999; Williams et al. 2002). VPA has been shown to increase chaperone levels, such as GRP78, GRP94, and calreticulin in neuronal cells and in the rat cerebral cortex and hippocampus (Chen et al. 2000; Wang et al. 2003). This may potentially protect cells from cellular dysfunctions caused by ER stress, a condition associated with several independent risk factors for CVD including hyperglycemia, hyperhomocysteinemia, obesity and high levels of unesterified cholesterol (Werstuck et al. 2006; Zhou et al. 2004; Werstuck et al. 2001; Ozcan et al. 2004; Li et al. 2005). Investigation of the effects of VPA on lipid accumulation and inflammation associated with hyperglycemia may provide a novel potential target(s) and a therapy in diabetes-induced atherosclerosis.

1.4.1 Intracellular targets of valproic acid

1.4.1.1 ER chaperones

Treatment with VPA in cultured neuronal cells and chronic exposure to VPA in rats have been shown to induce elevated levels of ER chaperones (Chen et al. 2000; Wang et al. 2003; Bown et al. 2002). ER chaperones play an essential role in the folding of secreted proteins and proteins targeted for other organelles within the cell (Ron and Walter. 2007; Lee 2004). The expression levels of the chaperones increase during ER stress, a state triggered by accumulation of unfolded and misfolded proteins in the ER, to provide higher folding capacity to the cell. However, when a cell fails to relieve ER stress through the unfolded protein response (UPR), it undergoes lipid accumulation, inflammation, and eventually apoptosis (Pahl 1999; Schroder and Kaufman. 2005; Ron and Walter. 2007). The over-expression of certain ER chaperones has been shown to protect against cellular injuries including cytotoxic chemicals, oxidative stress, and ER stress (Reddy et al. 2003; Morris et al. 1997; Liu et al. 1998). Therefore, examining the effects of VPA on ER chaperone levels in relation to lipid accumulation and lesion development may provide an explanation for anti-atherogenic effect of VPA *in vivo*.

1.4.1.2 Histone deacetylase

Histones are elements of nucleosomes where DNA is bound to form a chromatin structure (Gould et al. 2004). Histones can regulate gene transcription by influencing chromatin structure and the accessibility of transcription factors to their target genes (Haberland et al. 2009). A dynamic process of histone acetylation and deacetylation provides a mechanism for extracellular signals to control the regulation of specific genes

by inducing a different order of chromatin structure. Histone acetyltransferases (HATs) and histone deacetylases (HDACs) add and remove acetyl groups on/from histones to either enhance or reduce transcription (Haberland et al. 2009). VPA has been shown to directly inhibit HDAC at pharmacological concentrations which may potentially control transcription of specific genes (Phiel et al. 2001; Gottlicher et al. 2001). Interestingly, the ability of VPA to inhibit HDAC has been linked to diminished SREBP-1a mRNA and protein levels in adipocytes and down-regulation of human adipocyte differentiation (Lagace and Nachtigal. 2004). Hence, it is possible that the inhibition of HDAC may account for anti-atherogenic property seen *in vivo*.

1.4.1.3 Glycogen Synthase Kinase-3

There are several reports that therapeutic efficacy of VPA may lie in its ability to inhibit GSK3 (Chen et al. 1999a; Gould et al. 2004; Eldar-Finkelman 2002). It has also been shown that VPA can effectively inhibit GSK3 *in vitro* when assayed for its kinase activity (Chen et al. 1999a; Grimes and Jope. 2001; Song et al. 2002; Hoeflich et al. 2000). Given the variety of cellular responses regulated by GSK-3 including glucose metabolism, inflammation and apoptosis, GSK-3 may be a potential target by which VPA reduces hepatic steatosis and lesion development.

1.5 A MOUSE MODEL OF HYPERGLYCEMIA-INDUCED ATHEROSCLEROSIS

In the last few decades the development of transgenic mouse models in combination with the use of special diet has greatly advanced our understanding of cardiovascular disease progression (Renard et al. 2006). Wild type mouse strains are generally resistant to the development of atherosclerosis. This may result, in part, from the relatively high levels of circulating high density lipoproteins (HDLs) and low levels of LDLs that naturally occur in mice (Maeda et al. 2007). Deletion of the gene encoding ApoE or LDL receptor alters the murine lipoprotein profile to a form that is similar to that observed in humans. $ApoE^{-/-}$ mice spontaneously develop fatty streaks in aortic sinus as early as 6 weeks when maintained on a high fat diet or 12 weeks when maintained on a standard chow diet (Maeda et al. 2007; Hsueh et al. 2007; Renard et al. 2006). Specific cardiovascular risk factors have been introduced into the atherosclerosis-prone $ApoE^{-/-}$ strain in order to investigate their ability to accelerate the development of atherosclerotic lesions.

A number of diabetic mouse models that reflect the complexity of human diabetes have been developed by inducing hyperglycemia and/or dyslipidemia. Most type 1-like diabetic mouse models are generated by the destruction of β cells either by injecting exogenous toxins, such as STZ or alloxan, or through genetic modulation involving autoimmunity found in non-obese diabetic (NOD) mice. In order to examine atherogenesis under type 1-like diabetic conditions, we gave $ApoE^{-/-}$ mice multiple low

dose injections of STZ, creating severe hyperglycemia by 7 weeks of age (Table 1). There is much debate on which characteristics of diabetes contribute most to the development of cardiovascular complications. There is evidence that hyperglycemia, hyperinsulinemia, and hyperlipidemia each play a role in the development of diabetic complications, but it has been difficult to quantify the specific contribution of each independent phenomenon (Chait and Bornfeldt. 2008). STZ-injected $ApoE^{-/-}$ mice are deficient in insulin and they do not develop relative dyslipidemia until 20 to 24 weeks of age (Werstuck et al. 2006). Therefore, I examined the tissues of 15 week old STZ-injected $ApoE^{-/-}$ mice which exhibit hyperglycemia without dyslipidemia in order to isolate the effects of hyperglycemia on plaque development.

2 RATIONALE, HYPOTHESIS AND OBJECTIVES OF STUDY-PART I

2.1 RATIONALE

Diabetes mellitus is a major independent risk factor for accelerated atherosclerosis (Anand et al. 2008). There are several contributing factors that may lead to atherogenesis, one of which is elevated intracellular content of glucosamine, a metabolite of glucose. Increased levels of glucosamine have been implicated in hyperglycemia-induced cellular dysfunctions, and we have evidence showing that glucosamine treatment in HepG2 cells induces unesterified cholesterol accumulation and NF-κB activation (Figure 4) (Kim et al. 2005; Werstuck et al. 2006). VPA, a drug widely used as anti-convulsant and mood-modifier, has been shown to induce ER chaperone levels in cultured cells (Chen et al. 2000; Wang et al. 2003) and over-expression of ER chaperones has been shown to protect cultured cells from conditions of cellular injuries (Reddy et al. 2003; Morris et al. 1997; Liu et al. 1998). These studies suggest that VPA could protect against hyperglycemia-induced accumulation of pro-atherogenic pathways *in vitro* and accelerated atherosclerosis in a mouse model.

2.2 HYPOTHESIS

VPA attenuates the activation of pro-atherogenic pathways *in vitro* and the development of accelerated atherosclerosis in a hyperglycemic apolipoprotein E-deficient ($ApoE^{-/-}$) mouse model.

2.3 OBJECTIVES

2.3.1 Overall objective

To determine the anti-atherogenic potential of VPA under conditions of hyperglycemia and to identify the pathway(s) responsible for this effect.

2.3.2 Specific objectives

1. To determine the effect of VPA on lipid accumulation in cultured cells exposed to elevated concentrations of glucose and glucosamine

2. To determine the effect of VPA on inflammatory pathways in cultured cells exposed to elevated concentrations of glucose and glucosamine

3. To determine the effect of VPA supplementation on aortic lesion development and hepatic steatosis in a mouse model of hyperglycemia-induced atherosclerosis.

4. To identify the pathway(s) responsible for protecting cultured cells from glucosamine-induced lipid accumulation

3 EXPERIMENTAL PROCEDURES

3.1 MATERIALS

VPA, glucose, mannitol, glucosamine, tunicamycin, A23187, and filipin were purchased from Sigma (Oakville, ON). GSK-3 inhibitor II, 3-(3-carboxy-4-chloroanilino)-4-(3-nitrophenyl) maleimide, was purchased from CalBiochem (La Jolla, CA). 3 beta-(2-diethylaminoethoxy) androst-5-en-17-one (U18666A) was purchased from Biomol International (Plymouth Meeting, PA). Antibodies to calreticulin (SPA-600) and the anti-KDEL monoclonal antibody (SPA-827), which recognizes GRP78/BiP were purchased from StressGen Biotechnologies (Victoria, BC). Anti-GADD153/CHOP (sc-7351) monoclonal antibodies were purchased from Santa Cruz Biotechnology (Santa Cruz, CA). Anti-β actin (AC-15) antibodies were purchased from Sigma. Anti-acetyl-hisone H4 (Lys8) and total H4 antibodies were purchased from Upstate (Charlottesville, VA).

3.2 CELL LINES AND CULTURE CONDITIONS

3.2.1 Human Hepatocarcinoma cells

HepG2 were obtained from American Type Culture Collection (ATCC, Rockville, MD) and cultured in Dulbecco's Modified Eagle's Medium (Life Technologies, Burlington, ON) containing 10% fetal bovine serum (FBS) (HyClone, Logan, UT). Cells were maintained in a humidified incubator at 37°C with 5% CO_2.

3.2.2 Human Aortic Smooth Muscle Cells

Human aortic smooth muscle cells (HASMC) were purchased from Cascade Biologicals (Portland, OR) and cultured in Medium 231 supplemented with 20% smooth muscle growth supplement and PSA solution containing 100 U/ml penicillin, 100 μg/ml streptomycin and 0.25 μg/ml amphotericin (Cascade Biologicals). Cells were maintained in a humidified incubator at 37°C with 5% CO_2.

3.3 UNESTERIFIED CHOLESTEROL STAINING

The accumulation of unesterified cholesterol was determined by filipin staining (Kruth, 1984). Mouse embryonic fibroblasts (MEFs), grown on cover slips, were treated with 4 mM VPA or 200 nM GSK-3 inhibitor II for 1 hour and challenged with glucosamine (5 mM) for an additional 18 hours. Cells were washed three times with Medium 1 (150 mM NaCl, 5 mM KCl, 1 mM $CaCl_2$, 20 mM HEPES pH 7.4, 2 g/l glucose), fixed with 4% paraformaldehyde for 20 minutes at room temperature and then incubated for 2 hours with 50 μg/ml filipin in Medium 1 at room temperature. Cells were washed three times with Medium 1 and then filipin bound unesterified cholesterol complexes were visualized by fluorescence microscopy with excitation at 335-385 nm (emission at 420 nm). The accumulation of unesterified cholesterol in primary mouse hepatocytes was quantified using Sigma Scan. The intensity threshold was set to a range of 234-249 for measuring all intensities in the fluorescence pictures taken. The average intensity per cell surface area was plotted for each treatment group.

3.4 NF-κB ACTIVITY MEASUREMENT USING LUCIFERASE ACTIVITY

HASMC were cultured in 6-well plates and co-transfected at 50% confluency with 1.5μg of pNF-κB-luc reporter gene (Stratagene) and 1.5ng of pRL-luc reporter gene (Promega) using ExGen500 (Fermentas). 30 hours after transfection, the cells were pretreated with test compounds for 2 hours and then treated with 0-5mM of glucosamine and harvested 18 hours after the treatment. The luciferase activity of the lysates was determined using a luminometer (TD-20/20 Luminometer, Turner Designs). 20μL of the sample or standard was mixed with 50μL of the luciferase substrate (LAR II, Promega) and the relative light units were measured immediately at room temperature. 50μL of the Stop & Glo Reagent (Promega) was added subsequently to quench firefly luciferase and activate *Renilla* luciferase. The firefly luminescence was normalized to the *Renilla* luminescence of the transfection control.

3.5 MOUSE MODELS

Five week old female ApoE$^{-/-}$ (B6.129P2-ApoE^{tm1Unc}) mice were placed on a defined chow diet (Harlan Teklad, TD92078) and randomly divided into two groups (n=24/group). To induce hyperglycemia, one group was injected intraperitoneally with multiple low doses of streptozotocin (STZ) (40 mg/kg) as previously described (Werstuck et al. 2006; Kunjathoor et al. 1996). After one week, half of the mice in each group were switched to the control diet supplemented with 625 mg/kg VPA (TD02165). All mice had unrestricted access to both food and water throughout the study. Mice were sacrificed at

15 weeks of age and blood and tissues were collected for further analysis. The McMaster University Animal Research Ethics Board approved all procedures.

Figure 5. Study design: induction of hyperglycemia and diet treatment.

A and B. Five week old female ApoE$^{-/-}$ (B6.129P2-ApoE^{tm1Unc}) mice were placed on a defined chow diet and randomly divided into two groups (n=24/group). To induce hyperglycemia, one group was injected intraperitoneally with multiple low doses of streptozotocin (STZ) (40 mg/kg) or same volume of citrate buffer. After one week, half of the mice in each group were switched to the control diet supplemented with 625 mg/kg VPA (TD02165).

A.

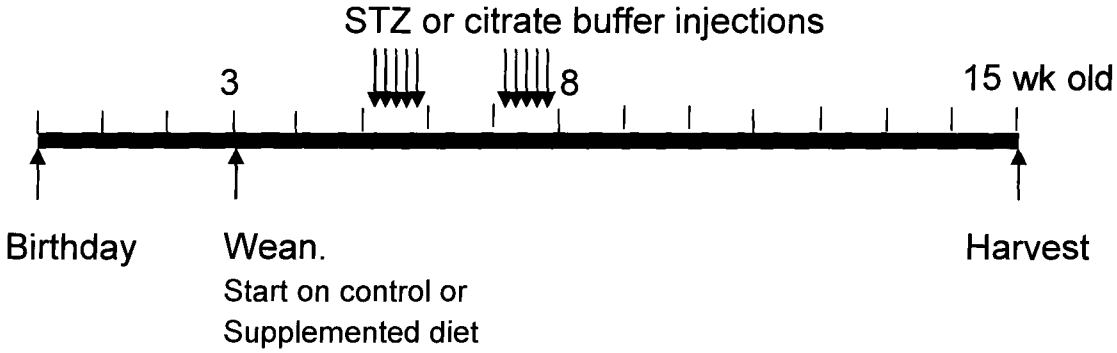
STZ or citrate buffer injections
3
8
15 wk old
Birthday
Wean.
Start on control or
Supplemented diet
Harvest

B.

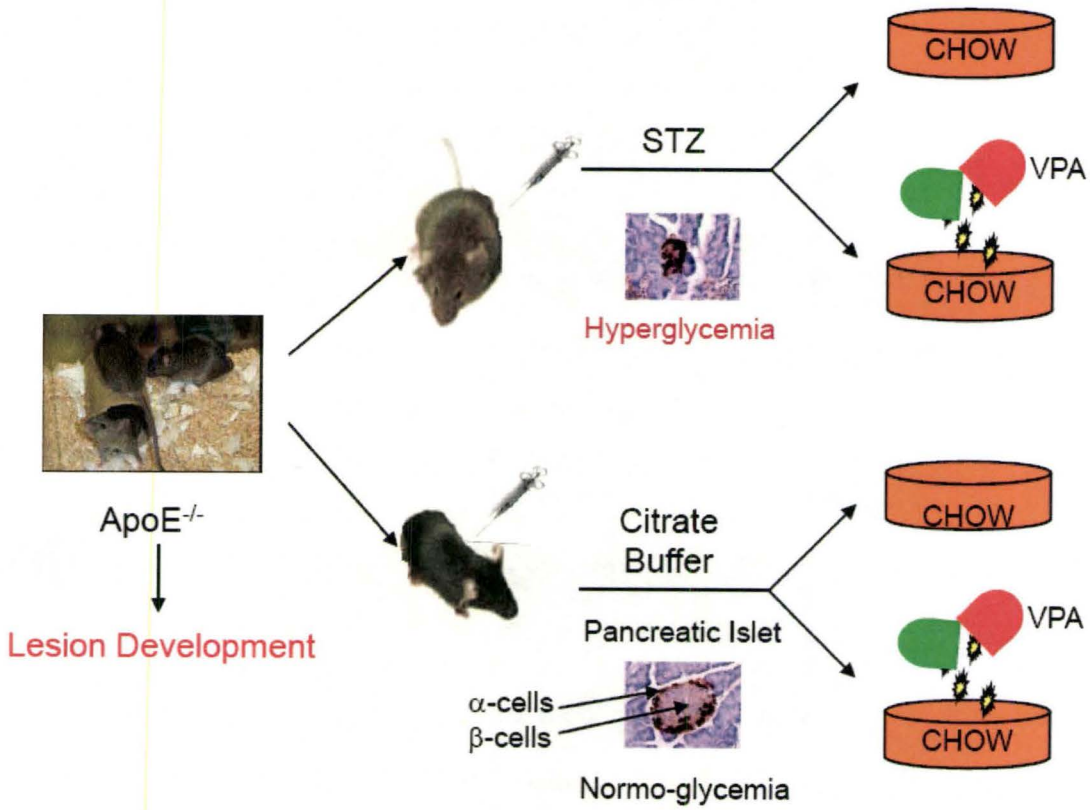
CHOW
STZ
VPA
CHOW
Hyperglycemia
ApoE-/-
Lesion Development
Citrate
Buffer
CHOW
Pancreatic Islet
VPA
α-cells
β-cells
CHOW
Normo-glycemia

3.6 PLASMA ANALYSIS

Random and fasting (12 hours) whole blood glucose levels were measured using a DEX glucometer (Bayer). Plasma glucose and lipid levels were determined in non-fasted mice using the colorimetric diagnostic kits for total cholesterol, triglycerides and glucose purchased from Thermal DMA Inc. Plasma VPA concentrations were determined using an AxSYM system (Abbott Laboratories, Mississauga, ON).

3.7 IMMUNOBLOT ANALYSIS

Cytoplasmic proteins were isolated from mouse liver using a NE-PER Kit (Pierce, Rockford, IL) and total protein lysates were prepared from mouse liver solubilized in RIPA buffer (150 mM NaCl, 5% DOC, 50 mM Tris-base, 1% NP-40, 0.1% SDS, 100 mM NaF, and 2mM PMSF). These lysates (40 μg) were solubilized in Sodium Dodecyl Sulfate-Polyacrylamide Gel Electrophoresis (SDS-PAGE) sample buffer (50 mM Tris, pH 6.8, 2% SDS, 10% glycerol, 0.01% bromophenol blue and 50 mM dithiothreitol) and separated on SDS-polyacrylamide gels under reducing conditions. Proteins were transferred to nitrocellulose membranes (Bio-Rad) using a wet transfer apparatus (Bio-Rad). Membranes were blocked overnight with 5% non-fat milk in 1X TBST (50 mM Tris; pH 7.5, 120 mM NaCl, 0.02% Tween20) at 4°C. After incubation with the appropriate primary and horseradish peroxidase (HRP)-conjugated secondary antibodies (Life Technologies, Burlington, ON), the membranes were developed using the Immobilon Western chemiluminescent HRP substrate (Millipore, Billerica, MA), and

Kodak X-OMAT Blue XB-1 film (Perkin-Elmer). Protein levels were normalized using anti-β-actin immunoblot on the same nitrocellulose membrane.

3.8 AORTIC LESION ANALYSIS

Mice were euthanized, hearts were flushed with 1X PBS and were then perfusion-fixed with 10% neutral buffered formalin. After removal, hearts, including the aortic root were cut transversely and embedded in paraffin. Serial sections (4 μm) of the aortic root were collected on pre-coated glass slides for measurement of lesion size (hematoxylin and eosin staining) or immunohistochemical staining (Paigen B et al. 1987). The Vectastain ABC System was used for immunohistochemical analyses. Sections were stained with primary antibodies and visualized using appropriate biotinylated secondary antibodies and Nova Red. Non-specific staining was controlled for using a similar section and pre-immune IgG. Images were captured with a charge coupled device (CCD) color video camera (Sony) and analyzed using Northern Exposure (Empix) and Wright Cell Imaging Facility (WCIF) customized ImageJ (NIH) software.

3.9 LIPID STAINING

Liver cryo-sections, 7 μm thick, were collected on slides and fixed in formal calcium for 30 minutes. Neutral lipids were visualized in sections that were rinsed and incubated in a saturated, filtered solution of Oil red O (Sigma) for 7 minutes. After rinsing

with H_2O, nuclei were stained with hematoxylin, and slides were mounted in Crystalmount (Sigma-Aldrich) (Westuck et al. 2001). Relative amounts of lipid staining were quantified using Image J 1.35 Software (NIH).

3.10 GSK-3 KINASE ASSAY

15 μM synthetic GSK-3 substrate (phospho-Glycogen Synthase Peptide-2) and 0.5 μCi/μL [γ^{32}P] ATP were added to recombinant GSK-3α/β in reaction mixture containing, 20 mM MOPS (pH7.4), 50 μM EDTA, 2.5 mM Mg acetate, 5 mM $MgCl_2$, 5 mM β-glycerol phosphate, 1 mM EGTA, 0.25 mM Na_3VO_4, 0.25 mM DTT, and 35 μM ATP in a total volume of 40 μL. 0-5 mM VPA was added to GSK-3 before the substrate and ATP were added. GSK-3 with 20 mM Li (a GSK-3 inhibitor) was used as a positive control. The samples were placed on ice immediately following a 30 min incubation at 30°C. 30 μL samples were spotted onto Whatman P81 phosphocellulose paper, washed 3X with 0.75% *o*-phosphoric acid and 1X with acetone. Scintillation counting was used to determine ^{32}P incorporation on to the substrate.

3.11 STATISTICAL ANALYSIS

Results are presented as the mean ± standard deviation. One-way analysis of variance (ANOVA) was used for repeated measurements of the same variable, and

Duncan's multiple range t-test was used to assess differences between experimental groups and controls. Probability values of <0.05 were considered statistically significant.

4 RESULTS

4.1 EFFECT OF VALPROIC ACID ON GLUCOSAMINE-INDUCED CELLULAR DYSFUNCTION

4.1.1 Valproic acid blocks glucosamine-induced lipid accumulation in HepG2 and HASMC

Our lab has demonstrated that elevated levels of glucosamine, a condition resulting from hyperglycemia, can cause cellular dysfunction through dysregulation of cholesterol and fatty acid metabolism in HepG2 cells (Figure 4) (Werstuck et al. 2001). We also discovered that VPA, a small fatty acid, can induce ER chaperone levels, which may offer cyto-protection in conditions of ER stress (Kim et al. 2005). In order to determine if VPA attenuates glucosamine-induced lipid accumulation, we monitored the levels of unesterified cholesterol by staining cells that are relevant to atherogenesis with filipin (Kruth. 1984). HepG2s, an immortal hepatocarcinoma cell line, were chosen for studying cholesterol accumulation.

The liver is the central organ in regulation of both lipid and glucose synthesis and metabolism (Taniguchi et al. 2006). Cholesterol is synthesized on the hepatic ER membrane where it is packaged with other lipids in the form of very low density lipoprotein (VLDL) for delivery to peripheral tissues. The liver is the main centre for gluconeogenesis when the body undergoes hypoglycemic conditions. Conversely, the liver is the site of glycogen and fatty acid synthesis during periods of hyperglycemia (Montminy and Koo. 2004; Taniguchi et al. 2006). Therefore, HepG2 cells, which retain

the ability to perform gluconeogenesis and lipid biosynthesis and packaging, were utilized to elucidate the effect of VPA on glucosamine-induced lipid accumulation.

HASMCs were also used as a model system to investigate the effect of VPA. SMCs, normally found in the medial layer of the artery wall, migrate into the intima in early atherosclerosis and participate in the production of inflammatory mediators (Dzau et al. 2002; Glass and Witztum. 2001). SMCs, like macrophages, also give rise to lipid-laden foam cells by taking up cholesterol (Doran et al. 2008). Human, rat, and rabbit SMCs have been shown to express receptors for cholesterol uptake, such as LDL receptor, CD36, and type I and type II scavenger receptors (Ruan et al. 2006; Lim et al. 2006; Matsumoto et al. 2000; Bickel et al. 1992). Therefore, the relevance of VPA with respect to glucosamine-induced lipid accumulation was also examined in HASMCs.

Treatment of cells with 10 mM glucosamine for 18 hours significantly increased the unesterified cholesterol content of HepG2 cells, consistent with our preliminary results (Figure 6. A. b). 10 mM of mannitol, a six carbon polyol that cannot be metabolized into glucose or glucosamine, was used as an osmotic control. Unesterified cholesterol accumulation was evident around the nuclei of glucosamine treated cells on what appears to be the ER membrane. This observation is consistent with the localization of endogenous cholesterol biosynthesis in the smooth ER. Cells treated with mannitol did not accumulate unesterified cholesterol, which confirms that 10 mM of six carbon polyol treatment alone does not induce osmotic stress associated lipid accumulation (Figure 6. A. c). Pretreatment of HepG2 cells with VPA significantly decreased unesterified

cholesterol accumulation associated with exposure to glucosamine in a dose responsive manner (Figure 6. A. d and e).

Treatment of HASMC with 5 and 10 mM glucosamine also resulted in higher luminosity than the untreated cells, indicating greater accumulation of unesterified cholesterol (Figure 6. B. b and c). Nonetheless, 4 mM VPA treatment decreased the effect of 5 and 10 mM glucosamine on lipid accumulation in HASMCs (Figure 6. B. d and e).

Figure 6. Valproic acid blocks glucosamine-induced unesterified cholesterol accumulation.

HepG2 cells (**A**) and human aortic smooth muscle cells (HASMC) (**B**) were pretreated with 0-4 mM valproic acid (VPA) for 2 hours and then with 5 or 10 mM glucosamine or mannitol (an osmotic control) for 18 hours. Cells were stained with filipin for 2 hours to visualize unesterified cholesterol and the images were captured using a fluorescence microscope with excitation at 335-385 nm and emission at 420 nm. Images were taken using a digital camera and the representative figures are shown.

(A) a. untreated, **b**. 10 mM glucosamine, **c**. 10 mM mannitol, **d**. 1 mM VPA + 10 mM glucosamine, **e**. 4 mM VPA + 10 mM glucosamine. **(B) a**. untreated, **b**. 5 mM glucosamine, **c**. 10 mM glucosamine, **d**. 4 mM VPA + 5 mM glucosamine, **e**. 4 mM VPA + 10 mM glucosamine.

A. HepG2 Cells

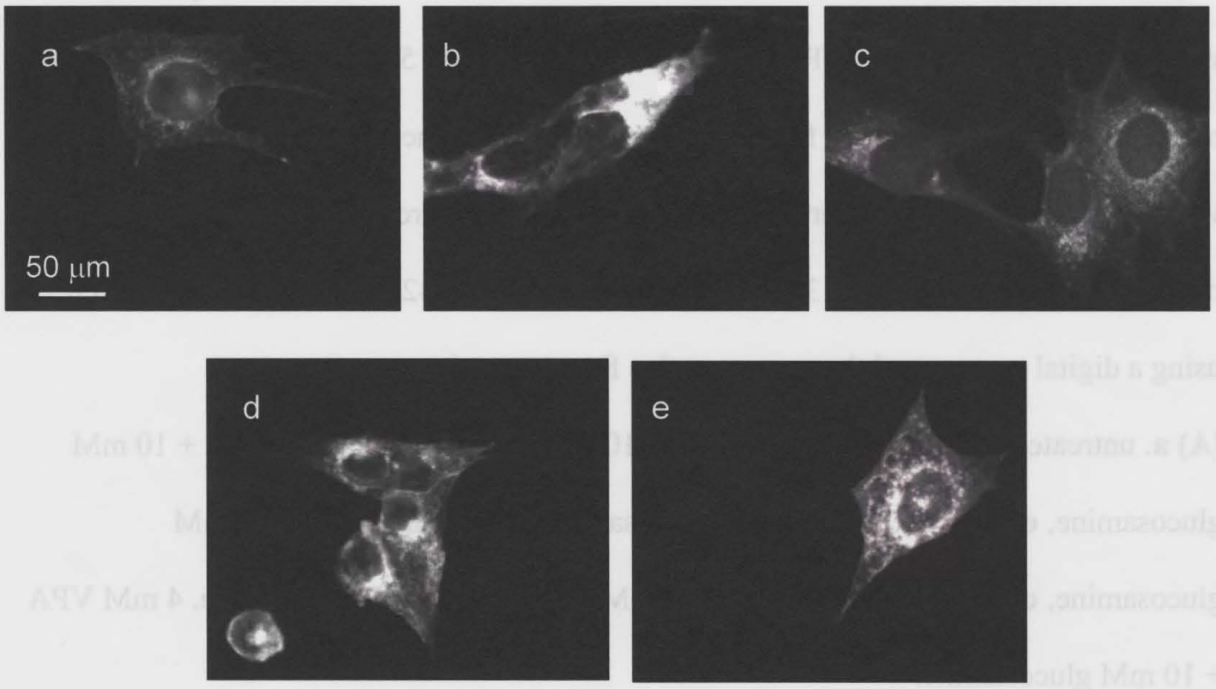

B. HASMC

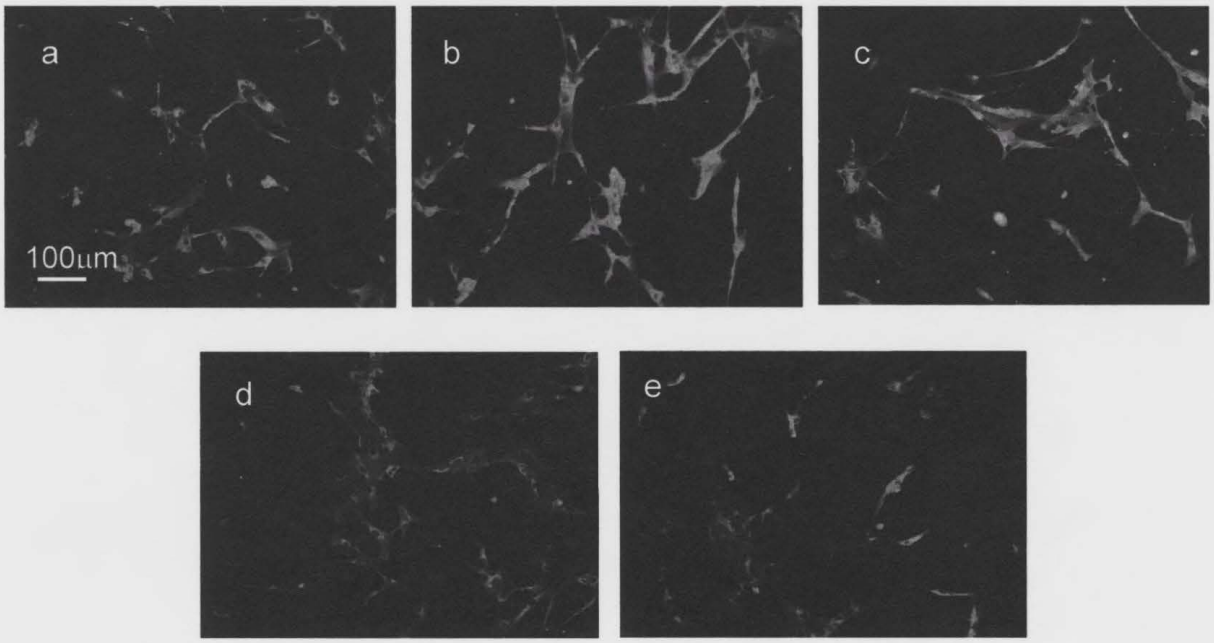

4.1.2 Valproic acid blocks glucosamine-induced NF-κB activation in HASMC

Inflammatory responses by macrophages and T-cells play a central role in all stages of atherosclerosis (Ross. 1999; Hansson and Libby. 2006). NF-κB is a key transcription factor in the expression of genes encoding inflammatory factors including ICAM-1, VCAM-1, E-selectin, tissue factor, TNF-α, IL-1α and IL-6 (Gleissner et al. 2007; Li and Verma. 2002). The effect of glucosamine on NF-κB activation and the ability of VPA to modulate this effect were examined. A luciferase assay was developed by transfecting HASMC with the plasmid pNF-κB-luc along with an internal transfection control Renilla luciferase (Promega). 1 and 5 mM glucosamine treatments of HASMC caused significant increases in luciferase signal, indicating elevated levels of NF-κB activity, relative to levels detected in untreated cells or cells treated with 5mM mannitol (an osmotic control) (Figure 7). In cells treated with VPA, the ability of glucosamine to induce NF-κB was attenuated. This result suggests that VPA may protect against inflammation caused by increased amounts of glucosamine.

Figure 7. Valproic acid blocks glucosamine-induced NF-κB activation in HASMC.

HASMCs were transfected with pNF-κB-luc (firefly luciferase) and pRL-SV40 plasmid (*Renilla* luciferase). After 30 hours, cells were pretreated with 0-4 mM valproic acid (VPA) for 2 hours and then exposed to 0 or 5 mM glucosamine (GlcN) or 5 mM mannitol. 18 hours later, the cells were lysed and luciferase activity was measured. The firefly luciferase activity was normalized to the *Renilla* luciferase activity of each sample and the average activity of untreated cells was set as 100%. (n=3. *P<0.05 vs. untreated, **P<0.05 vs. GlcN alone)

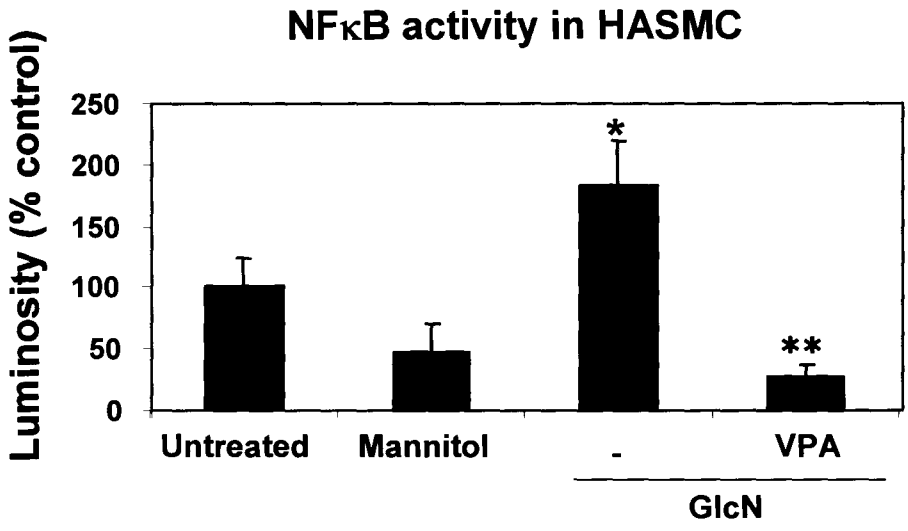
NFκB activity in HASMC
Luminosity (% control)
250
200
150
100
50
0
*
**
Untreated
Mannitol
-
VPA
GlcN

4.2 EFFECTS OF VALPROIC ACID SUPPLEMENTATION ON HYPERGLYCEMIC APOLIPOPROTEIN E-DEFICIENT MICE

4.2.1 Induction of hyperglycemia and effects of valproic acid supplementation on metabolic parameters

In cultured cells, we have shown that VPA attenuates glucosamine-induced unesterified cholesterol accumulation and NF-κB activation (Figures 6 and 7). These results suggest that VPA may exhibit anti-atherogenic effects *in vivo*. We tested this possibility in a hyperglycemic $ApoE^{-/-}$ mouse model of accelerated atherosclerosis. Hyperglycemia was induced in female $ApoE^{-/-}$ mice by multiple low dose intraperitoneal injections of STZ (Werstuck et al. 2006, Kunjathoor et al. 1996). STZ was used to induce apoptosis in pancreatic β cells, causing insulin deficiency and hyperglycemia (Kunjathoor et al. 1996; Park et al. 1998). Blood glucose levels were monitored weekly in all experimental groups. All STZ-injected mice were hyperglycemic by the time of the last injection. At the time of sacrifice (15 weeks of age), 12 hour fasting plasma glucose concentration in STZ-injected mice was 7.6±2.1 mmol/L versus 4.3±0.7 mmol/L ($P<0.05$) in control mice (Table 1). As previously reported, the lesion volume in STZ mice fed control diet was significantly larger than the lesion volume observed in control mice (Park et al. 1998; Werstuck et al. 2006). VPA supplementation, however, significantly reduced the elevated lesion volume in STZ mice (Table 1).

Supplementation of defined mouse chow with 625 mg/kg VPA increased plasma VPA levels from undetectable to 37.5±14.9 μmol/L in control ApoE$^{-/-}$ mice (Table 1). Plasma VPA levels were not significantly different in hyperglycemic ApoE$^{-/-}$ mice relative to normoglycemic mice fed the same diet. VPA supplementation had no significant effect on body or liver weight in any of the experimental groups relative to age matched mice fed a control diet.

In addition, VPA supplementation had no significant effect on plasma glucose and plasma cholesterol levels in fasted or fed animals (Table 1). Consistent with previous studies, the induction of hyperglycemia did not significantly affect plasma cholesterol levels in 15 week old ApoE$^{-/-}$ mice (Werstuck et al. 2006). There was a significant increase in plasma triglyceride levels in STZ mice fed control diet accompanied by a large standard deviation, which may be indicative of the start of dyslipidemia seen around week 20 (Werstuck et al. 2006). STZ mice fed VPA supplemented diet, however, did not show a significant increase in plasma triglyceride levels compared to control mice (Table 1). These findings indicate that this level of VPA supplementation is sub-symptomatic, which is consistent with previous pre-clinical analyses of VPA toxicity in rodents (Walker et al. 1990).

Table 1. Metabolic parameters in ApoE$^{-/-}$ mice

	Experimental Group			
	control	control + VPA	STZ	STZ + VPA
body weight (g)	20.9±1.8	20.9±1.1	19.5±0.6	20.1±1.6
liver weight (g)	0.85±0.1	0.80±0.9	0.88±0.13	0.94±0.21
lesion volume ($10^{-3}mm^3$)	3.80±0.55	3.21±0.56	8.62±1.23*	4.98±0.76†
Plasma				
VPA (μmol/L)	0	37.5±14.9	0	33.7±6.2
Fasting glucose (12h) (mmol/L)	4.3±0.7	4.7±0.5	7.6±2.1§	8.3±2.7§
Fed glucose (mmol/L)	14.0±2.7	12.6±3.5	23.2±5.6§	27. 0±0.9§
cholesterol (mmol/L)	11.6±2.1	13.1±3.7	12.7±3.1	13.5±3.5
triglyceride (mmol/L)	0.21±0.06	0.28±0.10	0.41±0.26*	0.29±0.14

STZ, streptozotocin-injected; n = 9-16/treatment group for each measurement

*P<0.05 relative to control mice fed control diet.

†P<0.05 relative to HG mice fed control diet

§P<0.05 relative to control mice fed the same diet

4.2.2 Hyperglycemic mice have elevated levels of hepatic O-linked protein glycosylation

Glucosamine is a product of glucose flux through the hexosamine pathway and an ER stress-inducing agent that we have previously linked to diabetic atherogenesis (Werstuck et al. 2006; Kim et al. 2005). Alterations in intracellular glucosamine concentration were determined by evaluating the extent of O-linked glycosylation of the nuclear pore protein p62 using immunoblot analysis with the RL2 antibody (Werstuck et al. 2006; Han et al. 2000). Hyperglycemic mice have significantly elevated levels of O-linked *N*-acetyl glycosylation (GlcNAc) of p62 in the liver relative to control mice (Figure 8). The supplementation of their diet with VPA did not affect the observed levels of O-linked glycosylation (Figure 8). These findings are consistent with the similar blood glucose concentrations observed in supplemented and non-supplemented mice. This result suggests that VPA does not significantly affect glucose flux through the hexosamine pathway.

Figure 8. Effect of valproic acid supplementation on intracellular O-linked glycosylation

Livers were frozen in liquid nitrogen during the organ harvest at 15 weeks of age. Livers were later thawed on ice to be homogenized in RIPA buffer for lysate preparation. Total protein lysates were resolved by SDS-PAGE, transferred to nitrocellulose membranes and immunoblotted with the RL-2 antibody. The relative amounts of the O-glycosylated nuclear pore protein, p62 (p62-O-GlcNAc) were quantified and plotted for each group. NG, normoglycemic; HG, hyperglycemic; VPA, valproic acid. n=3-6/group; $*P<0.05$ relative to controls.

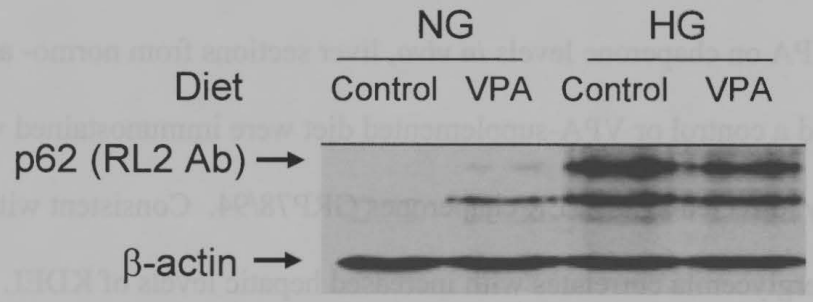
NG
HG
Diet
Control
VPA
Control
VPA
p62 (RL2 Ab)
β-actin

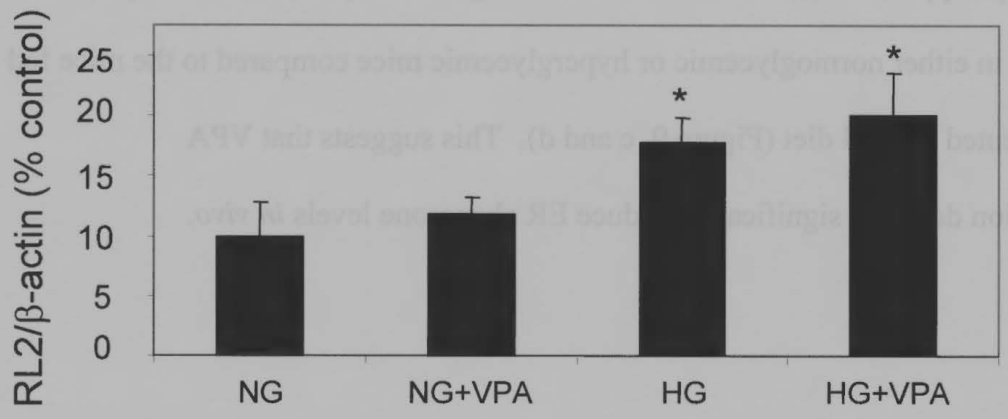
RL2/β-actin (% control)
25
20
15
10
5
0
*
*
NG
NG+VPA
HG
HG+VPA

4.2.3 Valproic acid supplementation does not increase chaperone levels in mice

VPA has been shown to induce ER and cytosolic chaperone levels in cultured cells and in rat brain (Cui et al. 2007; Shao et al. 2006). Increase in chaperone levels may provide protection against inflammation and lipid accumulation caused by oxidative stress and ER stress (Cui et al. 2007; Kim et al. 2005; Bowes et al. 2009). To investigate the effects of dietary VPA on chaperone levels *in vivo*, liver sections from normo- and hyperglycemic mice fed a control or VPA-supplemented diet were immunostained with an anti-KDEL antibody, directed against ER chaperones GRP78/94. Consistent with our previous findings, hyperglycemia correlates with increased hepatic levels of KDEL staining, most likely indicative of ER stress (Figure 9) (Werstuck et al. 2006; Bowes et al. 2009). Dietary supplementation with VPA did not significantly induce ER chaperone protein levels in either normoglycemic or hyperglycemic mice compared to the mice fed non-supplemented control diet (Figure 9. c and d). This suggests that VPA supplementation does not significantly induce ER chaperone levels *in vivo*.

Figure 9. Effect of valproic acid supplementation on ER chaperone levels

Paraffin-embedded sections of liver from each of the treatment groups were collected on pre-coated glass slides. Sections were stained with primary antibodies raised against the KDEL sequence and visualized using biotinylated secondary antibodies and Nova Red. Images were captured with a CCD color video camera (Sony) and analyzed using Northern Exposure (Empix) and SigmaScan Pro software. Dark burgundy colour indicates positive staining for the antibody.

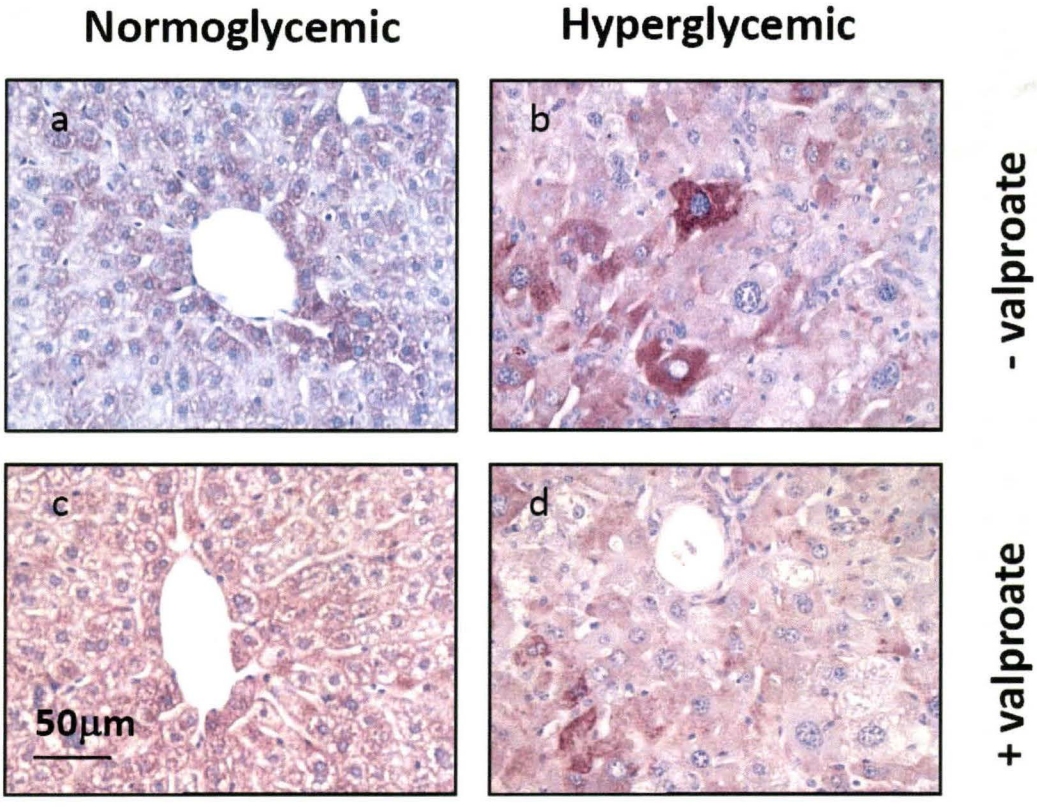
Normoglycemic
Hyperglycemic
a
b
c
d
50µm
- valproate
+ valproate

4.2.4 Valproic acid supplementation reduces hepatic steatosis

Hepatic steatosis, or fatty liver, is a complication frequently observed in individuals with DM and animal models of diabetes (Ohno et al. 2000; Werstuck et al. 2006; Cusi 2009). Since VPA attenuates lipid accumulation in HepG2 cells, I examined the effect VPA supplementation has on hepatic steatosis. Cryo-sections of liver isolated from each of the treatment groups were stained with Oil Red O to visualize neutral lipids (Figure 10). Consistent with our previous findings, conditions of hyperglycemia promote the accumulation of hepatic lipids in $ApoE^{-/-}$ mice (Werstuck et al. 2006). Significantly reduced levels of hepatic lipid were observed in hyperglycemic mice that received dietary supplementation with VPA relative to non-supplemented control (Figure 10). This finding is supported by an observed increase in hepatic mRNA transcripts encoding proteins involved in lipid biosynthesis, including SREBP-1c, FAS, and HMG-CoA reductase, in hyperglycemic mice fed control diet (Bowes et al. 2009). Hyperglycemic mice fed the VPA supplemented diet had significantly lower levels of these transcripts (Bowes et al. 2009). This suggests that VPA protects hyperglycemic mice from dysregulation of lipid metabolism in the liver.

Figure 10. Effect of valproic acid supplementation on hepatic steatosis.

Representative sections of liver from control or hyperglycemic ApoE$^{-/-}$ mice fed control diet or valproic acid (VPA) supplemented diet, as indicated, were stained with Oil Red O (red). 7 μm thick liver cryo-sections were collected on slides and fixed in Formal calcium solution before incubation with Oil red O solution. After rinsing with distilled water, nuclei were stained with hematoxylin (blue), and slides were mounted using Crystalmount. Images of several fields within the same treatment group were taken using a light microscope.

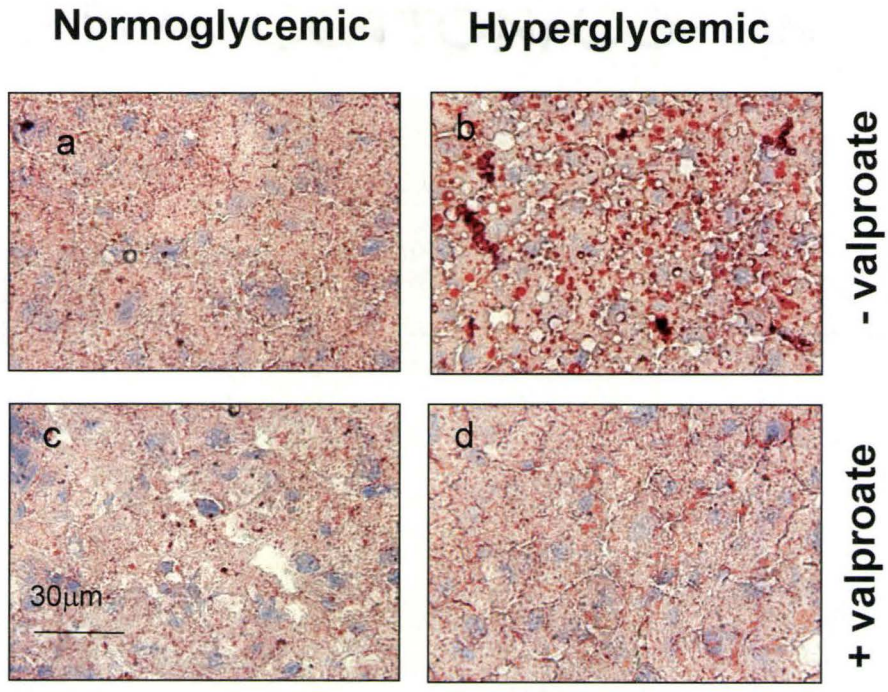
Normoglycemic
Hyperglycemic
a
b
c
d
30μm
- valproate
+ valproate

4.2.5 Valproic acid supplementation reduces lesion size in the aortic root of hyperglycemic mice

We next examined the effect VPA supplementation has on overall atherosclerosis by measuring the size of the lesion in aortic roots. Consistent with our observation in hepatic tissues, VPA supplementation did not increase chaperone levels in aorta (Bowes et al. 2009). Nevertheless, our *in vitro* data suggest that VPA may still exert a protective effect against lipid accumulation and inflammation in the absence of the elevation of chaperone levels (Kim et al. 2005). Hence, the effect of VPA on hyperglycemia-associated accelerated atherosclerosis was examined. Hyperglycemia significantly increased mean atherosclerotic lesion volume at the aortic root of $ApoE^{-/-}$ mice relative to control $ApoE^{-/-}$ mice (2.3 fold) (Figure 11) which is consistent with reported data (Levi et al. 2003). Interestingly, dietary supplementation with VPA correlated with a significant decrease in cross sectional lesion area and total mean lesion volume in hyperglycemic mice (4.98 ± 0.76 versus $8.62\pm1.23 \times 10^{-3}mm^3$, $P<0.05$) relative to non-supplemented controls (Table 1). In hyperglycemic mice the reduced lesion volume corresponded with a significant reduction in the number of Mac-3 positive macrophage-derived foam cells within the atherosclerotic plaque (Bowes et al. 2009). A non-significant trend toward smaller lesion volume was observed in normoglycemic $ApoE^{-/-}$ mice fed the VPA diet. In all mice, atherosclerotic lesion development was confined to a region within 120 μm of the aortic root and no lesions were observed in the descending aorta or the aortic arch of any of the treatment groups (Figure 28). The finding that VPA can protect hyperglycemic $ApoE^{-/-}$ mice from accelerated atherosclerosis and hepatic steatosis, leads to the next step

in identifying the *in vivo* target(s) of VPA which will advance our knowledge in developing potential therapeutic intervention.

Figure 11. Effect of valproic acid supplementation on atherosclerotic plaque area in hyperglycemic ApoE$^{-/-}$ mice

Lesion areas were determined at the aortic root (0 μm) and at 40 μm intervals in aortae isolated from 15 week old normoglycemic (NG) or hyperglycemic (HG) mice fed control diet or control diet supplemented with valproic acid (+VPA). The mice were perfusion-fixed with 10% neutral buffered formalin and hearts, including the aortic root, were cut transversely and embedded in paraffin. 4 μM sections of aortic root were collected on pre-coated glass slides for hematoxylin and eosin stain. The lesion area (average ± s.e.m.) was determined using WCIF ImageJ software and plotted against the distance across the aortic root. n=10-12/group; *P<0.05, relative to control mice; **P<0.05, relative to similar treatment group in the absence of VPA supplementation.

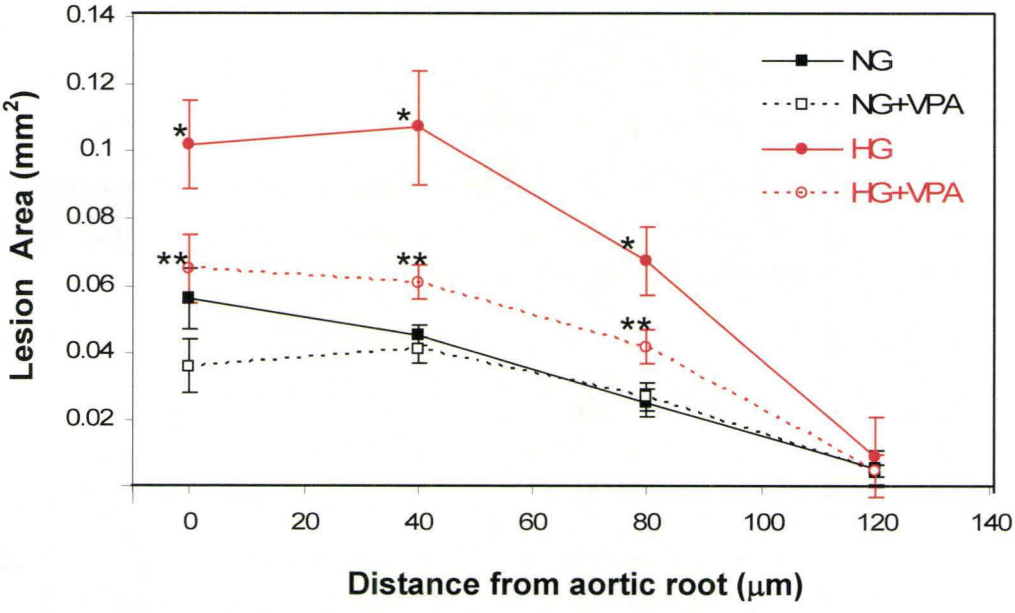
0.14
0.12
0.1
0.08
0.06
0.04
0.02
Lesion Area (mm²)
0
20
40
60
80
100
120
140
Distance from aortic root (μm)
NG
NG+VPA
HG
HG+VPA
*
*
*
**
**
**

4.3 INTRACELLULAR EFFECTS OF VALPROIC ACID

4.3.1 Effect of valproic acid on chaperone levels

Treatment with VPA can induce ER chaperone levels in neuronal cells and over-expression of chaperones has been shown to protect cells from inflammation caused by many cellular insults (Chen et al. 2000; Reddy et al. 2003; Morris et al. 1997; Liu et al. 1997). I examined whether there is a correlation between induction of chaperone levels and protection of cells from glucosamine-induced lipid accumulation. A time course study of 0.5 mM VPA treatment in HepG2 cells indicates that GRP78/BiP, HSP47, calreticulin, PDI and HSP70 protein levels are increased between 24 to 48 hours after the cells have been incubated with VPA (Figure 12. A). Previous results showed that VPA protects cells from glucosamine-induced lipid accumulation and NF-κB activation at around 18 or 24 hours of treatment (Figures 6 and 7). This suggests that the induction of chaperones, which happens at later time points, may not be responsible for the beneficial effects of VPA. In primary mouse hepatocytes, 12 to 120 hours of VPA treatment did not induce GRP78/BiP levels while the positive control, an ER stress-inducing agent tunicamycin, was able to induce GRP78 after 8 hours of treatment (Figure 12. B).

Figure 12. Valproic acid induces the expression of ER-resident chaperones in HepG2 cells but not in primary mouse hepatocytes.

A) Immunoblot analysis of protein chaperone levels in HepG2 cells. HepG2 cells were treated with 0.5 mM VPA for 0 – 96 hours. Total protein lysates were resolved by SDS-PAGE, transferred to nitrocellulose membranes and immunoblotted with antibodies against GRP78/BiP, HSP47, calreticulin, PDI or HSP70 as indicated. As a loading control, an identical blot was immunoblotted with an antibody against β-actin. **B)** Immunoblot analysis of GRP78/BiP and HSP47 in primary mouse hepatocytes for 0-120 h in the presence of 0-0.5 mM VPA or 8 h of 10 μg/ml tunicamycin (Tm).

A)

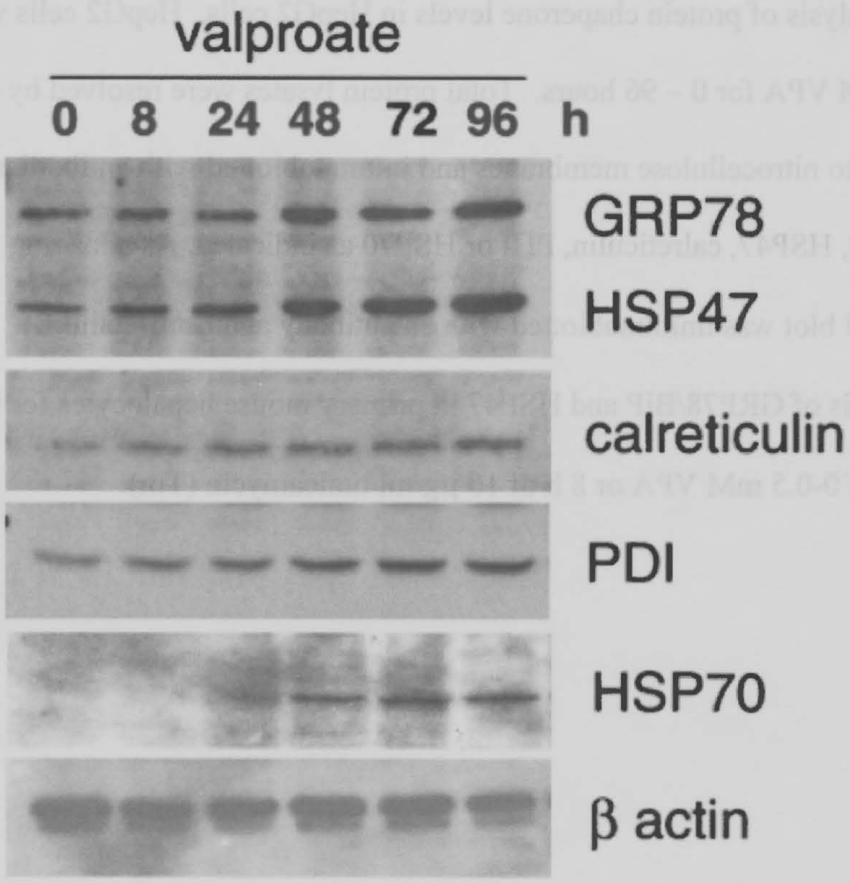

Kim *et al.* JCI 2005

B)

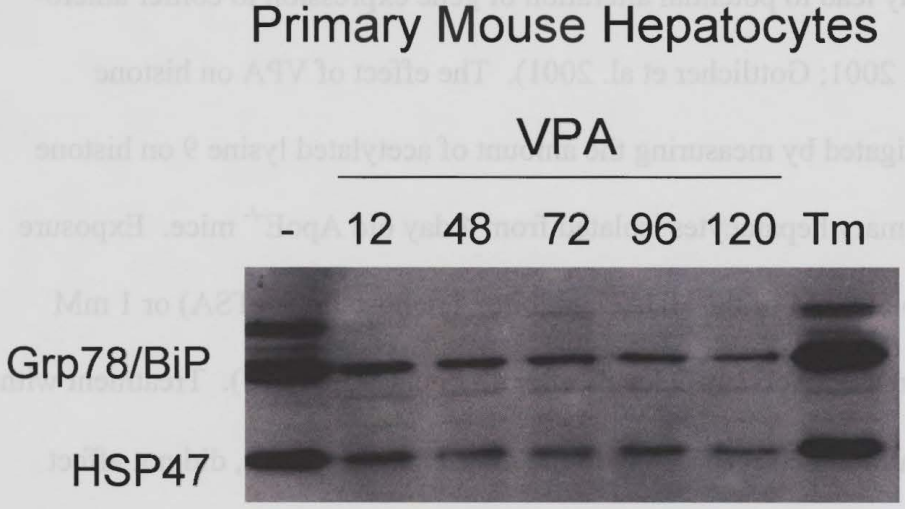
Primary Mouse Hepatocytes
VPA
- 12 48 72 96 120 Tm
Grp78/BiP
HSP47

4.3.2 Effect of valproic acid on histone deacetylase

Other groups have shown that VPA can inhibit HDAC at pharmacological concentrations and may lead to potential alteration of gene expression to confer athero-protection (Phiel et al. 2001; Gottlicher et al. 2001). The effect of VPA on histone acetylation was investigated by measuring the amount of acetylated lysine 9 on histone H3 (AcH3 lys9) in primary hepatocytes isolated from 4 day old $ApoE^{-/-}$ mice. Exposure of the cultured cells to 600 nM of the HDAC inhibitor Trichostatin A (TSA) or 1 mM VPA significantly increased AcH3 lys9 levels after 48 hours (Figure 13). Treatment with 50 μM VPA, a concentration corresponding to the mouse plasma levels, did not affect histone acetylation in primary hepatocytes (Figure 13). However, the result with 50 μM VPA is difficult to translate to its potential *in vivo* since plasma concentration of VPA does not fully represent intracellular concentration of VPA in a mouse chronically exposed to dietary VPA.

In vitro effects of VPA on histone acetylation indicate that it is possible that VPA may exert athero-protection via inhibition of HDAC.

Figure 13. Effect of valproic acid on HDAC activity.

Primary hepatocytes treated with 600 nmol/L TSA, or valproic acid (VPA) (50 μmol/L or 1 mmol/L) were resolved by SDS-PAGE and probed with antibodies specific for acetylated histone H3 (AcH3)-lys 9 or total histone H3. Immunoblots were quantified by densitometry and AcH3-lys9 was normalized to total H3 in each and plotted as a percent of control. n=3, $*P<0.05$ relative to untreated hepatocytes.

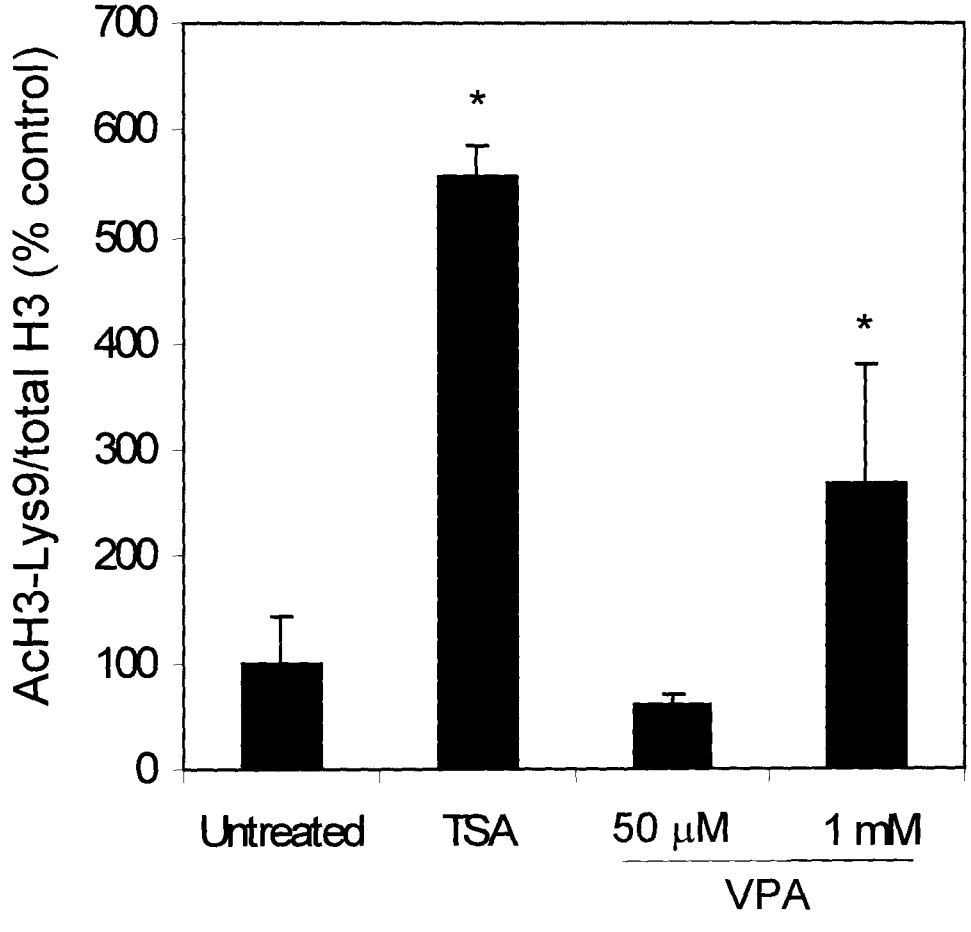
AcH3-Lys9/total H3 (% control)
700
600
500
400
300
200
100
0
*
*
Untreated
TSA
50 μM
1 mM
VPA

4.3.3 Effect of valproic acid and valproic acid derivatives on GSK-3

Several groups have suggested that the therapeutic effect of VPA requires its ability to inhibit GSK-3 activity. However, it is unclear if GSK-3 is a target of VPA or a target of enzymes upstream of GSK-3 that are modulated by VPA (Chen et al. 1999a; Eldar-Finkelman 2002; Gould et al. 2004). There are reports suggesting that VPA may inhibit GSK-3 through an indirect mechanism that is yet unknown as *in vitro* kinase assays failed to show VPA inhibiting GSK-3 at its therapeutic range (Hall et al. 2002). There is also a report suggesting that GSK-3 is unaffected by VPA in neurons (Williams et al. 2002).

In order to clearly determine if GSK-3 is a direct target of VPA, an *in vitro* cell-free kinase assay was utilized. Addition of lithium, a widely used inhibitor of GSK-3, showed dose-dependent inhibition of both α and β isoforms of recombinant GSK-3 (recGSK-3) (Figure 14. A). Using this assay system, VPA inhibited recGSK-3 in the absence of other enzymes capable of phosphorylating GSK-3, proving that VPA can directly inhibit GSK-3 (Figure 14. B). It also appears that VPA is more potent toward the β isoform than the α isoform. The effect of VPA on intracellular GSK-3 was examined by treating HepG2 cells with 0.5 mM VPA for 2-6 hours and purifying GKS-3α and β by immunoprecipitation using appropriate antibodies. Results of the kinase assay indicate that VPA can inhibit intracellular GSK-3 as well. However, VPA appears to be a more potent inhibitor in cellular systems when comparing its effect towards recGSK-3 at the same concentration (Figure 14. B and C). This potentially indicates that VPA may also be acting on proteins upstream of GSK-3 that modify GSK-3 through phosphorylation.

Figure 14. Valproic acid inhibits GSK-3α and β in both cell-free and cell culture systems.

Recombinant GSK3α and β activity in the presence of **A)** 0-50 mM lithium chloride (Li) or **B)** 0-5 mM valproic acid (VPA). The enzyme activity was determined *in vitro* by assaying the ability of the recombinant kinase to phosphorylate a synthetic substrate (p-GS2) at 30°C for 30 minutes. Quantitative values were converted to a percentage of recombinant GSK3α or β activity in the absence of inhibitor. **C)** GSK3α and β activity immunoprecipitated from HepG2 cells treated with 0.5 mM VPA for 2-6 hours. Quantitative values were converted to a percentage of recombinant GSK3α or β activity ± standard deviation in the absence of VPA. n=3, $*P<0.05$.

A. Lithium Dose Response

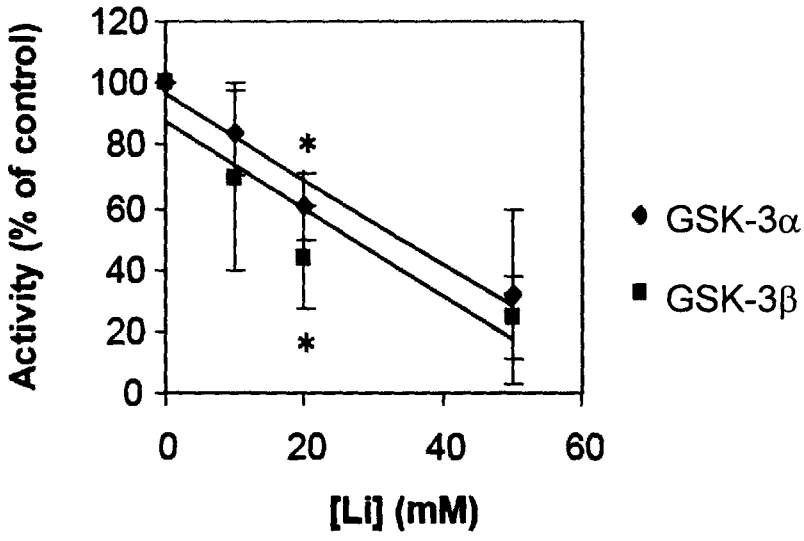

B. VPA Dose Response

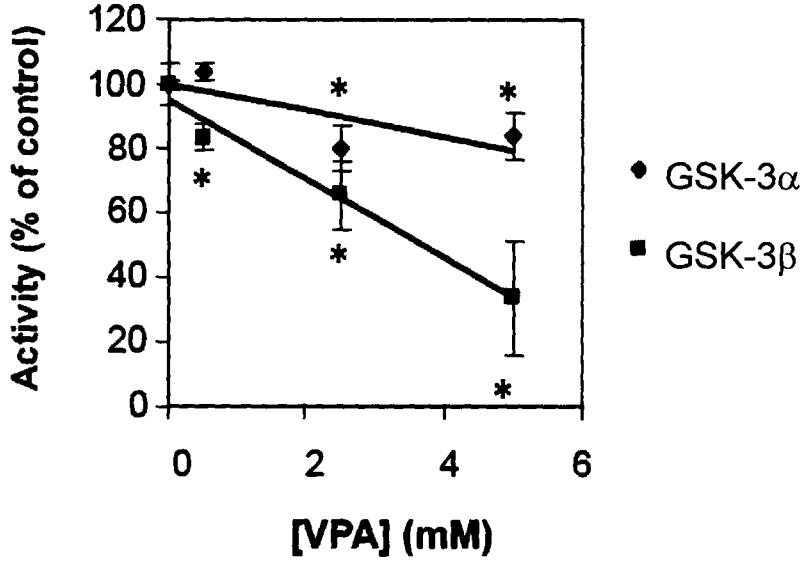

C.

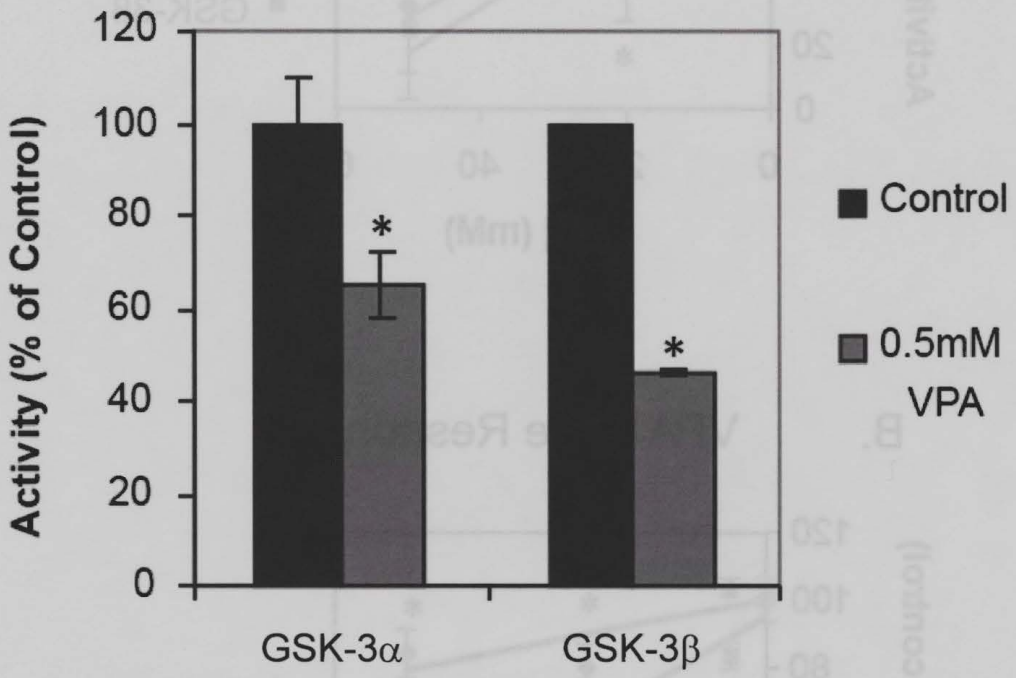
Activity (% of Control)
120
100
80
60
40
20
0
*
*
GSK-3α
GSK-3β
Control
0.5mM VPA

5 INTRODUCTION – PART II

5.1 GLYCOGEN SYNTHASE KINASE-3

5.1.1 GSK-3 isoforms and substrates

GSK-3 is a serine/threonine kinase expressed in all eukaryotic cells. It is expressed as two mammalian isoforms, GSK-3α and GSK-3β with molecular weights of 51 and 47 kDa respectively, that are each encoded by a distinct gene (Ali et al. 2001; Doble and Woodgett, 2003). GSK-3α has a glycine-rich domain at the N-terminus, which is responsible for the size difference, but both isoforms share a high degree of identity (nearly 98%) within their kinase domain (Doble and Woodgett, 2003; Jope and Johnson. 2004). Both isoforms have similar biochemical and substrate binding properties with very few exceptions. Substrates proposed to be specific for each of the isoforms include NF-κB, (GSK-3β) which regulates inflammatory pathways, and amyloid precursor protein (GSK-3α) which is linked to Alzheimer's disease (Hoeflich et al. 2000; Phiel et al. 2003). Proteins that are substrates for both isoforms include GS, caspase-3, β-catenin, microtubule associated protein Tau, and cubitus interruptus, among others involved in transcription, translation, intracellular vesicular transport, cell cycle progression, and circadian rhythm regulation (Jope and Johnson. 2004; Grimes and Jope. 2001). The broad regulatory influence of GSK-3 suggests that its activity must be carefully regulated by mechanisms customized for each substrate. GSK-3 has a peculiar

preference for primed substrates. Pre-phosphorylation at a serine or threonine residue located four residues towards the carboxy terminus of the site of GSK-3 phosphorylation increases its binding and activity by more than a thousand fold. This provides further control of GSK-3 substrate phosphorylation through priming kinases (Jope and Johnson. 2004).

5.1.2 Regulation of GSK-3

Unlike many signal transduction kinases, GSK-3 is constitutively active in resting cells. Its activity can be regulated by mitogens and growth factors including insulin, insulin-like growth factor-1, and epidermal growth factor, as well as conditions of cellular stress including heat shock, oxidative stress, and ER stress (Kockeritz et al. 2006; Jope et al. 2007). As outlined in section **1.2.2**, insulin activates the PI3K and PKB/Akt pathway to inactivate GSK-3α/β by phosphorylation at Ser21/9. In contrast, phosphorylation at Tyr279/216 has been shown to increase the activity of GSK-3α/β (Jope and Johnson. 2004; Cohen and Frame. 2001).

Access of GSK-3 to its substrates can also be regulated by intracellular localization. GSK-3 has been found in the cytosol, nucleus, and mitochondria (Jope and Johnson. 2004; Bijur and Jope. 2001). Increased nuclear GSK-3 has been linked to the stimulation of apoptosis which may be due to increased access to various transcription factors (Meares and Jope. 2007). Another important mechanism in regulating GSK-3 activity is through association with protein complexes. The regulation and

phosphorylation of β-catenin are dependent on a multi-protein Wnt signalling complex composed of Adenomatous polyposis coli (APC), Axin, and GSK-3 (Cohen and Frame. 2001). Regulation of GSK-3 through phosphorylation, cellular localization, and interaction with neighbouring proteins may allow individually tailored control of GSK-3 towards different substrates without affecting the diverse array of other cellular functions regulated by GSK-3 (Jope and Johnson. 2004).

5.1.3 GSK-3: a multi-tasking kinase

Dysregulation of GSK-3 has been associated with numerous pathological conditions, such as T1DM, T2DM, muscle hypertrophy, cancer, bipolar disorder, schizophrenia, and Alzheimer's disease (Song et al. 2002; Brownlee. 2001; Pilcher. 2003). As a result, GSK-3 has become a popular drug target. Due to the complexity of GSK-3's involvement in various cellular functions, complete inhibition of GSK-3 would likely have detrimental effects on the entire cell and perhaps to the body. An ideal GSK-3 inhibitor would therefore specifically inhibit the subset of GSK-3 involved in a particular pathway of interest. To date no such specific inhibitors have been identified.

GSK-3 was first identified as one of many enzymes capable of phosphorylating GS, the enzyme involved in the last step of glycogen synthesis (Embi et al. 1980). Constitutively active GSK-3 inhibits GS in resting cells, and insulin signalling alleviates this inhibition. Since its original discovery, numerous other essential cellular functions were found to be regulated by GSK-3. Some of the other metabolic enzymes that are substrates of GSK-3 include IRS-1, eIF2B, and pyruvate dehydrogenase (Eldar-Finkelman and Krebs. 1997; Hoshi et al. 1996; Grimes and Jope. 2001). Phosphorylation of structural proteins Tau and Amyloid-β by GSK-3 is thought to contribute to neurofibrillary tangles and senile plaque formation in relation to Alzheimer's disease (Martinez and Perez 2008). GSK-3 is also involved in regulation of apoptosis through activation of Caspase-3 and destabilization of p53 in neuronal cells and mouse embryonic fibroblasts (Song et al. 2002; Qu et al. 2004). Regulation of nuclear factor of activated T-

cells (NFAT) by GSK-3 can alter axonal growth and vertebrate development while activation of NF-κB is compulsory for embryonic hepatic development, activation of pro-inflammatory responses, and maintenance of leukaemic cell growth (Grimes and Jope. 2001; Hoeflich et al 2000; Holmes et al. 2008). Recently, much interest has been drawn to GSK-3 for its role in hematopoietic stem cell repopulation by regulating the Wnt, Hedgehog, and Notch pathways (Trowbridge et al. 2006; Doble et al. 2007).

Its multiple roles in metabolism and growth, and involvement in several pathologic conditions have drawn a great deal of interest to GSK-3 (Cohen and Frame. 2001; Frame and Cohen, 2001). There is ongoing research to characterize this enzyme and elucidate its relevance as a therapeutic target.

Figure 15. Effect of GSK-3 on inflammatory and apoptotic pathways.

Glycogen synthase kinase (GSK)-3 can stimulate inflammatory responses through the activation of Nuclear factor-κB (NF-κB), which induces transcription of pro-inflammatory molecules, including tumour necrosis factor (TNF)-α, Interleukin (IL)-1β, and IL-12. GSK-3 also inhibits cAMP response element binding protein (CREB), leading to decreased production of anti-inflammatory molecule IL-10. GSK-3 can regulate apoptosis by inducing caspase-3 and -9 activation, and through destabilization of p53.

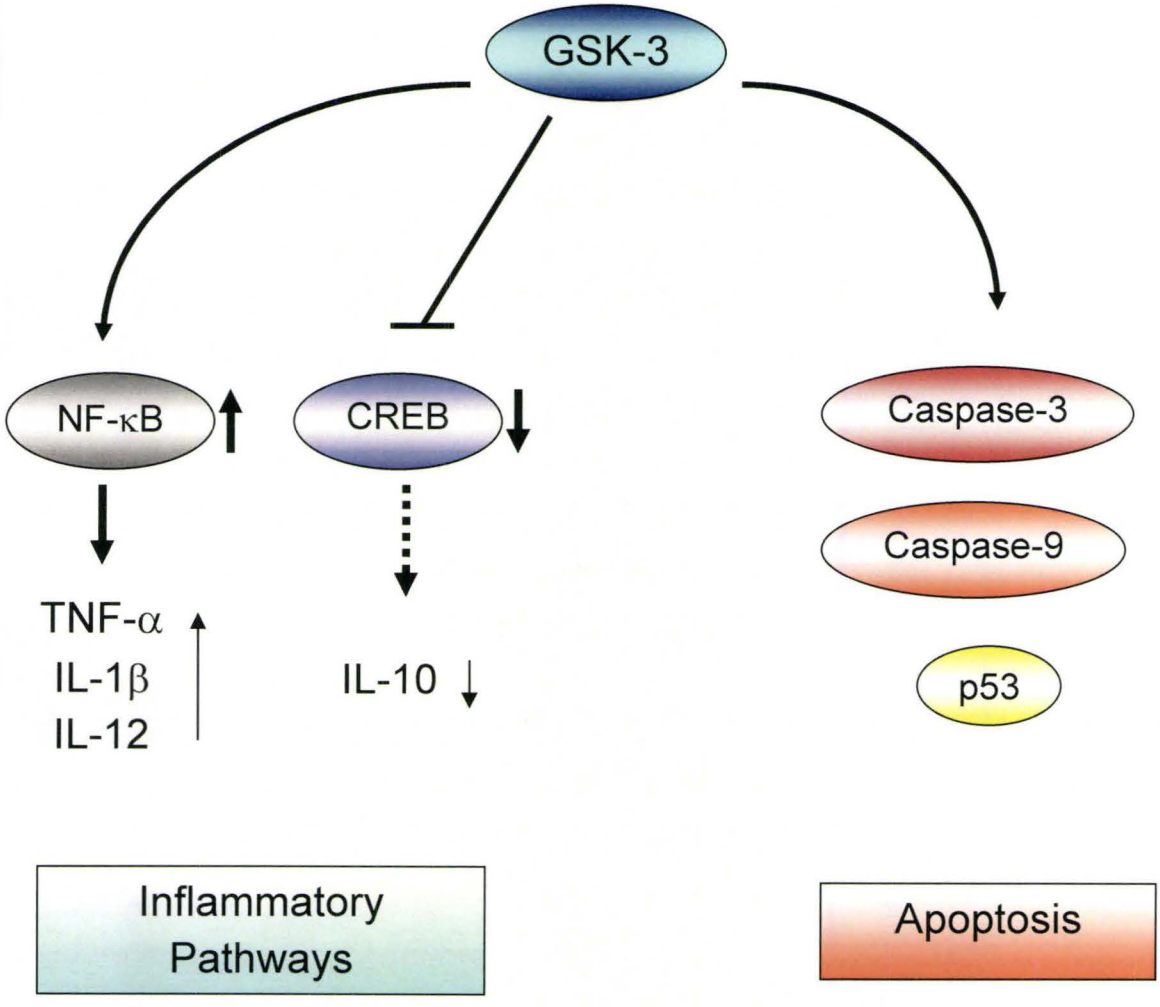
GSK-3
NF-κB
CREB
Caspase-3
Caspase-9
p53
TNF-α
IL-1β
IL-12
IL-10
Inflammatory Pathways
Apoptosis

5.1.4 GSK-3 and Diabetes Mellitus

The inability of cells to properly respond to insulin may result from increased GSK-3 activity which can lead to inhibition of GS even when plasma glucose levels are high (Eldar-Finkelman et al. 1999). Diabetic mice display decreased inhibitory phosphorylation at Ser21/9 of GSK-3α/β, resulting in hyper-stimulation of the enzyme (Lajoie et al. 2004; Laviola et al. 2001). Elevated expression and activity levels of GSK-3 have been reported in human muscle and mouse β-cells under hyperglycemic conditions (Liu et al. 2008; Nikoulina et al. 2000; Eldar-Finkelman et al. 1999; Ciaraldi et al. 2006). Direct involvement of GSK-3 in diabetes associated cellular dysfunction has been shown through a study demonstrating that GSK-3 inhibitors can lower blood glucose levels by stimulating glycogen synthesis in skeletal muscles (Nikoulina et al. 2002). These findings support the relevance of GSK-3 in insulin signalling and suggest that controlled inhibition of GSK-3 may improve cellular and molecular defects in diabetic individuals.

6 RATIONALE, HYPOTHESIS, AND OBJECTIVES OF THE STUDY-PART II

6.1 RATIONALE

In the previous study, I demonstrated that VPA protects cultured cells from glucosamine-induced unesterified cholesterol accumulation and NF-κB activation (Figures 6 and 7). The protective effect of VPA is also extended to an *in vivo* model of atherosclerosis of which dietary VPA supplementation significantly reduced hepatic steatosis and atherosclerotic lesion development in aortic root in hyperglycemic $ApoE^{-/-}$ mice (Figures 10 and 11). There are several intracellular pathways through which VPA may act to exert an anti-atherogenic effect. Exposure to VPA has been shown to induce the expression of chaperones such as HSP70, GRP78/BiP, HSP47, PDI, and calreticulin in rat neurons and HepG2 cells (Kim et al. 2005; Wang et al. 1999). However, no significant increase in ER chaperones was detected in HepG2 and primary mouse hepatocytes after 18 hours of treatment, which is the time point when the reduction of glucosamine-induced unesterified cholesterol accumulation and NF-κB activation were observed. Another potential mechanism by which VPA may affect atherogenesis is by regulation of gene expression patterns through the inhibition of HDACs (Phiel et al. 2001; Gottlicher et al. 2001). HDAC inhibitors have been shown to inhibit vascular SMC proliferation but actually exacerbate atherosclerosis in a LDL receptor-deficient mouse model (Okamoto et al. 2006; Choi et al. 2005).

There are several reports that therapeutic efficacy of VPA may lie in its ability to inhibit GSK-3 (Chen et al. 1999a; Gould et al. 2004; Eldar-Finkelman. 2002). The involvement of GSK-3 in the activation of inflammatory pathways and apoptosis has been suggested by various groups (Hoeflich et al. 2000; Song et al. 2002; Brewster et al. 2006; Bijur and Jope. 2001). There have been many studies conducted to elucidate the role of GSK-3 in relation to Diabetes, Alzheimer's disease, and bipolar disorder, however not much is known about its role in atherogenesis. Therefore, we carried out experiments to determine if GSK-3 is an *in vivo* target of VPA. We further investigated the involvement of GSK-3 in hyperglycemia-induced accelerated atherogenesis using a library of compounds based on the structure of VPA and GSK-3knock-out cell lines.

6.2 HYPOTHESIS

VPA reduces hyperglycemia/glucosamine-associated lipid accumulation and atherosclerosis by inhibition of GSK-3 activity.

6.3 OBJECTIVES

6.3.1 Overall objective

To characterize the role of GSK-3α and β in diabetic atherogenesis using a variety of GSK-3 inhibitors in cultured cells and a mouse model of hyperglycemia-accelerated atherosclerosis.

6.3.2 Specific objectives

1. To identify VPA derivatives with the ability to reduce glucosamine-induced lipid accumulation *in vitro*

2. To determine the involvement of GSK-3 in glucosamine-induced lipid accumulation using GSK-3 deficient MEFs

3. To determine the effect of VPA supplementation on hepatic GSK-3 *in vivo*

4. To determine the effect of dietary supplementation with a more potent GSK-3 inhibitor, EBA, on atherosclerosis and hepatic steatosis in hyperglycemic $ApoE^{-/-}$ mice

7 EXPERIMENTAL PROCEDURES

7.1 MATERIALS

VPA derivative compounds were synthesized and provided by Dr. Fred Capretta (McMaster University, Hamilton, ON). VPA, glucose, mannitol, glucosamine, tunicamycin, A23187, and filipin were purchased from Sigma (Oakville, ON). GSK-3 inhibitor II, 3-(3-carboxy-4-chloroanilino)-4-(3-nitrophenyl) maleimide, was purchased from CalBiochem (La Jolla, CA) and SB415286 was purchased from Sigma. The anti-KDEL monoclonal antibody (SPA-827), which recognizes GRP78/BiP was purchased from StressGen Biotechnologies (Victoria, BC). Monoclonal antibodies recognizing total GSK-3 were purchased from Upstate (Charlottesville, VA). Anti-β actin (AC-15) antibodies were purchased from Sigma.

7.2 CELL LINES AND CULTURE CONDITIONS

7.2.1 Human Hepatocarcinoma cells

HepG2 were obtained from American Type Culture Collection (ATCC; Rockville, MD) and cultured in Dulbecco's Modified Eagle's Medium (Life Technologies, Burlington, ON) containing 10% FBS (HyClone, Logan, UT). Cells were maintained in a humidified incubator at 37°C with 5% CO_2.

7.2.2 Primary Mouse Hepatocytes

One to twelve days old mice were anaesthetized with CO_2 prior to cervical dislocation and immersed in 70% ethanol for 5 minutes in a biological hood. The liver

was exposed and 500 mg of the tissue was removed using autoclaved scissors and forceps. The tissue was washed twice in Hank's solution (Hank's balanced salt solution with penicillin and streptomycin). The tissue was diced into small pieces and washed three times with Hank's solution. 1 ml of 1x trypsin was added and the mixture was incubated in a water bath for 30 minutes at 37°C. The supernatant was removed and 5 ml of DMEM with 10% FBS was added. The trypsinized liver tissue was pipeted up and down ten times and let stand for 10 minutes. The cell suspension was collected and plated onto a dish to grow in a humidified incubator at 37°C with 5% CO_2.

7.2.3 Mouse Embryonic Fibroblasts

Wild type, GSK-3$\alpha^{-/-}$, and GSK-3$\beta^{-/-}$ MEFs were generous gifts from Dr. B. Doble and Dr. J. Woodgett (McMaster University and University of Toronto, ON). The cells were cultured in DMEM (Life Technologies, Burlington, ON) containing 10% FBS and maintained in a humidified incubator at 37°C with 5% CO_2.

7.3 IMMUNOBLOT ANALYSIS

Total protein lysates (40 μg) from cultured cells were solubilized in SDS-PAGE sample buffer (50 mM Tris, pH 6.8, 2% SDS, 10% glycerol, 0.01% bromophenol blue and 50 mM dithiothreitol) and separated on SDS-polyacrylamide gels under reducing conditions. Proteins were transferred to nitrocellulose membranes (Bio-Rad) using a wet transfer apparatus (Bio-Rad). Membranes were blocked overnight with 5% non-fat milk

in 1X TBST (50 mM Tris; pH 7.5, 120 mM NaCl, 0.02% Tween20). After incubation with the appropriate primary and HRP-conjugated secondary antibodies (Life Technologies, Burlington, ON), the membranes were developed using the Immobilon Western chemiluminescent HRP substrate (Millipore, Billerica, MA) and Kodak X-OMAT Blue XB-1 film (Perkin-Elmer). Protein levels were normalized using an anti-β-actin immunoblot on the same nitrocellulose membrane.

7.4 GSK-3 KINASE ASSAY

15 μM synthetic GSK-3 substrate (phospho-Glycogen Synthase Peptide-2) and 0.5 μCi/μL [γ^{32}P] ATP were added to recombinant GSK-3α/β in a reaction mixture containing, 20 mM MOPS (pH7.4), 50 μM EDTA, 2.5 mM Mg acetate, 5 mM $MgCl_2$, 5 mM β-glycerol phosphate, 1 mM EGTA, 0.25 mM Na_3VO_4, 0.25 mM DTT, and 35 μM ATP in a total volume of 40 μL. 4 mM VPA derivatives or 2 μL of DMSO were added to GSK-3 before the substrate and ATP were added. GSK-3 with 20 mM Li (a GSK-3 inhibitor) and 20 μM of SB415286 (a synthetic GSK-3 inhibitor) were used as positive controls. The samples were placed on ice immediately following a 30 min incubation at 30°C. 30 μL sample was spotted onto Whatman P81 phosphocellulose paper, washed 3X with 0.75% *o*-phosphoric acid and once with acetone. Scintillation counting was used to determine ^{32}P incorporation on to the substrate.

7.5 UNESTERIFIED CHOLESTEROL STAINING

The accumulation of unesterified cholesterol was determined by filipin staining (Kruth, 1984). MEFs, grown on cover slips, were treated with 4 mM VPA or 200 nM GSK-3 inhibitor II for 1 hour and challenged with glucosamine (5 mM) for an additional 18 hours. Cells were washed three times with Medium 1 (150 mM NaCl, 5 mM KCl, 1 mM $CaCl_2$, 20 mM HEPES pH 7.4, 2 g/l glucose), fixed with 4% paraformaldehyde for 20 minutes at room temperature and then incubated for 2 hours with 50 μg/ml filipin in Medium 1 at room temperature. Cells were washed three times with Medium 1 and then filipin bound unesterified cholesterol complexes were visualized by fluorescence microscopy with excitation at 335-385 nm (emission at 420 nm). The accumulation of unesterified cholesterol in primary mouse hepatocytes was quantified using Sigma Scan. The intensity threshold was set up at a range of 234-249 for measuring all intensities in the fluorescence pictures taken. The average intensity per cell surface area was plotted for each treatment group.

7.6 ANALYSIS OF UNESTERIFIED CHOLESTEROL STAINING USING FLUORESCENCE-ACTIVATED CELL SORTING (FACS)

MEFs were grown on 100 mm diameter culture dishes to 50% confluency and treated with drugs as described above. The cells were washed three times with Medium 1, fixed in 4% paraformaldehyde at room temperature for 20 minutes, and incubated with 50 μg/ml filipin for 2 hours at room temperature. Cells were washed with PBS,

trypsinized, and stored in PBS containing 1% FBS. Filipin fluorescence was measured using a FACS VantageSE™ instrument with 350-70 nm UV laser and emission detection at 420-460 nm. Data were analyzed using FlowJo software (Treestar).

7.7 RNA ISOLATION AND QUANTITATIVE REVERSE TRANSCRIPTASE-POLYMERASE CHAIN REACTION (qRT-PCR)

Total RNA was extracted from MEFs using commercially available TRIzol^{R} Reagent (Invitrogen, Carlsbad, CA) following the manufacturer's instructions. The concentration and purity of the RNA were determined by measuring the absorbance at 260 and 280 nm. cDNA was synthesized from 2 μg of total RNA using a commercially available kit (High Capacity cDNA Reverse Transcription Kit, Applied Biosystems) following the guidelines provided by the manufacturer. Real-Time PCR was conducted at the following settings: one cycle at 95 °C for 10 min followed by 40 cycles at 95 °C for 1 min and at 60 °C for 1 min using a GeneAmp 7300 sequence detection system (Applied Biosystems, Foster City, CA) and SYBR^{R} GreenER qPCR SuperMix for ABI PRISM^{R} (Invitrogen, Carlsbad, CA). Template cDNAs were amplified using the following primers: for SREBP-2, the forward primer was 5'-GCGTTCTGGAGACCATGGA-3' and reverse was 5'-ACAAAGTTGCTCTGAAAACAAATCA-3', the amplicon size is 131 bp; for 3-hydroxy-3-methyl-glutaryl-CoA reductase (HMG-CoAR), the forward primer was 5'-CTTGTGGAATGCCTTGTGATTG-3' and reverse was 5'-AGCCGAAGCAGCACATGAT-3', the amplicon size is 76 bp; for β-actin, the forward

primer was 5'-GGCACCACACCTTCTACAATG-3' and the reverse was 5'-GGGGTGTTGAAGGTCTCAAAC-3'; the amplicon size is 132 bp. The standard method was used for the quantification of the mRNA expression in the livers using β-actin as a normalization control gene.

7.8 MOUSE MODELS

Five week old female ApoE$^{-/-}$ (B6.129P2-ApoE^{tm1Unc}) mice were placed on a defined chow diet (Harlan Teklad, TD92078) and randomly divided into two groups (n=24/group). To induce hyperglycemia, one group was injected intraperitoneally with multiple low doses of STZ (40 mg/kg) as previously described (Bowes et al. 2009). After one week, one third of the mice in each group were switched to the control diet supplemented with 625 mg/kg 2-ethylbutyric acid (TD07473) and another third to the control diet supplemented with 312.5 mg/kg 2-ethylbutyric acid (TD07427). All mice had unrestricted access to both food and water throughout the study. Mice were sacrificed at 15 weeks of age and blood and tissues were collected for further analysis. The above experiment was repeated using control diet, 625 mg/kg VPA diet (TD02165), and 312.5 mg/kg 2-ethylbutyric acid (TD07427). The McMaster University Animal Research Ethics Board approved all procedures.

Figure 16. *In vivo* study design

Five week old female ApoE$^{-/-}$ (B6.129P2-ApoE^{tm1Unc}) mice were placed on a defined chow diet and randomly divided into three groups (n=18/group). To induce hyperglycemia, one group was injected intraperitoneally with multiple low doses of streptozotocin (STZ) (40 mg/kg) or the same volume of citrate buffer. After one week, one third of the mice in each group were switched to **A**) the control diet supplemented with 312.5 mg/kg 2-ethylbutyric acid (EBA) (TD07427) and another third to 625 mg/kg EBA (2X EBA) (TD07473), or **B)** the control diet supplemented with 312.5 mg/kg EBA (TD07427) and another third to 625 mg/kg VPA (TD02165).

A.

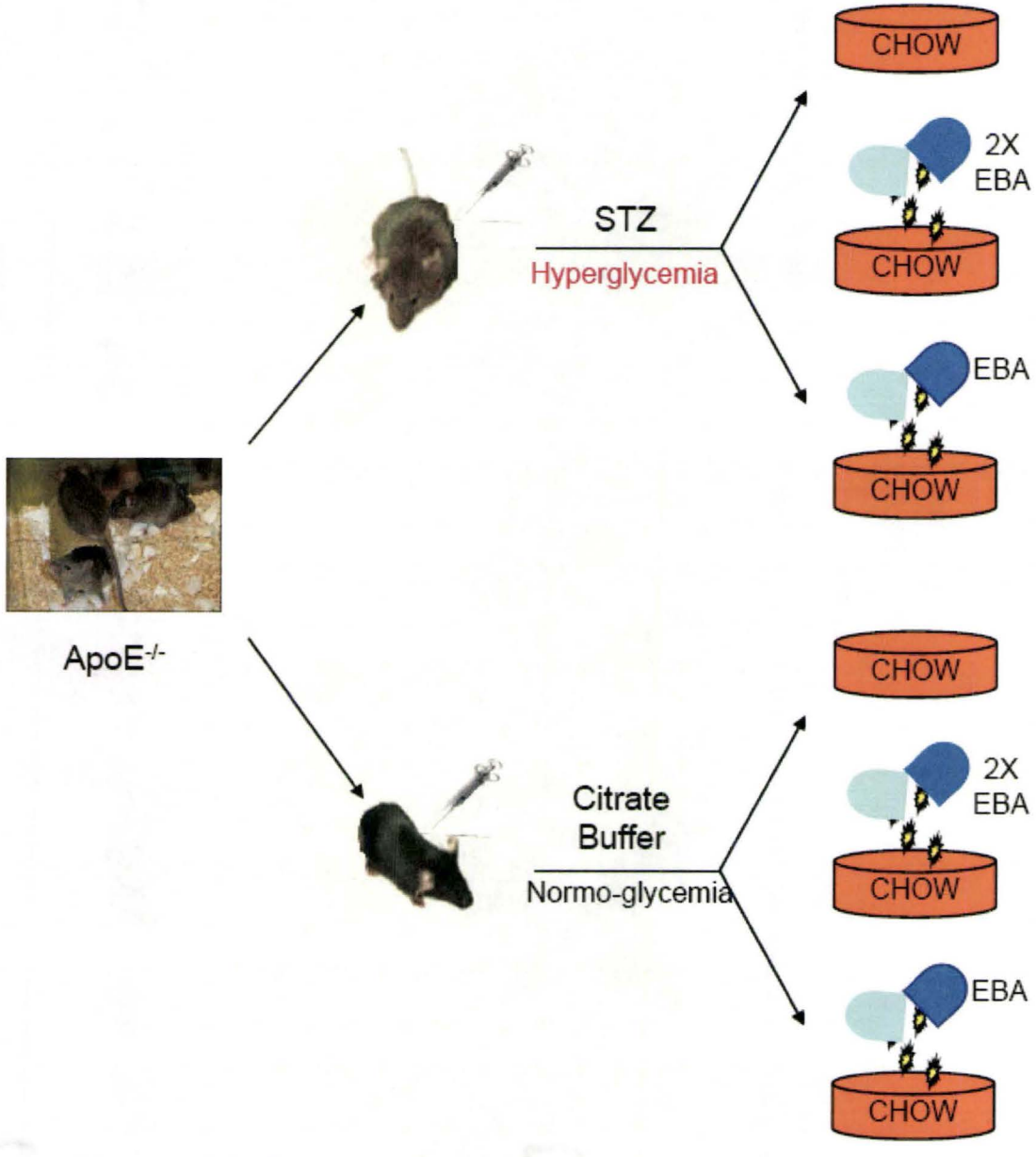
CHOW
2X
EBA
CHOW
STZ
Hyperglycemia
EBA
CHOW
ApoE-/-
CHOW
2X
EBA
CHOW
Citrate
Buffer
Normo-glycemia
EBA
CHOW

B.

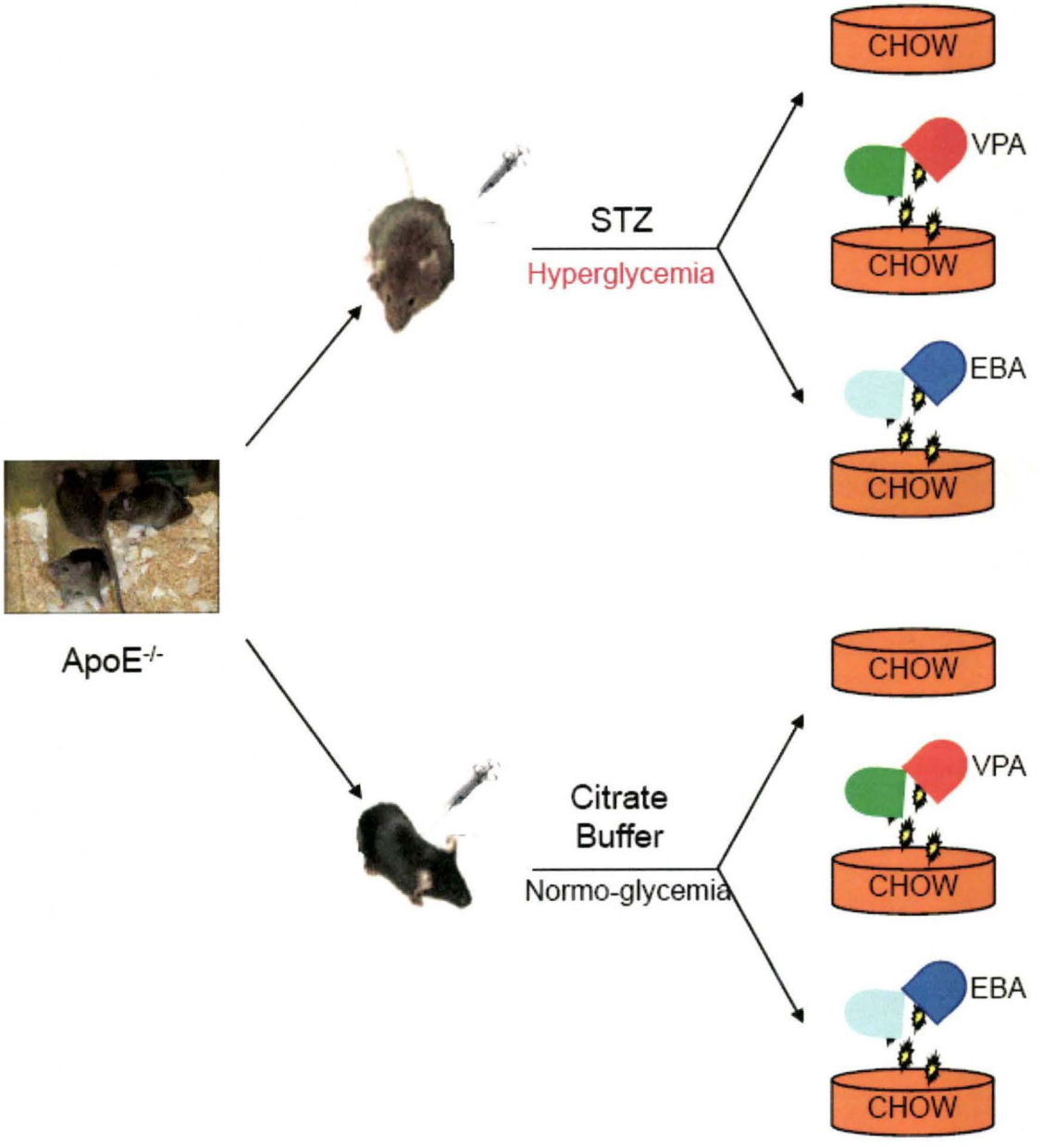
CHOW
VPA
CHOW
EBA
CHOW
STZ
Hyperglycemia
ApoE-/-
CHOW
VPA
CHOW
EBA
CHOW
Citrate
Buffer
Normo-glycemia

7.9 PLASMA ANALYSIS

Random and fasting (12 hours) whole blood glucose levels were measured using a DEX glucometer (Bayer). Plasma glucose and lipid levels were determined in non-fasted mice using the colorimetric diagnostic kits for total cholesterol, triglycerides and glucose purchased from Thermal DMA Inc. Plasma VPA concentrations were determined using an AxSYM system (Abbott Laboratories, Mississauga, ON).

7.10 SUDAN IV STAINING OF AORTAE

Descending aortae were collected and periadventitial tissue was removed. Clean aortae were washed in 70% ethanol, stained with 0.5% Sudan IV for 15 minutes, destained with 80% ethanol and rinsed with dH_2O. After longitudinal dissection, stained aortae were mounted *en face* and the images were visualized using a microscope (Yokogawa CSU22 on an Olymus BX61WI base) and captured using a CCD colour video camera (Sony).

7.11 AORTIC LESION ANALYSIS

After the mice were euthanized, hearts were flushed with 1X PBS and perfusion-fixed with 10% neutral buffered formalin. After removal, hearts, including the aortic root were cut transversely and embedded in paraffin. Serial sections (4 μm) of aortic root were

collected on pre-coated glass slides for measurement of lesion size (hematoxylin and eosin staining) or immunohistochemical staining (Paigen et al. 1987). The Vectastain ABC System was used for immunohistochemical analysis. Sections were stained with primary antibodies and visualized using appropriate biotinylated secondary antibodies and Nova Red. Non-specific staining was controlled for using a similar section and pre-immune IgG. Images were captured with a CCD color video camera (Sony) and analyzed using Northern Exposure (Empix) and WCIF ImageJ software.

7.12 LIPID STAINING

Liver cryo-sections, 7 μm thick, were collected on slides and fixed in Formal calcium for 30 minutes. Neutral lipids were visualized in sections that were rinsed and incubated in a saturated, filtered solution of Oil red O (Sigma) for 7 minutes. After rinsing with H_2O, nuclei were stained with hematoxylin for 10 seconds, and slides were mounted in Crystalmount (Werstuck et al. 2001). Relative amounts of lipid staining were quantified using Image J Software.

7.13 IMMUNOBLOT ANALYSIS OF MOUSE LIVER PROTEINS

Cytoplasmic proteins were isolated from mouse liver using a NE-PER Kit (Pierce, Rockford, IL) and total protein lysates were prepared from mouse liver solubilized in RIPA buffer. Equivalent amounts of total protein were separated on SDS-polyacrylamide

gels and transferred to nitrocellulose membranes (BioRad, Hercules, CA), as described previously (Kim et al. 2005, Werstuck et al. 2001). After incubation with the appropriate primary and HRP-conjugated secondary antibodies, the membranes were developed using the Immobilon Western chemiluminescent HRP substrate (Millipore, Billerica, MA). Specific bands were quantified using ImageQuant (GE Healthcare).

7.14 GSK-3β KINASE ACTIVITY ASSAY

GSK-3β was immunoprecipitated from total protein lysates prepared from mouse liver with antibodies directed against the β isoform (2 μg, BD Bioscience). 15 μM synthetic GSK-3 substrate (phospho-Glycogen Synthase Peptide-2) and 0.5 μCi/μL [γ^{32}P] ATP were added to immunoprecipitated GSK-3α/β in reaction mixture containing, 20 mM MOPS (pH7.4), 50 μM EDTA, 2.5 mM Mg acetate, 5 mM $MgCl_2$, 5 mM β-glycerol phosphate, 1 mM EGTA, 0.25 mM Na_3VO_4, 0.25 mM DTT, and 35 μM ATP in a total volume of 40 μL. The samples were placed on ice immediately following a 30min incubation at 30°C. 30 μL sample was spotted onto Whatman P81 phosphocellulose paper, washed 3X with 0.75% *o*-phosphoric acid and once with acetone. Scintillation counting was used to determine ^{32}P incorporation on to the substrate.

7.15 STATISTICAL ANALYSIS

Results are presented as the mean ± standard deviation. ANOVA was used for repeated measurements of the same variable, and Duncan's multiple range t-test was used to assess differences between experimental groups and controls. Probability values of <0.05 were considered statistically significant.

8 RESULTS

8.1 EFFECTS OF VALPROIC ACID DERIVATIVES

8.1.1 Screening valproic acid derivatives to identify novel GSK-3 inhibitors

In previous studies, I have demonstrated that VPA can protect HepG2 cells and HASMCs from glucosamine-induced lipid accumulation and NF-κB activation (Figures 6 and 7). I also observed that VPA can reduce hepatic steatosis and lesion development in aortic root in hyperglycemic ApoE$^{-/-}$ mice (Figures 10 and 11). In order to identify the pathway(s) responsible for anti-atherogenic effect of VPA, the effect of VPA on ER chaperone levels, HDAC activity, and GSK-3 activity was examined *in vitro*. We narrowed down the potential target to GSK-3 based on our results showing VPA inhibition of GSK-3 and other reports suggesting its involvement in apoptosis and inflammation. To establish the role of GSK-3 in atherogenesis, a library of compounds were synthesized based on the structure of VPA through collaboration with Dr. Alfredo Capretta (McMaster University) (Figure 17).

Eleven VPA derivatives, along with established inhibitors of GSK-3 (LiCl and SB415286), were tested for their ability to inhibit recGSK-3. 4 mM, the concentration at which VPA showed approximately 50% inhibition of GSK-3β, was chosen for the initial kinase assay. When the inhibition at 4 mM of a compound was greater than 75%, the effect of reduced concentrations was also tested. The kinase assay showed several compounds that were able to inhibit both isoforms to various degrees, such as C14 and C15 (Figure 17). Several compounds with preferential inhibition towards the β isoform

were discovered, including 4 mM of C3, C5, C9, C11, and 0.5 mM C15. 4 mM of C1, C2, C6, C8, and C13 did not affect either GSK-3α or β (Figure 18).

A dose response curve was used to determine the potency of one of the novel inhibitors of GSK-3. The most promising compound C15 is 2-ethylbutyric acid (EBA) which differs from VPA by the absence of two methyl groups. EBA almost completely inhibited both GSK-3 isoforms at 2.5 mM concentration and showed higher potency towards the β isoform at 0.5 mM concentration (Figure 19).

Figure 17. Valproic acid and valproic acid derivatives.

The structure of valproic acid (VPA) and VPA derivatives synthesized and purified in Dr. Capretta's laboratory (Werstuck et al. 2004). C12 is VPA and C15 is 2-ethylbutyric acid (EBA).

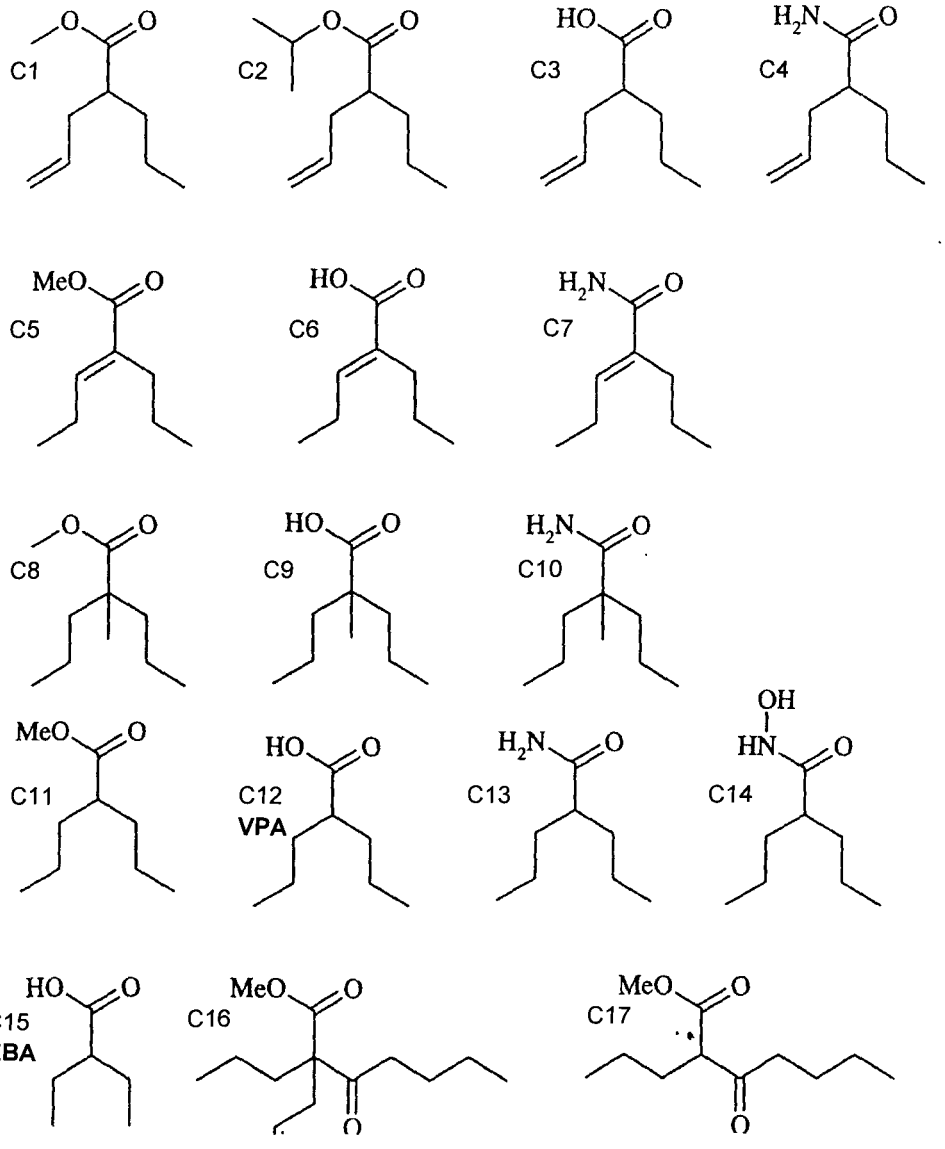
C1
C2
C3
C4
C5
C6
C7
C8
C9
C10
C11
C12
VPA
C13
C14
C15
EBA
C16
C17

Figure 18. Effect of valproic acid derivatives on recombinant GSK-3.

Recombinant GSK3α and β activity in the presence of 4 mM VPA derivatives (C1-C15), 20 mM lithium chloride (Li) or 20 μM SB415286. The enzyme activity was determined *in vitro* by assaying the ability of the recombinant kinase to phosphorylate a synthetic substrate (p-GS2) at 30°C for 30 minutes. Quantitative values were converted to a percentage of recombinant GSK3α or β activity in the absence of testing compound or inhibitor. n=3, $*P<0.05$

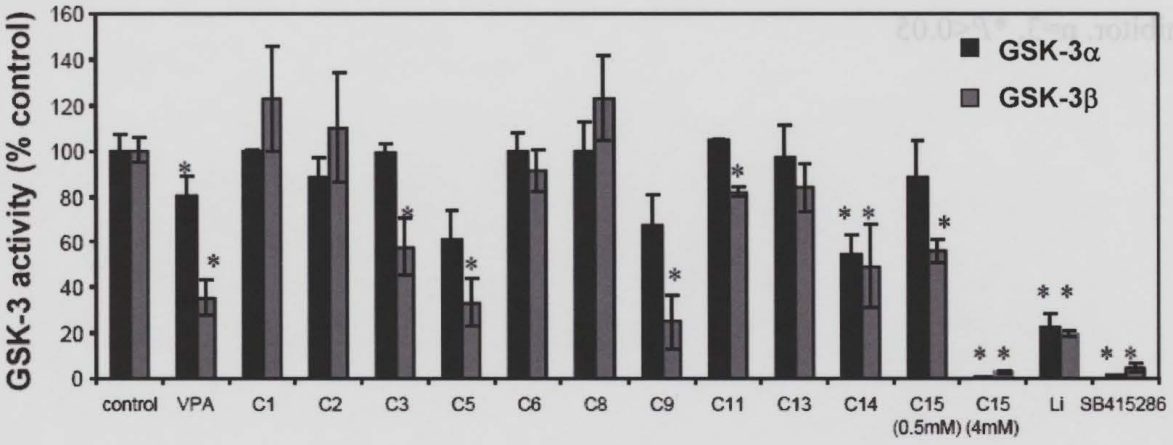
GSK-3 activity (% control)
160
140
120
100
80
60
40
20
0
GSK-3α
GSK-3β
control
VPA
C1
C2
C3
C5
C6
C8
C9
C11
C13
C14
C15 (0.5mM)
C15 (4mM)
Li
SB415286

Figure 19. Dose response curve for inhibition of recombinant GSK-3α and β by 2-ethylbutyric acid.

Recombinant GSK3α **(A)** and β **(B)** activity in the presence of 0-5 mM valproic acid (VPA) or 2-ethylbutyric acid (EBA). The enzyme activity was determined *in vitro* by assaying the ability of the recombinant kinase to phosphorylate a synthetic substrate (p-GS2) at 30°C for 30 min. Quantitative values were converted to a percentage of recombinant GSK3α or β activity in the absence of inhibitor. n=3, $*P<0.05$

A. GSK-3α

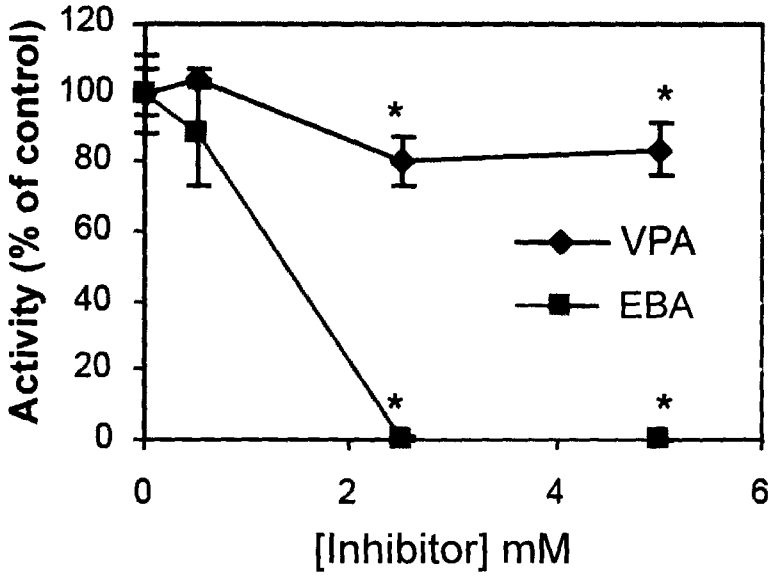

B. GSK-3β

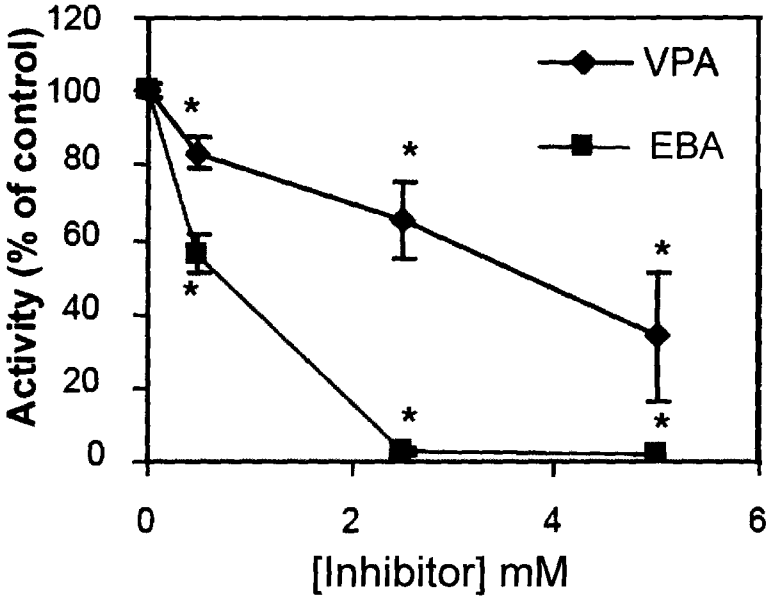

8.1.2 Testing valproic acid derivatives for their effect on glucosamine-induced lipid accumulation

To determine the role of GSK-3 in glucosamine-induced lipid accumulation, the novel GSK-3 inhibitors were tested for their ability to inhibit unesterified cholesterol accumulation induced by glucosamine in primary mouse hepatocytes using filipin staining. In comparison to untreated primary mouse hepatocytes, 30 mM glucose treatment for 18 hours showed a modest increase in fluorescence while 10 mM glucosamine treatment induced significantly higher fluorescence levels, indicating accumulation of unesterified cholesterol in these cells (Figure 20. A and B). Pretreatment with 1 and 4 mM VPA gave dose dependent protection against glucosamine-induced unesterified cholesterol accumulation which is consistent with previous findings (Figure 20) (Kim et al. 2005). While C1 showed no significant effect, EBA, C3, C5, and C11 demonstrated various degrees of reduction in glucosamine-induced unesterified cholesterol accumulation. The compounds that showed an ability to inhibit GSK-3α or β were also able to block glucosamine-induced unesterified cholesterol accumulation as observed in VPA, C3, C5, C11, and C15 (EBA) (Figure 20). Consistently, C1, the compound which had no inhibitory effect on GSK-3, did not reduce glucosamine-induced lipid accumulation. This suggests that there is an association between the ability of a compound to inhibit GSK-3 and the ability to decrease glucosamine-induced unesterified cholesterol accumulation. EBA, the most potent inhibitor of GSK-3 among VPA derivatives, was chosen to be tested for its efficacy in preventing hyperglycemia-induced atherosclerosis in our *in vivo* mouse model.

Figure 20. Effect of valproic acid derivatives on glucosamine-induced unesterified cholesterol accumulation.

A) Primary mouse hepatocytes were pretreated with 0 or 4 mM of indicated compounds for 1 hour and challenged with 0 or 10 mM glucosamine (GlcN) for an additional 18 hours. Cells were stained with filipin and fluorescence was examined by fluorescence microscopy with excitation at 335-385 nm and emission at 420 nm. **B)** The fluorescence was quantified using SigmaScan. $^{**}P<0.05$ relative to control, $^{*}P<0.05$ relative to GlcN treatment. N > 4000 cells

A)

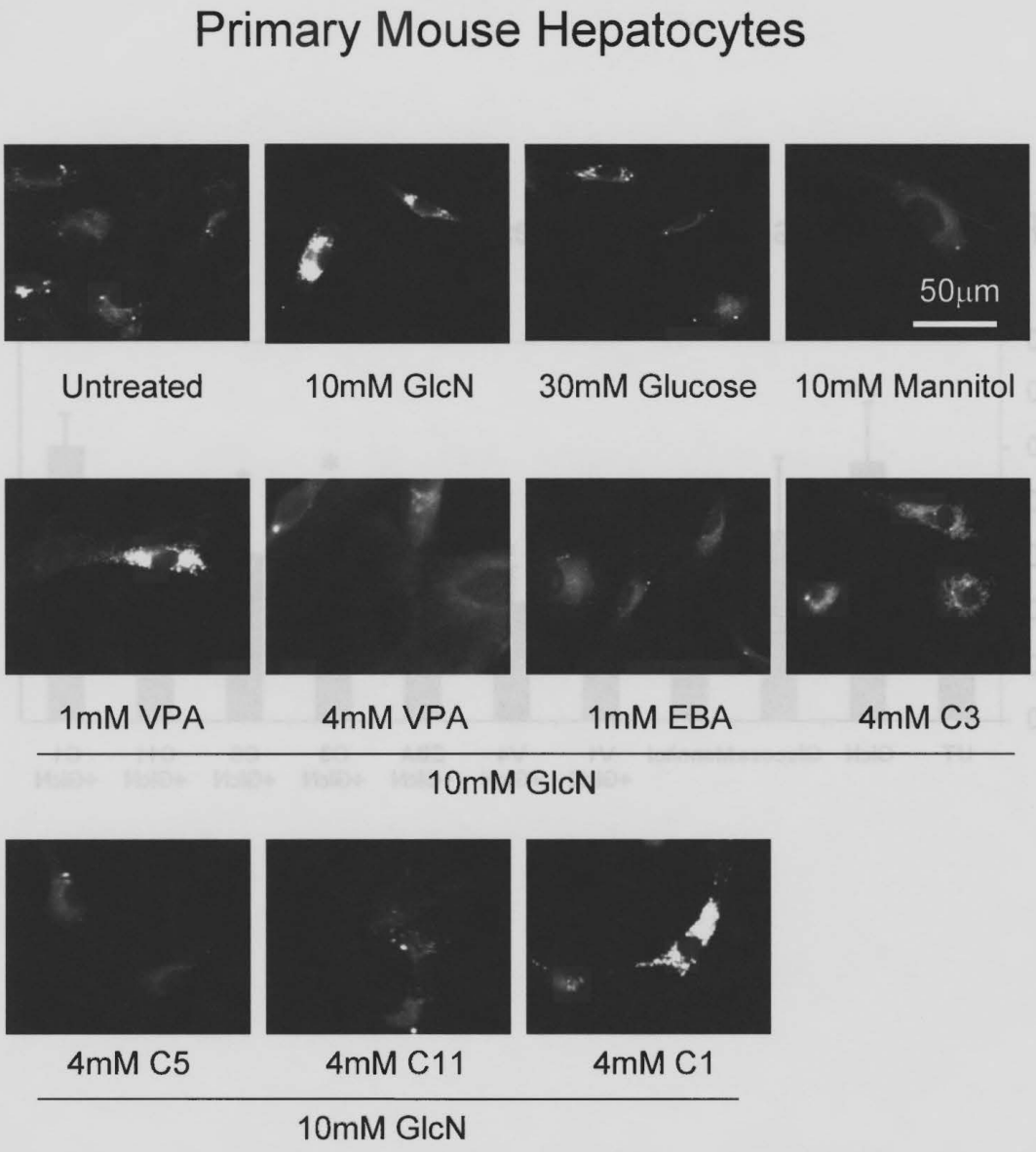
Primary Mouse Hepatocytes
50μm
Untreated
10mM GlcN
30mM Glucose
10mM Mannitol
1mM VPA
4mM VPA
1mM EBA
4mM C3
10mM GlcN
4mM C5
4mM C11
4mM C1
10mM GlcN

B)

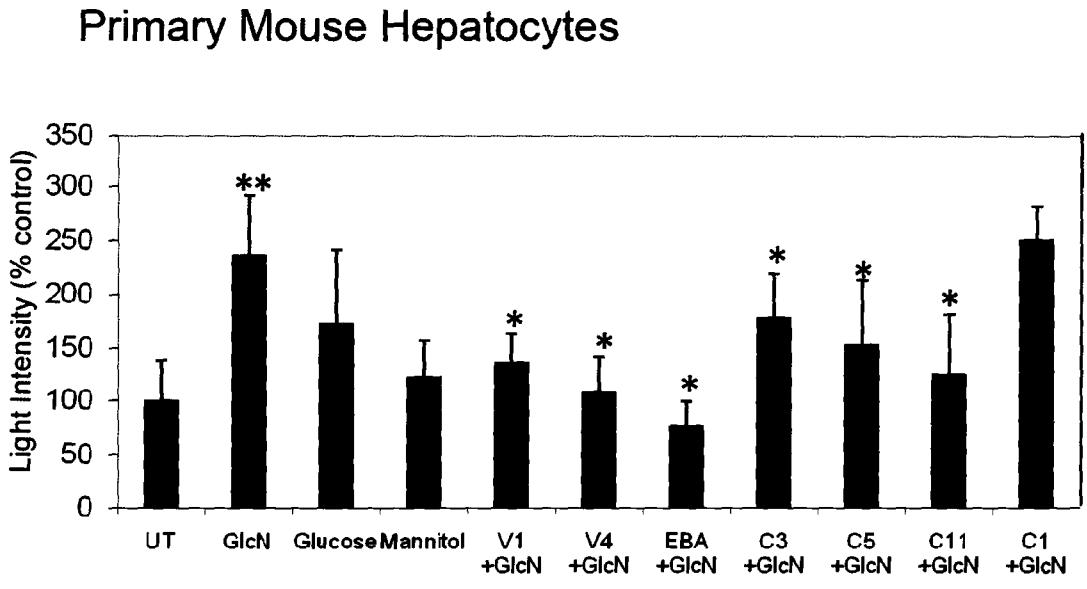
Primary Mouse Hepatocytes
Light Intensity (% control)
350
300
250
200
150
100
50
0
**
*
*
*
*
*
*
UT
GlcN
Glucose
Mannitol
V1 +GlcN
V4 +GlcN
EBA +GlcN
C3 +GlcN
C5 +GlcN
C11 +GlcN
C1 +GlcN

8.2 EFFECT OF GSK-3 DEFICIENCY ON GLUCOSAMINE-INDUCED LIPID ACCUMULATION

8.2.1 Verification of GSK-3 deficiency in knock-out MEFs

Small molecule inhibitors are a valuable tool for testing the involvement of an enzyme in cellular and physiological pathways. However, small molecule inhibitors often affect other intracellular pathways, and thus, it is hard to interpret the results from these experiments and to distinguish between different pathways that may be responsible for the protective effect. One of the other ways to determine the involvement of a gene is by using a knock-out (KO) cell line. Further analyses of the role of GSK-3α/β in glucosamine-induced lipid accumulation was performed using GSK-3α or β deficient MEFs generated by Drs. Bradley Doble and Jim Woodgett.

Upon the receipt of the KO cell lines, I verified knock-out of specific genes using an antibody against total GSK-3. Immunoblot analysis confirmed that GSK-3α KO cells only contain the β isoform of GSK-3 and GSK-3β KO only contains the α isoform (Figure 21).

Figure 21. Verification of GSK-3α and β knock-out in mouse embryonic fibroblasts. Immunoblot analysis of GSK-3α and β protein levels in wild-type (WT), GSK-3$\alpha^{-/-}$ ($\alpha^{-/-}$), and GSK-3$\beta^{-/-}$ ($\beta^{-/-}$) mouse embryonic fibroblasts (MEFs). MEFs were grown to 80% confluency and harvested using 4X SDS loading buffer. 25 μg of total protein lysates were resolved by SDS-PAGE, transferred to nitrocellulose membranes and immunoblotted with antibodies against total GSK-3.

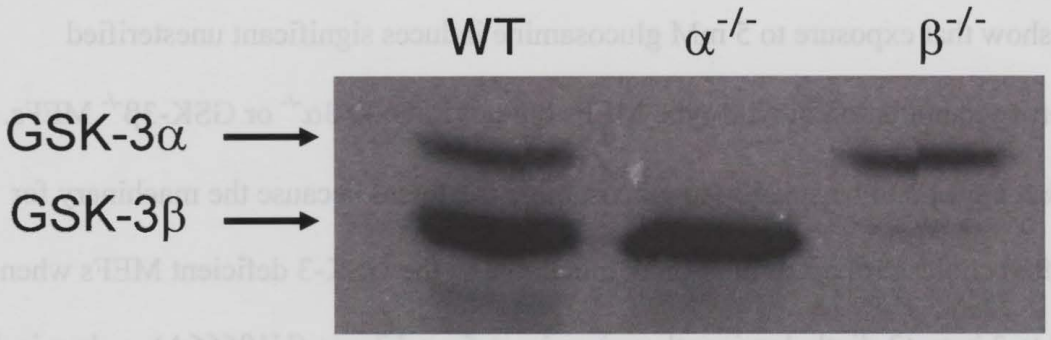
WT
α-/-
β-/-
GSK-3α
GSK-3β

8.2.2 GSK-3 deficiency reduces glucosamine-induced lipid accumulation in MEFs

I have established that elevated levels of glucosamine can promote unesterified cholesterol accumulation in specific cell types including HepG2 cells (Figures 4 and 6) (Kim et al. 2005). Next, the potential role of GSK-3 activity in this response was determined using the GSK-3 deficient MEFs. Filipin staining of MEFs treated with glucosamine was analyzed using FACS and fluorescence microscopy (Figure 22). Results show that exposure to 5 mM glucosamine induces significant unesterified cholesterol accumulation in wild-type MEFs but not in GSK-3$\alpha^{-/-}$ or GSK-3$\beta^{-/-}$ MEFs. This effect appears to be specific to glucosamine treatment because the machinery for unesterified cholesterol accumulation is functional in the GSK-3 deficient MEFs when exposed to 3 beta-(2-diethylaminoethoxy) androst-5-en-17-one (U18666A), a chemical that induces cholesterol biosynthesis by blocking intracellular trafficking of cholesterol (Underwood et al. 1996) (Figure 23). These findings suggest that both the α and β GSK-3 isoforms are required for glucosamine-induced unesterified cholesterol accumulation.

Figure 22. Effect of GSK-3 deficiency on glucosamine-induced cholesterol accumulation

Wild-type, GSK-3$\alpha^{-/-}$, and GSK-3$\beta^{-/-}$ MEFs were challenged with 0 or 5 mM glucosamine (GlcN) for 18 hours. Cells were stained with filipin for 2 hours at room temperature and fluorescence was examined by **A**) fluorescence activated cell sorting (FACS) and **B**) fluorescence microscopy with excitation at 335-385 nm and emission at 420 nm. For FACS, >10,000 cells were analyzed from each treatment group using excitation wavelengths of 350-370 nm and emission detection at 420-460 nm. The data was analyzed using FlowJo software (Treestar).

A.

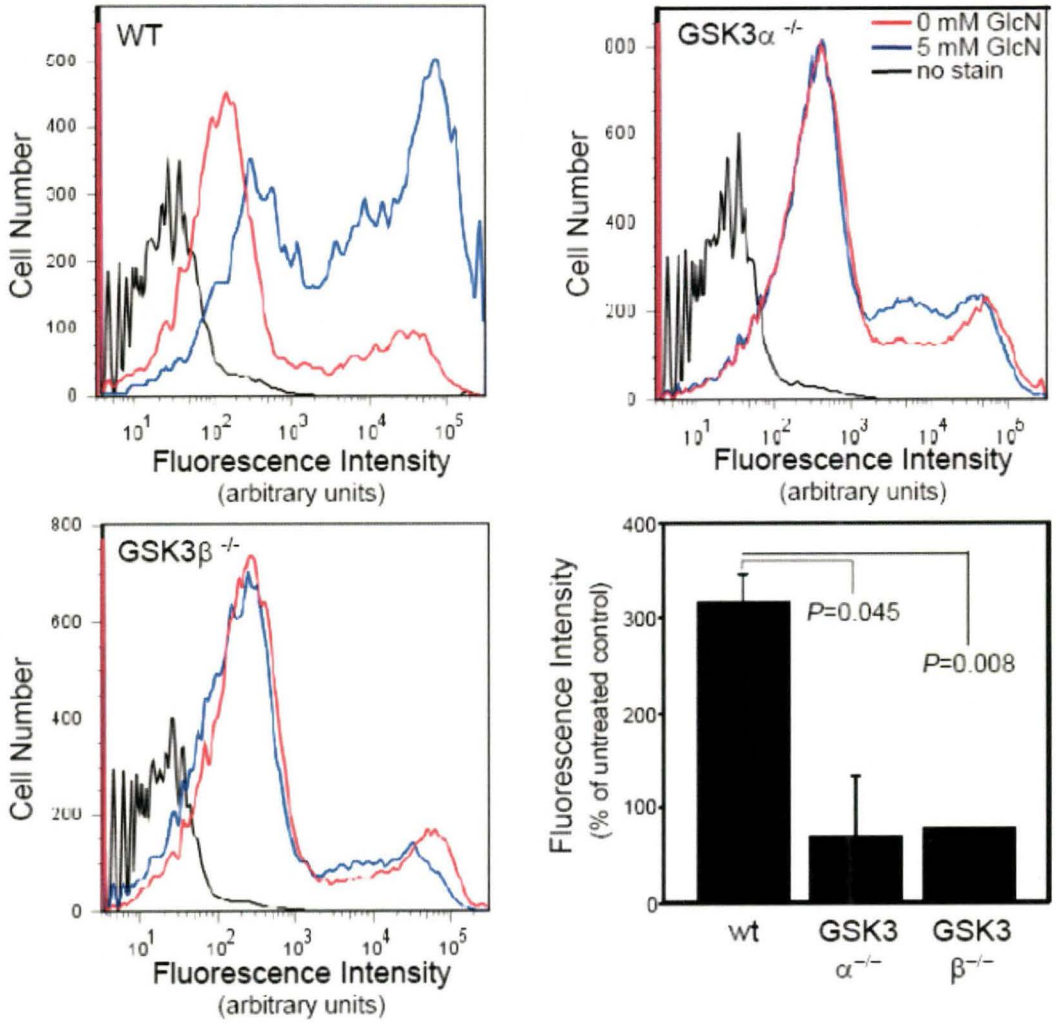
WT
GSK3α -/-
GSK3β -/-
0 mM GlcN
5 mM GlcN
no stain
Cell Number
Fluorescence Intensity
(arbitrary units)
Fluorescence Intensity
(% of untreated control)
P=0.045
P=0.008
wt
GSK3 α-/-
GSK3 β-/-

B.

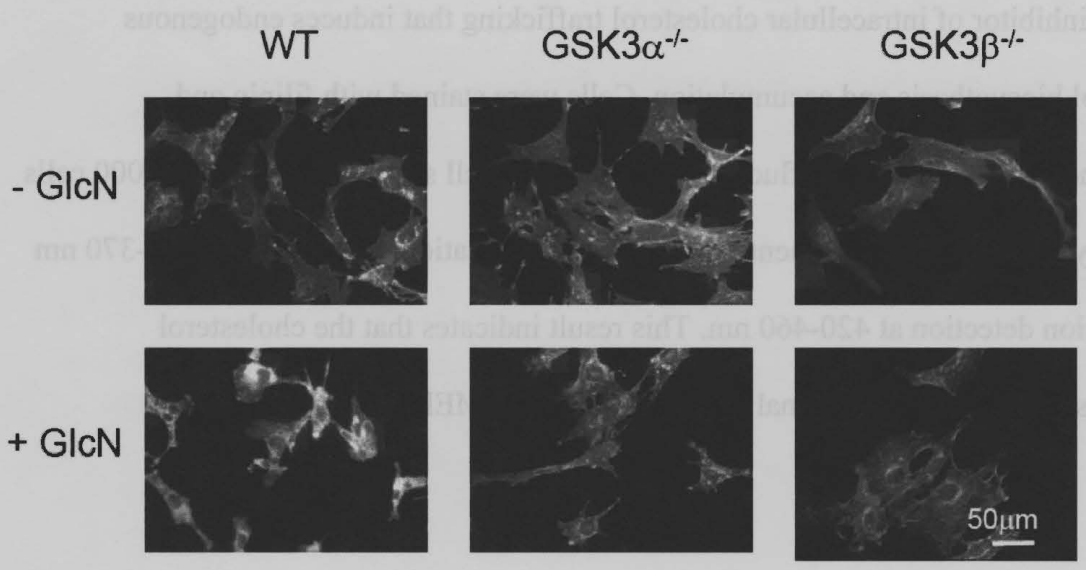

Figure 23. Effect of GSK-3 deficiency on U18666A-induced cholesterol accumulation.

Wild-type, GSK-3$\alpha^{-/-}$ and GSK-3$\beta^{-/-}$ MEFs were exposed to 2 μg/mL 3 beta-(2-diethylaminoethoxy) androst-5-en-17-one (U18666A) for 18 hours. U18666A is a small molecule inhibitor of intracellular cholesterol trafficking that induces endogenous cholesterol biosynthesis and accumulation. Cells were stained with filipin and fluorescence was examined by fluorescence activated cell sorting (FACS). >10,000 cells were analyzed from each treatment group using an excitation wavelength at 350-370 nm and emission detection at 420-460 nm. This result indicates that the cholesterol biosynthesis pathway is functional in GSK-3 deficient MEFs.

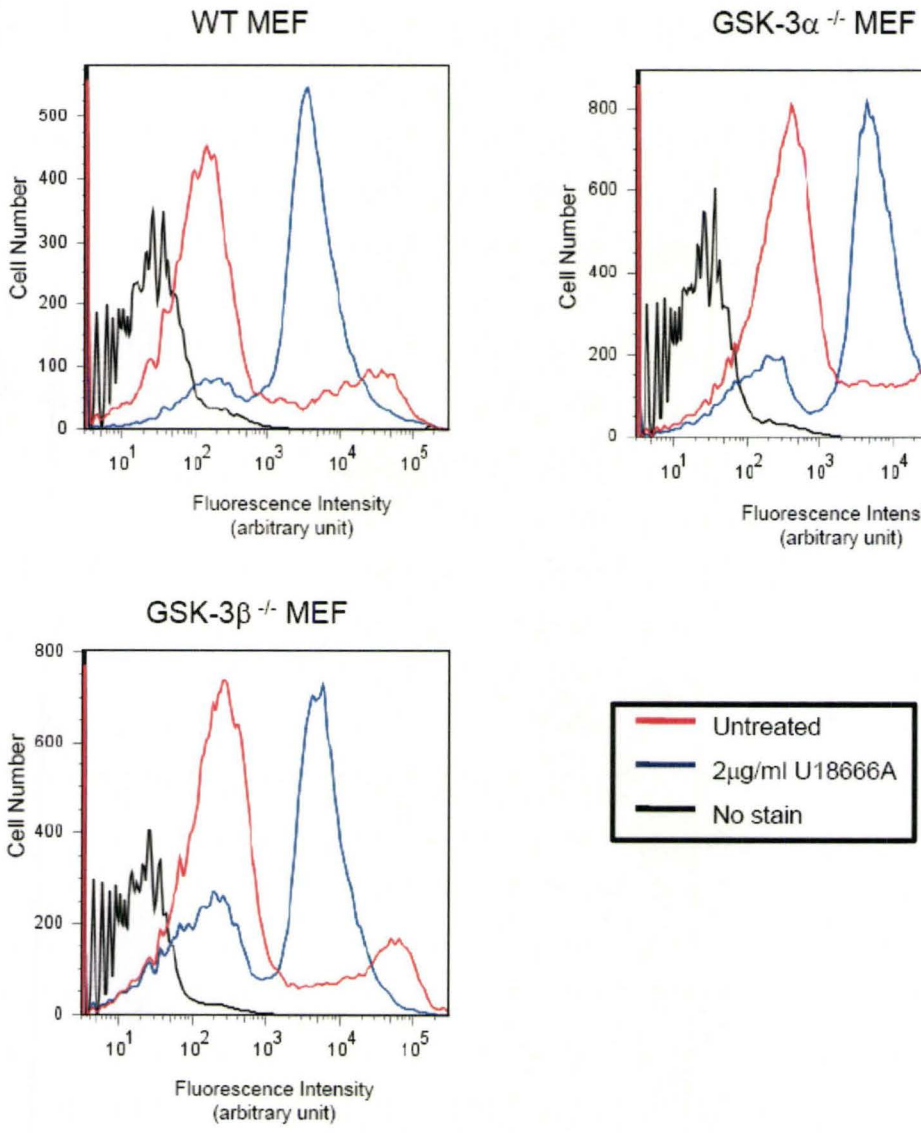
WT MEF
GSK-3α -/- MEF
GSK-3β -/- MEF
Cell Number
Fluorescence Intensity
(arbitrary unit)
Untreated
2μg/ml U18666A
No stain

8.2.3 Inhibition of GSK-3 using small molecules reduces glucosamine-induced lipid accumulation in wild-type MEFs

I have previously shown that VPA can inhibit both recombinant and intracellular GSK-3α/β activity (Figure 14). I have also shown that VPA and other GSK-3 inhibitors attenuate glucosamine-associated unesterified cholesterol accumulation in cultured HASMC and HepG2 cells (Figure 20) (Kim et al. 2005; Bowes et al. 2009 supplementary data). Here I examined the effect of VPA and a potent maleimide-based GSK-3 inhibitor on glucosamine-induced cholesterol accumulation in wild-type MEFs. FACS analysis of filipin stained wild-type MEFs indicates that glucosamine-induced unesterified cholesterol accumulation is significantly lower in cells pretreated with VPA or GSK-3 Inhibitor II (Figure 24). This result is consistent with my previous findings suggesting that GSK-3 activity plays a role in glucosamine-associated unesterified cholesterol accumulation.

Figure 24. Effect of GSK-3 inhibition on glucosamine-induced lipid accumulation. Wild-type MEFs were challenged with 0 or 5 mM glucosamine (GlcN) in the presence of 4 mM valproic acid (VPA) or 200 μM GSK-3 inhibitor II. Cells were stained with filipin and analyzed by **A**) FACS and **B**) fluorescence microscopy. For FACS, >10,000 cells were analyzed from each treatment group using excitation wavelengths of 350-370 nm and emission detection at 420-460 nm.

A.

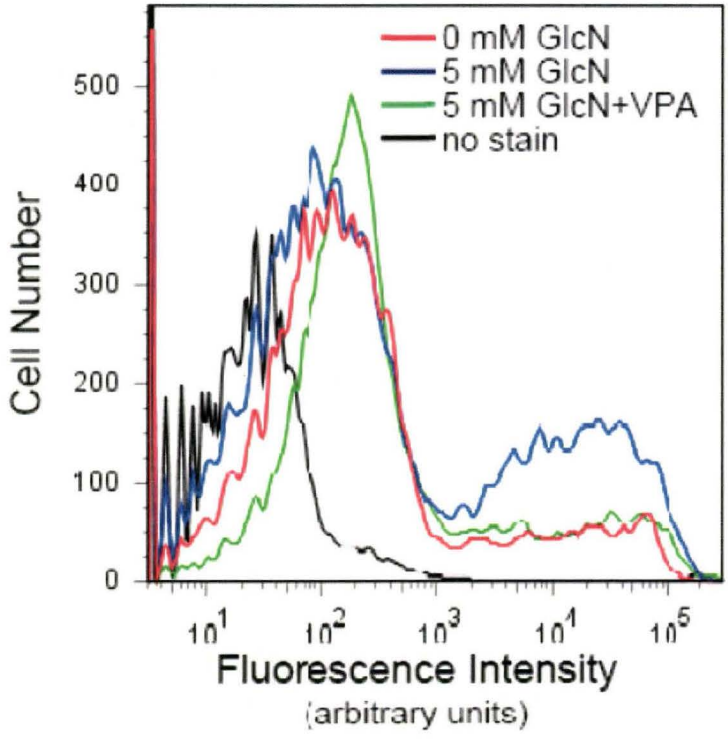
0 mM GlcN
5 mM GlcN
5 mM GlcN+VPA
no stain
Cell Number
500
400
300
200
100
0
10^1
10^2
10^3
10^4
10^5
Fluorescence Intensity
(arbitrary units)

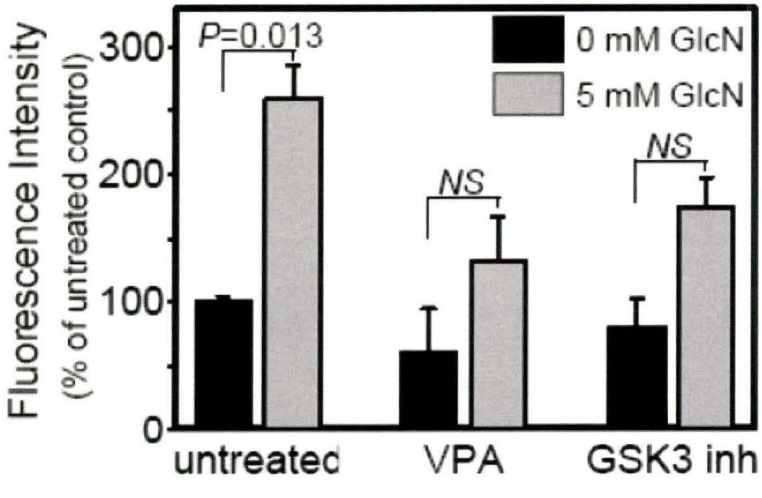
P=0.013
0 mM GlcN
5 mM GlcN
NS
NS
Fluorescence Intensity
(% of untreated control)
300
200
100
0
untreated
VPA
GSK3 inh

B.

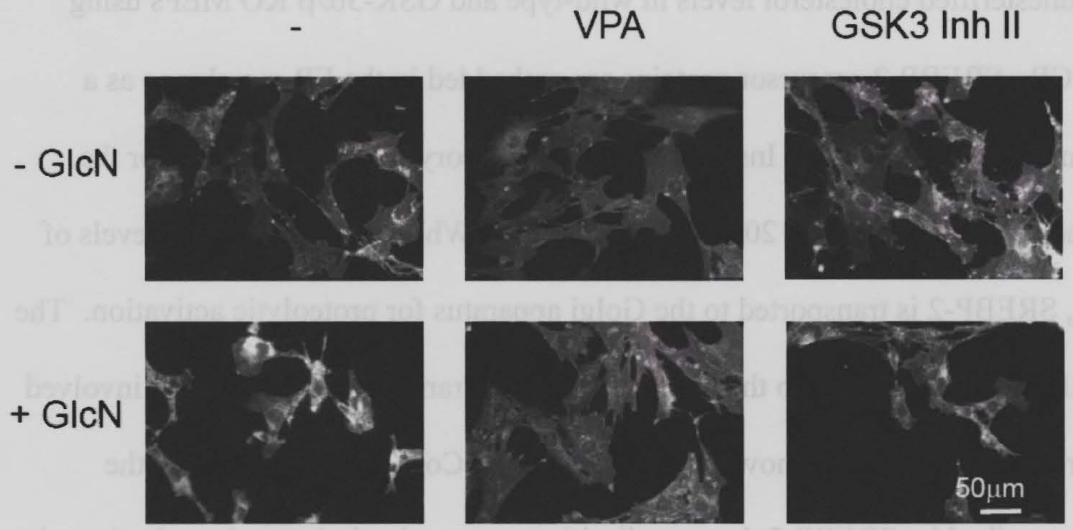

8.3 EFFECT OF GSK-3 DEFICIENCY ON STEROL REGULATORY ELEMENT BINDING PROTEIN TRANSCRIPTION LEVELS

I have shown that deficiency or inhibition of GSK-3α or β interferes with glucosamine-induced unesterified cholesterol accumulation in MEFs using filipin staining. In order to elucidate possible mechanism(s) by which GSK-3 is affecting cholesterol metabolism in these cells, I examined the transcription levels of genes regulating unesterified cholesterol levels in wild-type and GSK-3α/β KO MEFs using real-time PCR. SREBP-2 precursor proteins are embedded in the ER membrane as a protein complex with SCAP and Insig, which act as sensory proteins that monitor the levels of cholesterol (Yang et al. 2002; Rawson 2003). When Insig senses low levels of cholesterol, SREBP-2 is transported to the Golgi apparatus for proteolytic activation. The active SREBP-2 translocates into the nucleus to initiate transcription of proteins involved in cholesterol biosynthesis (Raghow et al. 2008). HMG CoA Reductase, one of the enzymes transcribed by SREBP-2, is a rate-limiting enzyme in cholesterol synthesis and is often used as an indication of increased biosynthesis of cholesterol (Rawson 2003).

Transcripts encoding SREBP-2 were doubled in wild-type MEFs when treated with glucosamine but this elevation was not seen in either of the GSK-3 KO cells under the same condition (Figure 25). There was a slight increase in the transcription levels of HMG CoA Reductase with glucosamine treatment in wild-type cells but the levels were not significantly different from untreated controls. These results indicate that GSK-3α

and β signal through SREBP-2 to increase unesterified cholesterol levels upon treatment with glucosamine.

Figure 25. Effects of glucosamine treatment on the cholesterol biosynthetic pathway.

Quantification of mRNA levels of sterol regulatory element binding protein (SREBP)-2 and 3-hydroxy-3-methyl-glutaryl-CoA reductase (HMG CoA R) using quantitative RT-PCR in wild-type (WT), GSK-3$\alpha^{-/-}$ and GSK-3$\beta^{-/-}$ MEFs treated with 5mM glucosamine (GlcN) for 18 hours. Total RNA was extracted from the cells and real-time PCR was conducted using SYBR GreenER (Applied Biosystems). β-actin mRNA levels were used as an internal control. n=3

A. SREBP mRNA levels

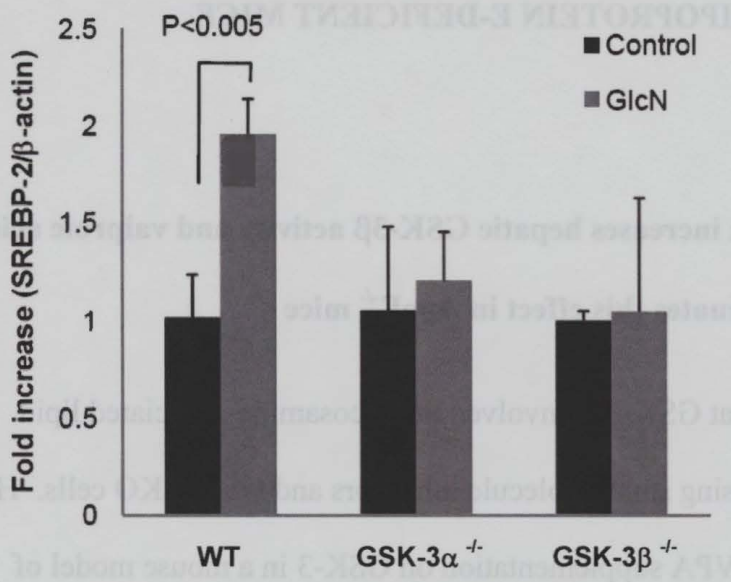

B. HMG CoA Reductase mRNA levels

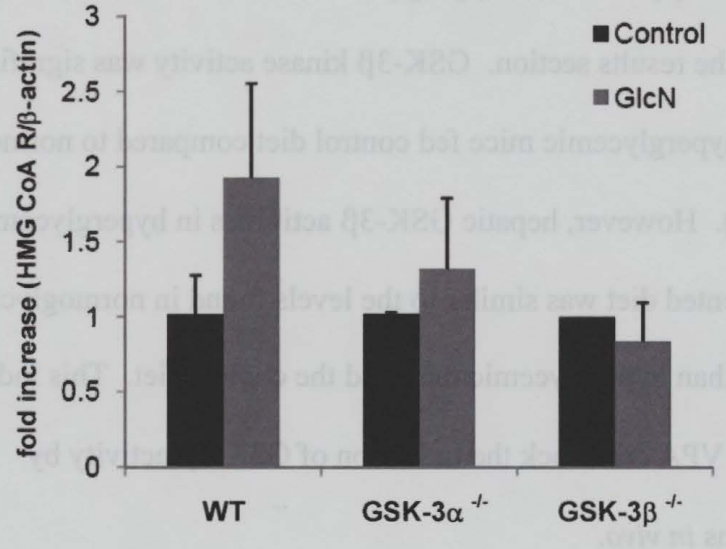

8.4 EFFECTS OF VALPROIC ACID SUPPLEMENTATION ON GSK-3 ACTIVITY IN APOLIPOPROTEIN E-DEFICIENT MICE

8.4.1 Hyperglycemia increases hepatic GSK-3β activity and valproic acid supplementation attenuates this effect in ApoE$^{-/-}$ mice

I have shown that GSK-3 is involved in glucosamine-associated lipid accumulation *in vitro* using small molecule inhibitors and GSK-3 KO cells. Here, I examined the effect of VPA supplementation on GSK-3 in a mouse model of hyperglycemia-induced atherosclerosis. GSK-3β was immunoprecipitated from hepatic protein lysates from normoglycemic and hyperglycemic mice to determine its kinase activity as described in the results section. GSK-3β kinase activity was significantly elevated in the liver of hyperglycemic mice fed control diet compared to normoglycemic control mice (Figure 26). However, hepatic GSK-3β activities in hyperglycemic ApoE$^{-/-}$ mice fed VPA supplemented diet was similar to the levels found in normoglycemic mice and significantly lower than hyperglycemic mice fed the control diet. This indicates that oral supplementation of VPA can block the induction of GSK-3β activity by hyperglycemic conditions *in vivo*.

Figure 26. Effect of valproic acid supplementation on hepatic GSK-3 activity.

GSK-3β was immunoprecipitated from protein lysates prepared from the livers of normoglycemic (NG) and hyperglycemic (HG) mice fed control or VPA supplemented diet using a GSK-3β antibody. GSK-3β kinase activity was determined by measuring ^{32}P incorporation on to a synthetic substrate. n=3, $*P<0.05$ relative to non-supplemented control. $**P<0.05$ relative to non-supplemented HG.

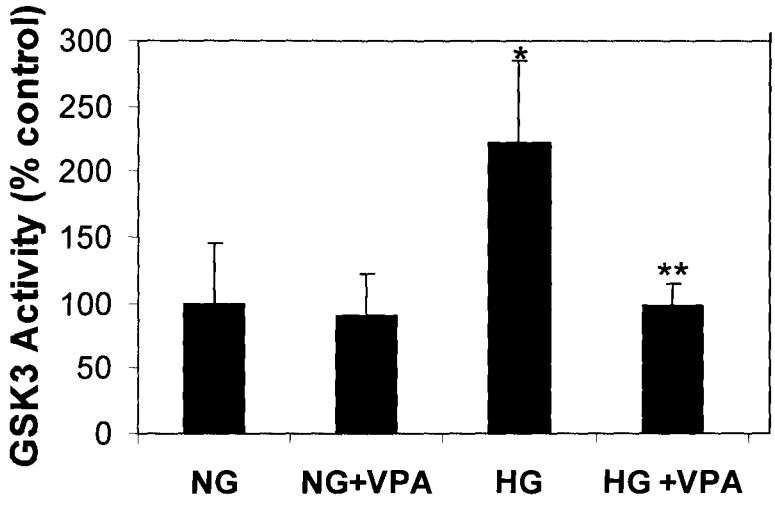
GSK3 Activity (% control)
300
250
200
150
100
50
0
*
**
NG
NG+VPA
HG
HG +VPA

8.5 EFFECTS OF 2-ETHYLBUTYRIC ACID SUPPLEMENTATION ON APOLIPOPROTEIN E-DEFICIENT MICE

8.5.1 Effect of 2-ethylbutyric acid supplementation on metabolic parameters

Supported by my *in vitro* data showing that treatment with small molecule inhibitors of GSK-3 prevents accumulation of lipid when cells are exposed to glucosamine (Figure 20), we hypothesized that GSK-3 plays a role in the development of hyperglycemia-accelerated atherosclerosis. This hypothesis was further strengthened by our data on the effects of glucosamine in cells deficient in GSK-3α or β (Figure 22). In previous studies, I demonstrated that EBA, a novel, more potent and selective GSK-3 inhibitor, is effective in reducing glucosamine-induced unesterified cholesterol accumulation in model cell types (Figure 19) (Werstuck et al. 2004; Shi et al. 2007). I tested if supplementation with EBA slows the progression of atherosclerosis in diabetic mice. I have identified non-toxic concentrations of EBA to use as a dietary supplement in $ApoE^{-/-}$ mice and have tested its effect on atherogenesis *in vivo*. We have first looked at any differences in body weight, blood glucose, plasma total cholesterol and triglyceride levels.

Hyperglycemia was induced in female $ApoE^{-/-}$ mice by multiple low dose intraperitoneal injections (Werstuck et al. 2005, Kunjathoor et al. 1996). Two sets of experiments were carried out to study the effects of EBA supplementation: **1)** 0, 312.5 mg/kg, or 625 mg/kg EBA supplemented diet was given to both normo- and hyperglycemic groups, **2)** 0, 312.5 mg/kg EBA or 625 mg/kg VPA was given to both

groups (Figure 16). Hyperglycemia and EBA supplementation had no significant effect on the body weight of age-matched ApoE$^{-/-}$ mice in this study. There was a slight but significant increase in non-fasted blood glucose levels of normoglycemic mice supplemented with a higher dose (625mg/kg) of EBA compared to the group fed a regular chow diet (15.4±1.2mM versus 13.5±1.4mM, $P<0.05$). In an attempt to minimize any complication caused by an elevation of blood glucose levels seen in the group receiving the higher dose of EBA, 312.5 mg/kg EBA was used for the parallel study with VPA supplementation. All mice that received STZ injections had significantly higher non-fasted blood glucose levels compared to the group receiving citrate buffer (24.2±5.8mM versus 14.5±1.7mM, $P<0.000001$) whereas EBA supplementation did not significantly change the blood glucose levels in either normo- or hyperglycemic groups (Figure 27. B). Plasma total cholesterol levels were not influenced by EBA supplementation, but plasma triglyceride levels were significantly increased by EBA supplementation in both normo- and hyperglycemic mice (Figure 27. C and D).

Figure 27. Effects of 2-ethylbutyric acid supplementation on metabolic parameters in ApoE$^{-/-}$ mice.

ApoE$^{-/-}$ mice (normoglycemic (NG) and hyperglycemic (HG)) were fed a control chow diet or a chow diet supplemented with two doses of 2-ethylbutyric acid (+E1 or E2) (312.5mg/kg or 625mg/kg) from 5 to 15 weeks of age. The mice were sacrificed at the end of 15 weeks and their body weight was measured (**A**). The blood glucose levels (**B**) were measured using a DEX glucometer (Bayer) at the time of sacrifice. Plasma lipid levels were determined in non-fasted mice using the colorimetric diagnostic kits for total cholesterol (**C**), and triglycerides (**D**) from Thermo DMA Inc. n=5-6, *P<0.05 versus normoglycemic mice, **P<0.05 versus corresponding group fed a control diet.

A.

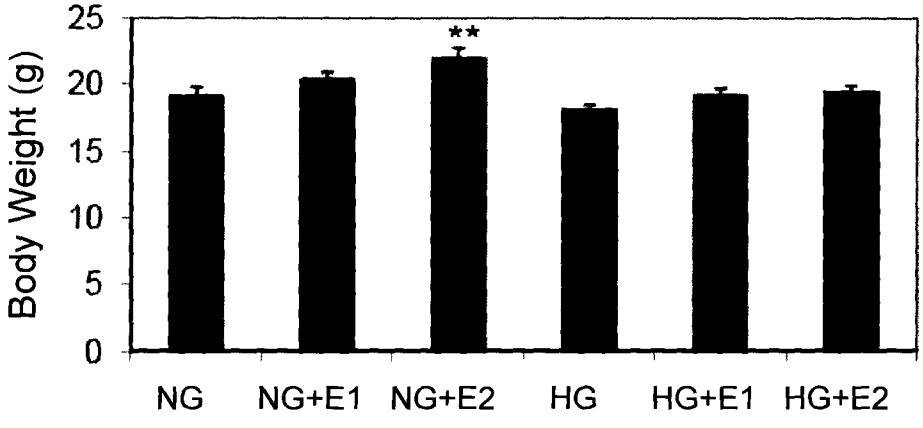
Body Weight (g)
25
20
15
10
5
0
**
NG
NG+E1
NG+E2
HG
HG+E1
HG+E2

B.

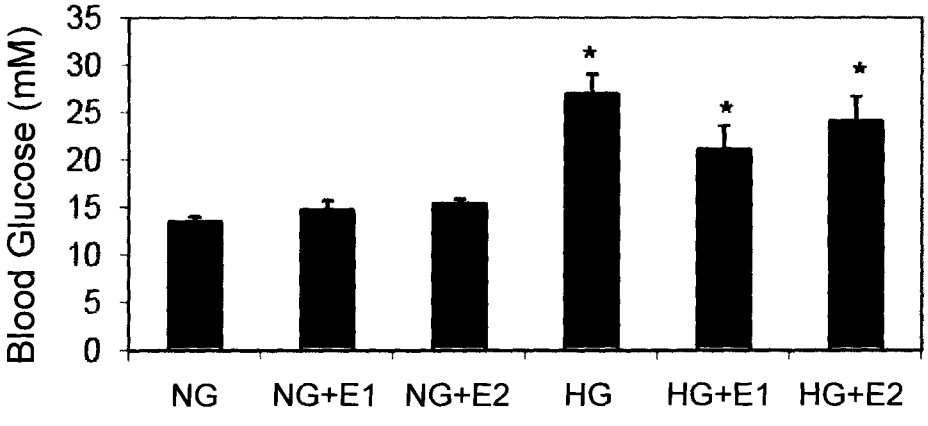
Blood Glucose (mM)
35
30
25
20
15
10
5
0
*
*
*
NG
NG+E1
NG+E2
HG
HG+E1
HG+E2

C.

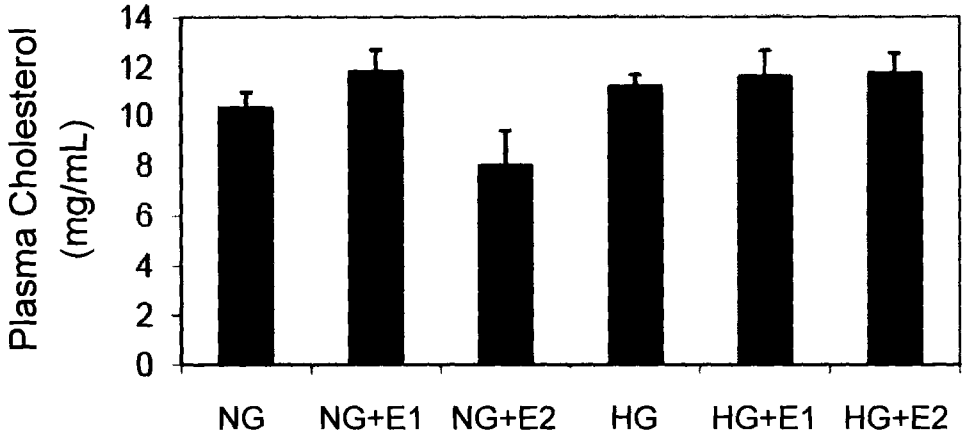
Plasma Cholesterol (mg/mL)
14
12
10
8
6
4
2
0
NG
NG+E1
NG+E2
HG
HG+E1
HG+E2

D.

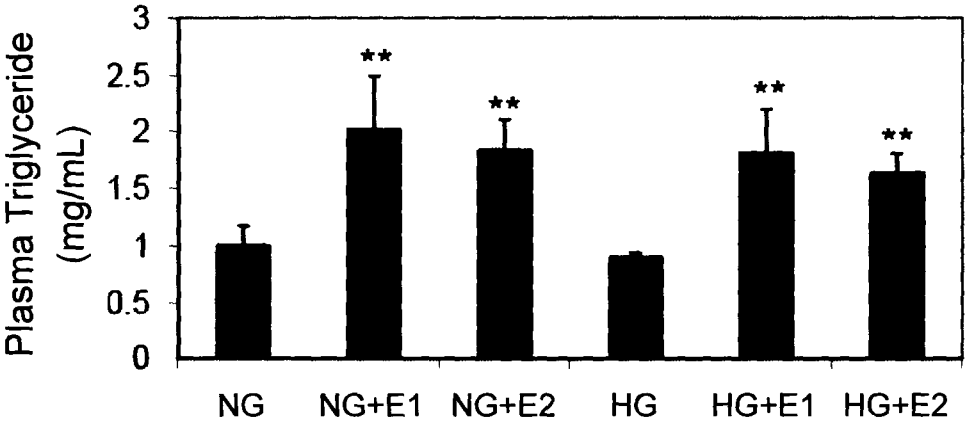
Plasma Triglyceride (mg/mL)
3
2.5
2
1.5
1
0.5
0
**
**
**
**
NG
NG+E1
NG+E2
HG
HG+E1
HG+E2

8.5.2 Effect of hyperglycemia and 2-ethylbutyric acid supplementation on lesion development in the aorta at 15 weeks of age

The effect of hyperglycemia and supplementation of EBA on lesion development in mouse aorta was determined using Sudan IV staining, a procedure used to visualize neutral fat (Kim et al. 1976). Before staining the lesions present inside of the aortic wall, all the visible adipose and connective tissues on the exterior of the aorta was removed under a microscope.

No measurable lesion was found in any of the control or treatment groups at the age of 15 weeks (Figure 28). This is consistent with previous reports regarding $ApoE^{-/-}$ mice which do not acquire significant plaque development in the descending aortae until the later age of 18-20 weeks (Hoen et al. 2003). Therefore, the effect EBA supplementation may have on lesion development in the aorta was unable to be assessed.

Figure 28. Effect of valproic acid and 2-ethylbutyric acid supplementation on lesions in aortae of normo- and hyperglycemic mice.

Representative Sudan IV-stained descending aortae of normoglycemic and hyperglycemic mice fed control, valproic acid (VPA), and 2-ethylbutyric acid (EBA) supplemented diets. Aortae were collected at 15 weeks and fixed in 10% neutral buffer formalin immediately. Periadventitial tissue and fat was removed before staining with Sudan IV and the stained aortae were mounted *en face* for the images to be taken.

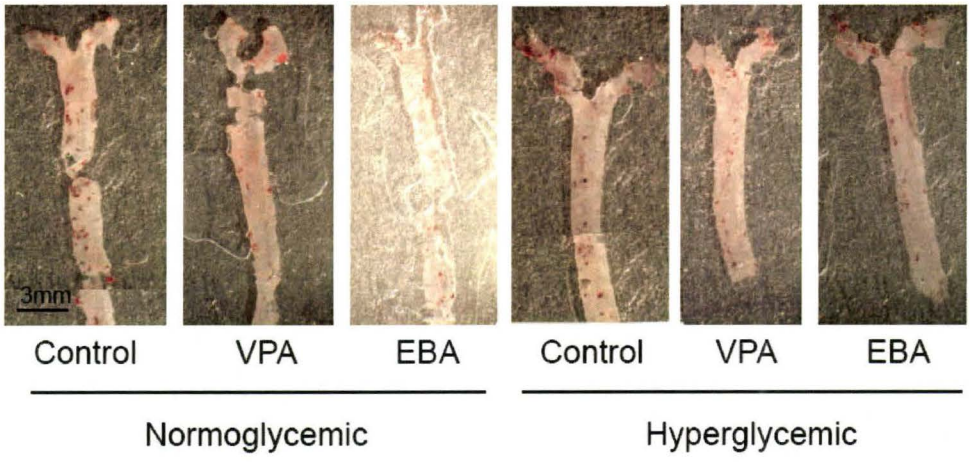
3mm
Control
VPA
EBA
Control
VPA
EBA
Normoglycemic
Hyperglycemic

8.5.3 Effect of 2-ethylbutyric acid supplementation on hepatic steatosis in hyperglycemic mice

In our earlier studies, VPA supplementation to hyperglycemic ApoE$^{-/-}$ mice reduced hepatic steatosis, which correlated with decreased GSK-3 activity (Figures 10 and 27). Therefore, we examined the effect of EBA supplementation on hyperglycemia-induced lipid accumulation in the liver. However, I observed inconsistent results regarding Oil red O staining on frozen liver sections of some treatment groups including the hyperglycemic group supplemented with EBA. In general, hyperglycemic mice fed the control diet displayed more lipid staining compared to the normoglycemic mice as previously reported (Figure 29) (Bowes et al. 2009). The EBA supplemented diet seemed to increase lipid accumulation in normoglycemic mice compared to control mice fed non-supplemented diet. EBA supplementation, however, showed reduced staining in the hyperglycemic group (Figure 29). This may imply a beneficial effect of EBA supplementation only when hyperglycemia is prevalent but not in the normal condition, although this result needs to be interpreted with caution due to variation within each treatment group.

Figure 29. Effect of 2-ethylbutyric acid supplementation on hepatic steatosis

Representative sections of liver from control or hyperglycemic ApoE$^{-/-}$ mice fed control diet, valproic acid (VPA), or 2-ethylbutyric acid (EBA) supplemented diet were stained with Oil Red O. 7 μm thick liver cryo-sections were collected on slides and fixed in Formal calcium solution before incubation with Oil red O solution. After rinsing with distilled water, nuclei were stained with hematoxylin, and slides were mounted using Crystalmount. Images of several fields within the same treatment group were taken using a light microscope.

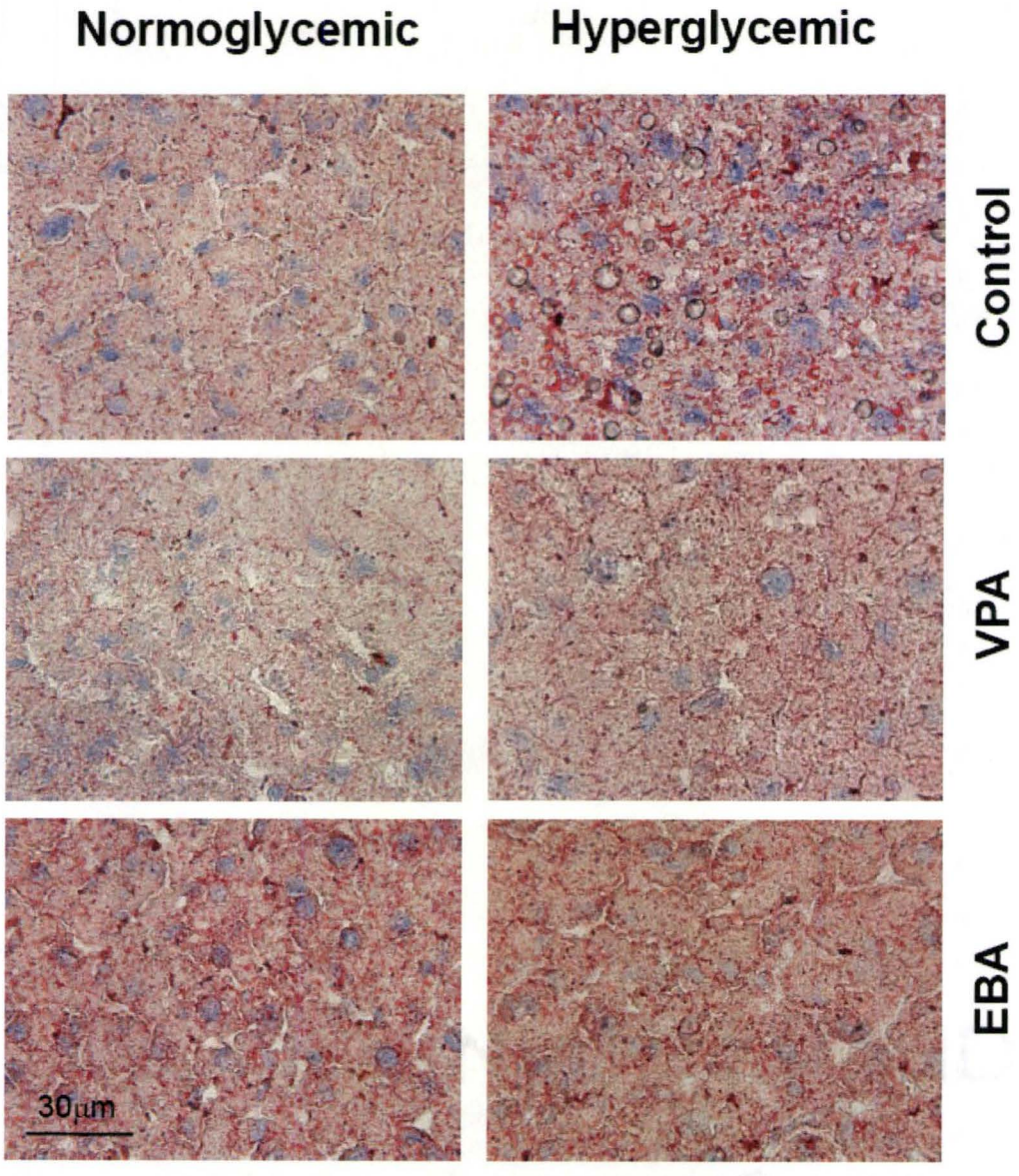
Normoglycemic
Hyperglycemic
Control
VPA
EBA
30μm

8.5.4 Effect of 2-ethylbutyric acid supplementation on lesion size at the aortic root of hyperglycemic mice

Even though there is minimal plaque development in the descending arota, the root of the aorta has significant development of atherosclerotic lesions at 15 weeks of age in ApoE$^{-/-}$ mice (Bowes et al. 2009). H&E staining was performed on paraffin embedded aortic root sections to visualize the structure of this region. From each section, the size of the lesion was measured and plotted against the distance from the aortic root where the lesion first appeared. Increases in overall lesion size with a large degree of variation were observed in normoglycemic mice fed EBA supplemented diet compared to normoglycemic mice fed control diet (Figure 30). Even though this was not a desired effect, it appears consistent with a slight increase in hepatic lipid levels and significantly higher levels of plasma triglyceride levels seen in these mice (Figures 28 and 30). There was a significant increase in lesion size in hyperglycemic mice compared to normoglycemic mice, consistent with previous findings (Figures 11 and 31) (Bowes et al. 2009). However, neither 312.5 nor 625 mg/kg concentration of EBA supplementation had any effect on lesion size in the aortic root. This may have occurred for several reasons. First, oral supplementation of EBA may not be an efficient way to deliver the drug into the circulation or to target organs. Secondly, if EBA has been delivered to the target organs, it may have failed to inhibit GSK-3 *in vivo*. Thirdly, EBA may have been rapidly metabolized to an ineffective form in the liver, or may have been excreted from the mice before it could have had any effect on peripheral tissues. Hence, we examined the activity of hepatic GSK-3β in the following experiment.

Figure 30. Effect of 2-ethylbutyric acid supplementation on atherosclerotic plaque area in hyperglycemic ApoE$^{-/-}$ mice

Lesion areas were determined at the aortic root (0 μm) and at 40 μm intervals in aortae isolated from normoglycemic (NG) or hyperglycemic (HG) mice fed control diet or control diet supplemented with a low dose of 2-ethylbutyric acid (EBA1) or a higher dose EBA (EBA2). The mice were perfusion-fixed with 10% neutral buffered formalin and hearts, including the aortic root, were cut transversely and embedded in paraffin. 4 μM sections of aortic root were collected on pre-coated glass slides and hematoxylin and eosin staining was performed. The lesion area (average ± s.e.m.) was determined using WCIF ImageJ software and plotted against the distance across the aortic root. n=3-6/group; *P<0.05, relative to control mice; **P<0.05, relative to similar treatment group in the absence of EBA supplementation.

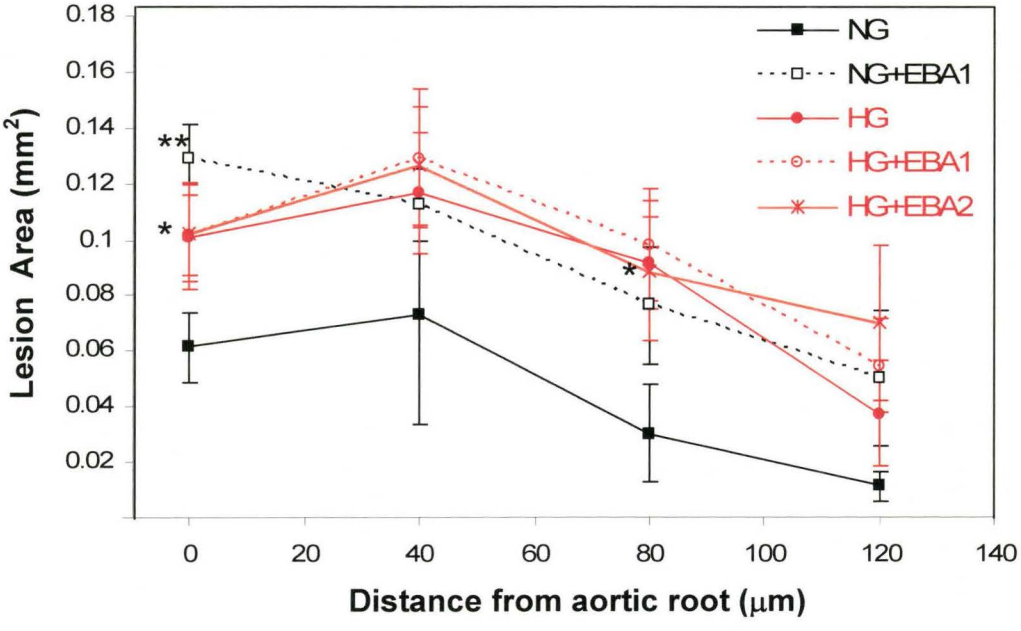
0.18
0.16
0.14
0.12
0.1
0.08
0.06
0.04
0.02
Lesion Area (mm²)
0
20
40
60
80
100
120
140
Distance from aortic root (μm)
NG
NG+EBA1
HG
HG+EBA1
HG+EBA2
**
*
*

9 DISCUSSION

Atherosclerosis is a macro-vascular complication of DM, and accounts for the majority of mortality in individuals diagnosed with DM (Haffner et al. 1998). There has been a great deal of effort aimed at delineating the cellular and molecular mechanisms by which hyperglycemia promotes CVD in order to develop an effective therapeutic interventions.

Many basic and clinical research efforts have focused upon the role of oxidative stress in hyperglycemia-associated accelerated atherosclerosis and CVD. However, the therapies targeting oxidative stress have led to insignificant impact on improving cardiovascular outcomes in clinical trials (Lonn et al. 2001; McQuillan et al. 2001; Lonn et al. 2005; Thomson et al. 2007). This suggests that alternative mechanisms might play a role in the progression of atherosclerosis.

Our lab has postulated a working model involving hyperglycemia-induced ER stress in the activation of pro-atherogenic pathways. My thesis is focused on defining some of the molecular mechanisms that are involved in this pathway. Specifically, i) the mechanism by which VPA attenuates hyperglycemia-induced atherogenesis in cultured cells and in an animal model, ii) the role of GSK-3 in hyperglycemia/glucosamine-induced activation of pro-atherogenic pathways and iii) the role of GSK-3 in diabetes-associated accelerated atherosclerosis.

9.1 VALPROIC ACID ATTENUATES HYPERGLYCEMIA-INDUCED ATHEROSCLEROSIS BY INHIBITING GSK-3

VPA has been used as an anticonvulsant and is also one of the primary drugs used to treat bipolar disorder (Bowden et al. 1994; Penry and Dean 1989). VPA has been shown to inhibit low-K^+-induced apoptosis by acting on the PI3K/PKB pathway in cerebellar granule cells (Mora et al. 1999). Neuroprotective properties of VPA have been shown in an amyotrophic lateral sclerosis mouse model where it delays disease onset and prolongs survival (Feng et al. 2008). Its effect on inflammation has been shown in experimental autoimmune neuritis rats by suppressing the mRNA levels of IFN-γ, TNF-α, IL-1β, and IL-6 (Zhang et al. 2008). The same report also showed that VPA suppressed the accumulation of immune cells in sciatic nerves, including macrophages, T cells and B cells (Zhang et al. 2008).

Our data indicate that VPA attenuates both hyperglycemia-induced accelerated atherosclerosis and hepatic steatosis. VPA has been shown to initiate a variety of cellular responses that may be responsible for these effects. . It has been reported that VPA and other anti-convulsant drugs can stabilize neuronal growth cones by depleting intracellular inositol concentrations (Williams et al. 2002). VPA also has been shown to regulate gene expression by activating the AP-1 family of transcription factors and through the inhibition of HDAC (Chen et al. 1999; Phiel et al. 2001). Immunoblot analysis in cultured primary mouse hepatocytes showed that exposure to 1 mM VPA significantly increased acetylation of histone 3, indicative of HDAC inhibition. However, 50 μM

VPA, the plasma concentration typically observed in mice fed a VPA supplemented diet, was unable to inhibit HDAC (Figure 13). This suggests that HDAC in VPA supplemented hyperglycemic mice is also not inhibited. Nonetheless, it is still possible that VPA has an effect *in vivo* since its intracellular concentration may be higher than in the plasma of chronically-exposed mice. However, HDAC was not chosen to be further examined *in vivo* taking into consideration the report that TSA, a potent inhibitor of HDAC, resulted in intensifying atherosclerosis in LDL receptor-deficient mice rather than protecting them from lesion development (Choi et al. 2005).

It has been demonstrated that GRP78/BiP protein and mRNA levels are increased in rat brains injected with VPA and we have shown that VPA increases protein levels of GRP78/BiP, GRP94, calreticulin, PDI, and HSP70 in cultured HepG2 cells (Figure 9) (Wang et al. 1999; Bown et al. 2000; Kim et al. 2005). Chaperones are required during the folding of nascent proteins in the ER and cytoplasm. The over-expression of specific chaperones has been shown to protect against cellular injury and apoptotic signals resulting from various cellular stresses (Reddy et al. 2003; Morris et al. 1997; Liu et al. 1998). There has been a suggestion that VPA induces ER chaperones by inducing ER stress (Lee. 2001). However, the mechanism by which VPA induces expression levels of GRP78/BiP and other chaperones seems to be independent of the UPR through the ER-resident PKR-ER-related kinase (PERK)-dependent phosphorylation of eIF2α (Kim et al. 2005). Unlike other ER stress inducing agents, including tunicamycin and A23187 (an ionophore), VPA treatment does not activate other arms of UPR such as GADD153/CHOP or ATF4 (Kim et al. 2005). Also, there is rapid induction (4-8 hours)

of ER chaperone levels by the UPR when the cells are exposed to tunicamycin, glucosamine, or A23187. This is in contrast to the observation that prolonged incubation with VPA for at least 48 hours is required to observe elevation of chaperone proteins (Figure 9) (Kim et al. 2005). Therefore, it appears that VPA is able to induce cellular chaperone levels without causing ER stress, which can enhance the cell's ability to cope with injury. However, the possibility that a reduction in glucosamine-induced lipid accumulation and NF-κB activation results from this increase in chaperones was discounted due to the time discrepancies in observed effects. The reduction of lipid accumulation and NF-κB activation in cultured cells occurred at the 18 hour point whereas the chaperone levels were not increased in these cells until after 24 hours (Figures 6, 7, and 9). Furthermore, normoglycemic mice which were fed a VPA supplemented diet did not show elevation in GRP78/BiP, GRP 94, or HSP47 protein levels as revealed by immunostaining of liver and aortic lesions compared to the corresponding controls (Figure 9) (Bowes et al. 2009). Hyperglycemic mice, do show indications of ER stress that are independent of diet (Werstuck et al. 2006; Bowes et al. 2009).

Previously, VPA has been reported to inhibit GSK-3α and β through direct and indirect mechanisms (Chen et al. 1999; De Sarno et al. 2002). The essential role of GSK-3β for the activation of NF-κB has been demonstrated by its genetic knock-out, resulting in liver degeneration and embryonic lethality (Hoeflich et al. 2000). This is consistent with findings that both VPA and lithium are teratogenic in humans (Klein and Melton 1996; Phiel et al. 2001). Direct inhibition of GSK-3α/β by VPA was clearly

demonstrated using recombinant human GSK-3 in a cell-free system (Figure 14). Interestingly, greater inhibition of both GSK-3α and β was observed in HepG2 cells after treatment with 0.5 mM VPA than with the same concentration used on recombinant GSK-3 in the cell-free system (Figure 14). This may be an indication that VPA also influences GSK-3 activation indirectly by inducing Ser21/9 phosphorylation through kinases upstream of GSK-3. The observation that inhibition of GSK-3 was conserved after immunoprecipitation also shed light on the potential mechanism by which VPA inhibits GSK-3. During the immunoprecipitation protocol, weak interactions between GSK-3 and any compounds or proteins should be disrupted. Therefore, the retention of GSK-3 inhibition after immunoprecipitation from VPA treated cultured cells suggests that VPA binds tightly to GSK-3, and/or that intracellular VPA causes covalent modification(s) on GSK-3 such as serine phosphorylation. In the case where the immunoprecipitated GSK-3 becomes serine phosphorylated, the percentage inhibition observed during the kinase assay may have been an underestimation of the effect of VPA in cultured cells. Inhibitory serine phosphorylation at Ser21/9 introduces a primed pseudosubstrate that binds to the positively charged pocket of GSK-3, the catalytic domain where primed substrates position themselves for the phosphorylation by GSK-3 (Frame et al. 2001). However, when there is high concentration of primed substrates, the substrates can out-compete the inhibition by pSer21/9 (Frame et al. 2001). This may have been the case in my assay condition given that an excess amount of substrate p-GS was used. This implies that VPA may indeed inhibit GSK-3 in cultured cells to a much greater extent than observed in the kinase assay.

Increased GSK-3β activity has been reported in adipose tissue from diet-induced diabetic mouse model and in skeletal muscle from individuals with T2DM (Eldar-Finkelman et al. 1999; Nikoulina et al. 2000). I have determined that hepatic GSK-3β activity in STZ-induced hyperglycemic ApoE$^{-/-}$ mice is more than twofold higher than in normoglycemic controls (Figure 26). This increase also corresponds to an increase in intracellular glucosamine levels shown by heavy glycosylation of p62 in hyperglycemic mice (Figure 8). In support of our hypothesis that GSK-3 inhibition is responsible for the anti-atherogenic effect of VPA, we observed that hyperglycemic ApoE$^{-/-}$ mice fed a VPA supplemented diet had a significant reduction in hepatic GSK-3β activity (Figure 26). This may be directly responsible for reduced hepatic steatosis in hyperglycemic mice fed the VPA supplemented diet. However, it is still unclear if the vascular effect of VPA is linked to decreased activity of hepatic GSK-3. It is possible that GSK-3 is affecting plasma lipid metabolism and in turn, influencing atherosclerosis development, but it is difficult to determine the causative role of hepatic GSK-3 at peripheral sites.

9.2 ROLE OF GSK-3 IN GLUCOSAMINE-INDUCED UNESTERIFIED CHOLESTEROL ACCUMULATION

GSK-3, a multifunctional Ser/Thr kinase, was first identified as one of the inhibitory kinases capable of phosphorylating glycogen synthase, the enzyme involved in the last step of glycogen synthesis (Embi *et al.* 1980). One of the effects of insulin is to reduce blood glucose levels by initiating glycogen and protein synthesis. This involves

the activation of the PI3K/PKB pathway, which attenuates GSK-3 activity (Ali et al. 2001; Cohen and Frame 2001; Cohen 2001). It has been observed that diabetic mice have decreased inhibitory phosphorylation at Ser21/9 of GSK-3α/β, causing over-stimulation of the enzyme (Lajoie et al. 2004; Laviola et al. 2001). Moreover, it has been reported that glucosamine treatment, as well as GFAT over-expression, increases GSK-3 activity, resulting in reduced insulin-stimulated GS activity in rat-1 fibroblasts (Singh and Crook. 2000).

The mechanism by which enhanced flux of glucose into the hexosamine pathway increases GSK-3 activity may involve several pathways, including the insulin signalling pathway and the ER stress pathway. Firstly, glucosamine has been shown to inhibit tyrosine-phosphorylation of IR and IRS1/2, causing the impaired ability of the PI3K/PKB pathway to inhibit GSK-3 (D'Alessandris et al. 2004). Inhibiting O-GlcNAc removal from proteins with PUGNAc (O-(2-acetamido-2-deoxy-d-glucopyranosylidene)amino-N-phenylcarbamate), thus prolonging the effect of the hexosamine pathway, resulted in the reduction in Thr308 phosphorylation of PKB and Ser9 phosphorylation of GSK-3β (Vosseller et al. 2002). These findings suggest that elevated levels of glucosamine and/or O-GlcNAc modification of proteins can block insulin signalling and thereby attenuate the inhibition of GSK-3.

Secondly, glucosamine can stimulate GSK-3 hyper-activity through the ER stress pathway. Glucosamine was identified as an ER stress inducer more than 20 years ago, however the ability of glucosamine to cause accumulation of misfolded or unfolded

proteins in the ER has been widely overlooked in relation to insulin resistance and diabetes (Lin et al. 1993). Although it has not been clearly shown, it is presumed that glucosamine causes ER stress by altering glycosylation of nascent proteins (Lee. 2001). Many secretory cells, such as pancreatic β-cells, often undergo transient ER stress as the demand for secretory proteins or membrane proteins increases (Hotamisligil and Erbay. 2008; Ron and Walter. 2007). Cells cope with a demand for rapid protein folding through the UPR which involves a reduction of overall protein translation and an increase in chaperone levels, to amplify folding capacity (Ron and Walter. 2007). However, when the ability of a cell to relieve ER stress is compromised, the cell undergoes inflammation, lipid accumulation, and eventually programmed cell death (Schroder and Kaufman. 2005).

Our lab has shown that accumulation of intracellular glucosamine is associated with hyperglycemia, ER stress, and accelerated atherosclerosis by observing colocalization of O-glycosylated proteins and phospho-PERK (an ER stress marker) in the aortic lesion of STZ-induced ApoE$^{-/-}$ mice (Werstuck et al. 2006). Previously, we and others have demonstrated that GSK-3 mediates ER stress-induced apoptotic signalling (Kim et al. 2005; Song et al. 2002; Pluquet et al. 2005; Brewster et al. 2006; Takadera et al. 2007; Huang et al. 2009). Song et al. first demonstrated this by showing that when GSK-3 was inhibited using lithium, the activation of caspase-3 by various ER stress-inducing agents could be inhibited in neuronal cells. A stable pancreatic β-cell line with 80% reduction in the expression level of GSK-3β was also found to resist ER stress-induced apoptosis (Srinivasan et al. 2005). In addition, our group has shown that

pretreatment with VPA blocks ER stress-induced caspase-3 activity in HepG2 cells (Kim et al. 2005). These reports suggest that GSK-3 plays a role in mediating ER stress associated cellular dysfunction.

Disruption of the ER homeostasis and activation of the UPR have been suggested to play a significant role during the development and progression of atherosclerosis (Marciniak and Ron. 2006). Independent cardiovascular risk factors including hyperhomocysteinemia, cholesterol, obesity, and DM have been linked to the activation of the UPR and increased markers for ER stress (Zhou et al. 2004; Li et al. 2004; Ozcan et al. 2004; Werstuck et al. 2005; Bowes et al. 2009). Increased staining of KDEL, which stains for the retention sequence abundant in ER chaperones, was observed in liver sections of STZ-induced ApoE$^{-/-}$ mice (Figure 9). Elevated levels of ER chaperones in these mice are likely due to the presence of ER stress, taking into consideration that increased levels of phospho-PERK, a diagnostic marker of ER stress, were also observed in aortic lesions of STZ-induced mice (Werstuck et al. 2006). In both control and STZ-induced mice, VPA supplementation did not appreciably alter chaperone levels (Figure 9). This is consistent with our hypothesis that VPA reduces accelerated lesion development by inhibiting GSK-3, a step subsequent to ER stress, and therefore has no effect on the UPR (Song et al. 2002; Srinivasan et al. 2005; Kim et al. 2005).

Hepatic steatosis is a complication associated with DM in humans and a characteristic of hyperglycemic rodent models (Ohno et al. 2000; Werstuck et al. 2006; Cusi 2009). We proposed that glucosamine induces lipid accumulation by a pathway that involves GSK-3 activation. This hypothesis is supported by the observation that GSK-3$^{-/-}$

MEFs do not accumulate unesterified cholesterol when exposed to elevated levels of glucosamine (Figure 22). The cholesterol biosynthetic pathway appeared to be functional in GSK-3$^{-/-}$ cells as revealed by an independent cholesterol up-regulator, U18666A, which produced higher levels of unesterified cholesterol in these cells compared to the untreated cells (Figure 23). These results suggest that a pathway involving GSK-3 is specific to glucosamine treatment.

There are many enzymes involved in cholesterol biosynthesis, which contribute to glucosamine-induced unesterified cholesterol accumulation, that could be affected by GSK-3. Our group has shown previously that exposure of HepG2 cells to glucosamine induces unesterified cholesterol accumulation by activation of SREBP-2, and that VPA pretreatment reduces the formation of mature SREBP-2, the active form of this transcription factor (Kim et al. 2005). The SREBPs are a family of transcription factors that control cholesterol and lipid metabolism (Brown and Goldstein. 1999). Of the three proteins in this family, SREBP-1a and SREBP-1c are involved in triglyceride and fatty acid metabolism, and SREBP-2 is known to induce the expression of proteins involved in cholesterol synthesis such as HMG CoA Reductase (Rawson 2003). When the WT and GSK-3$^{-/-}$ MEFs were examined for the transcription levels of these genes, there was a significant increase in SREBP-2 transcription levels in WT MEFs treated with glucosamine but not in GSK-3$^{-/-}$ cells (Figure 25). A similar but non-statistically significant trend was seen with HMG CoA Reductase. These results suggest that SREBP-2 is involved in glucosamine-induced GSK-3 activation leading to unesterified cholesterol accumulation.

9.3 EFFECT OF A NOVEL INHIBITOR OF GSK-3 IN A HYPERGLYCEMIC MOUSE MODEL OF ATHEROSCLEROSIS

EBA is a small branched fatty acid that is very similar in structure to VPA (Figure 17). EBA shares some characteristics that are similar to VPA but also possesses several different cellular and physiological effects. Previously, EBA has been shown to exhibit anticonvulsant activity without increasing the content of GABA in the mouse brain (Keane et al. 1983). Recently, EBA has been demonstrated to possess an inositol-depleting effect without exerting adverse effects on cell growth, making it less toxic than VPA and a potential candidate for mood-stabilizing therapy (Azab et al. 2009). We have also shown that EBA has no effect on HDAC inhibition unlike VPA (Shi et al. 2007). When tested for its effect on ER chaperone levels and the UPR, EBA did not induce GRP78/BiP, GRP94, or GADD153, suggesting that EBA does not alter the protein folding capacity of the ER (Shi et al. 2007). Therefore, the ability of EBA to inhibit GSK-3 at higher potency than VPA without affecting many other intracellular pathways made it a great tool to assess the involvement of GSK-3 in hyperglycemia-induced atherogenesis and to test its potential as a novel anti-atherogenic agent.

EBA supplementation, however, had no significant effect on overall aortic lesion development and only a slight effect on hepatic steatosis in STZ-induced ApoE$^{-/-}$ mice (Figures 29 and 30). The underlying reason for the lack of an athero-protective effect *in vivo* is currently not known although there are several possible explanations. First, the bio-availability of dietary EBA may be insufficient. It is possible that EBA is not efficiently absorbed in the gut. It is also possible that EBA is rapidly excreted or

metabolized into an inactive compound. These hypotheses are consistent with the observation that hepatic GSK-3 activity levels were not significantly affected in EBA-supplemented mice. Plasma EBA concentrations could be tested using mass spectrometry and high-performance liquid chromatography (HPLC) (Miwa and Yamamoto. 1990).

It appeared, however, that EBA also had some unforeseen effects on normoglycemic mice. EBA did not alter plasma cholesterol levels in any of the test groups, but significantly increased plasma triglyceride levels in control and STZ-induced ApoE$^{-/-}$ mice (Figure 27). Although there was some variation between animals, many of the control mice fed an EBA supplemented diet showed elevated hepatic lipid levels compared to control mice fed normal chow diet (Figure 29). In addition, there was a significant increase aortic lesion size of normoglycemic mice fed an EBA supplemented diet. The significant increase in triglyceride levels may be due to prolonged transcriptional activation by SREBP-1, a transcription factor regulating triglyceride and fatty acid synthesis (Raghow et al. 2008; Rawson 2003). It has been shown that GSK-3 plays a direct role in the regulation of SREBP-1 (Figure 3). Specifically, GSK-3 phosphorylates multiple sites on SREBP-1 in response to DNA binding to initiate its subsequent ubiquitination and proteosomal degradation (Punga et al. 2006; Bengoechea-Alonso and Ericsson. 2009). This may be a control mechanism for the down-regulation of SREBP-1 (Punga et al. 2006). Increased levels of plasma triglyceride and increased atherosclerosis in normoglycemic mice may be a side effect of inhibiting a multifunctional kinase using a potent inhibitor such as EBA, leading to uncontrolled synthesis of triglyceride and fatty acids. Thus, by "over-inhibiting" GSK-3 the beneficial

effect is over-whelmed by detrimental consequences of other pathways targeted by GSK-3. If this is the case, it suggests that less potent inhibitors of GSK-3, like VPA, may be a better candidate for anti-atherogenic therapy. This hypothesis could be directly tested by monitoring hepatic GSK-3 and SREBP-1 activity in VPA and EBA fed $ApoE^{-/-}$ mice. In addition, EBA may also be having effects on pathways that are independent of GSK-3.

9.4 THE OVERALL WORKING MODEL

Through the current thesis work I have identified that conditions of chronic hyperglycemia associated with DM can accelerate the development and progression of atherosclerosis by a novel mechanism involving glucosamine-induced cellular dysfunction (Figure 31) (Werstuck et al. 2006; Bowes et al. 2009). Hyperglycemia increases intracellular glucose levels in some cells including vascular smooth muscle cells and endothelial cells. Elevated intracellular glucose enhances flux into the hexosamine pathway, generating glucosamine. Increased glucosamine levels induce NF-κB activation and unesterified cholesterol accumulation processes involved in progression of atherosclerosis in cultured HASMC, HepG2 cells, and MEFs. Glucosamine-induced cellular dysfunction can be blocked *in vitro* by inhibition of GSK-3 using small molecule inhibitors such as VPA, or by knock-out of the gene. VPA also slows the progression of hyperglycemia-induced accelerated atherosclerosis by inhibition of GSK-3.

9.5 SIGNIFICANCE OF THIS WORK

The incidence of DM is increasing rapidly within Canada and is already on its way to becoming a global epidemic (Ohinmaa et al. 2006; Hossain et al. 2007). With cardiovascular complications being the major cause of morbidity and mortality among individuals with DM, understanding how diabetes promotes atherosclerosis is critical in developing strategies to prevent CVD. Identification and establishment of this novel therapeutic target will promote a rational approach to prevent cardiovascular complications in diabetic patients.

Figure 31. Overall working model: development of atherosclerosis in diabetic patients.

Both type I and type II diabetes are characterized by hyperglycaemia which increases intracellular glucosamine levels in some cells including vascular smooth muscle cells and endothelial cells. Elevated glucosamine promotes the increased activation of GSK-3, an enzyme that regulates sterol responsive element binding protein (SREBP), and nuclear factor-κB (NF-κB). SREBP activation leads to increased lipid synthesis and its uptake, and NF-κB is responsible for transcriptional activation of inflammatory pathways. We hypothesize that GSK-3-induced lipid accumulation and inflammation plays a causative role in accelerated atherosclerosis.

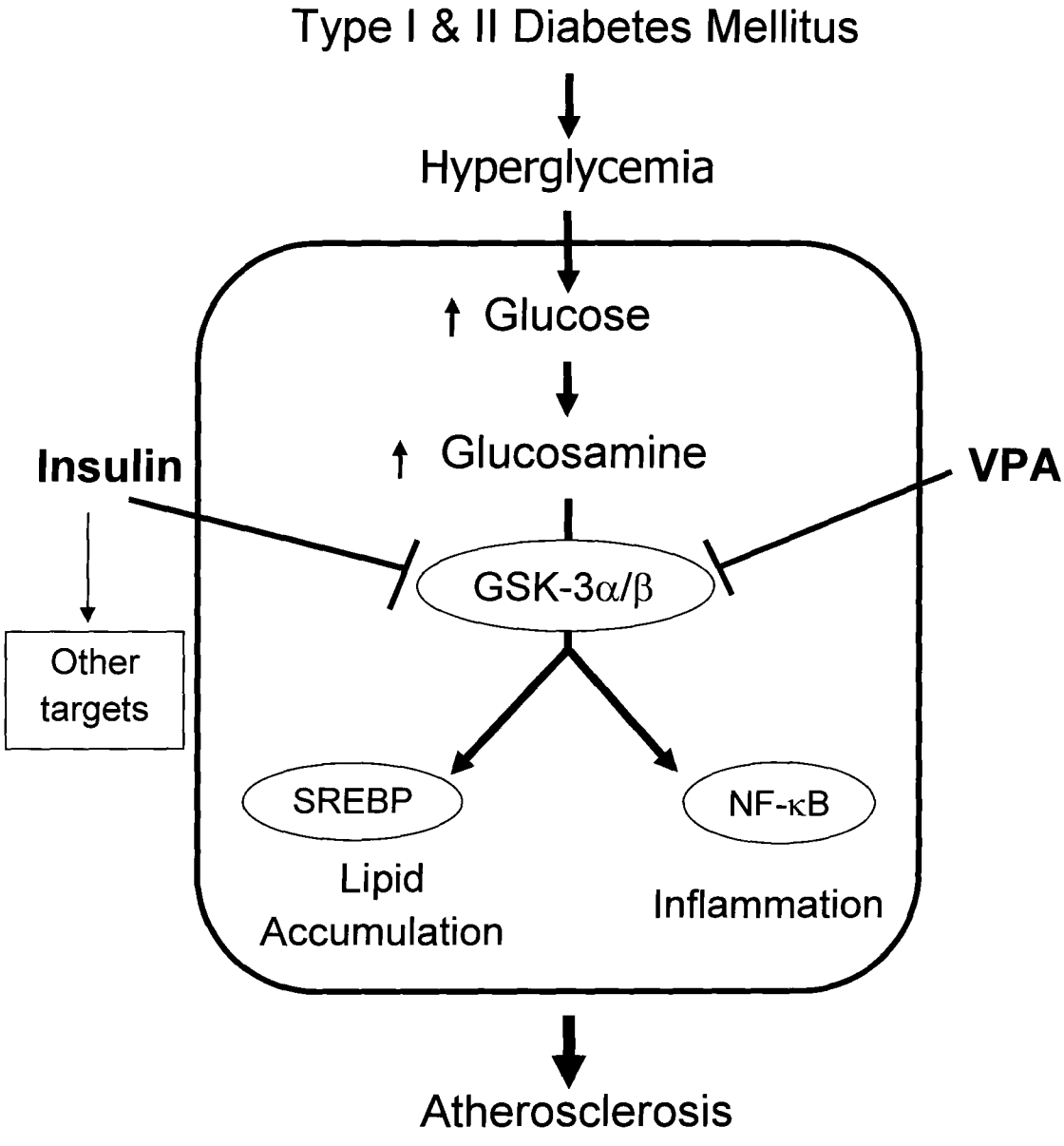
Type I & II Diabetes Mellitus
Hyperglycemia
↑ Glucose
↑ Glucosamine
Insulin
VPA
GSK-3α/β
Other targets
SREBP
NF-κB
Lipid Accumulation
Inflammation
Atherosclerosis

9.6 FUTURE DIRECTIONS

Based on the findings of this project, the following future experiments would shed light on the detailed mechanism(s) by which GSK-3 may activate glucosamine-induced cellular dysfunction leading to atherogenesis in conditions of hyperglycemia.

A. Test the effect of glucosamine on insulin signalling pathway. Currently, very little is known about which pathways are involved in glucosamine-induced GSK-3 activation. One of the potential mechanisms may involve deactivation of the insulin signalling pathway (D'Alessandris et al. 2004). First, an experiment testing tyrosine-phosphorylation of IR, IRS1/2, and PKB/Akt after glucosamine treatment will provide information regarding the involvement of this pathway. If there is an alteration in the phosphorylation levels of these proteins, a follow-up experiment using mutated IR, IRS1/2, or PKB/Akt that cannot be de-phosphorylated, can be used to examine the effect of glucosamine on GSK-3 activation and insulin-stimulated glucose uptake.

B. Test the involvement of ER stress and PERK upstream of GSK-3. With the finding that glucosamine is an ER stress inducer and that GSK-3 regulates ER stress-induced apoptosis, it is necessary to examine the proteins involved in the UPR to determine their involvement in glucosamine-induced GSK-3 activation (Lee. 2001; Song et al. 2002; Baltzis et al. 2007). PERK has been shown to affect degradation of p53 during the early phase of ER stress through the activation of GSK-3 (Baltzis et al. 2007). The involvement of PERK in the activation of GSK-3 can be determined by examining the effect of glucosamine treatment on GSK-3 activity and accumulation of unesterified cholesterol in PERK-deficient MEFs.

C. Test the mRNA levels of SREBP-1 in mice fed EBA supplemented diet. Observation that EBA supplemented diet increases atherogenesis in normoglycemic ApoE$^{-/-}$ mice but not in hyperglycemic ApoE$^{-/-}$ mice suggests that various degrees of GSK-3 inhibition *in vivo* may complicate the outcome of GSK-3 effects on lipid metabolism. In order to verify the hypothesis that "over-inhibition" of GSK-3 is responsible for elevated lesion development in normoglycemic mice fed EBA supplemented diet, the transcription levels of SREBP-1 should be determined.

D. Test the activity of aortic GSK-3. Hepatic GSK-3β activity in hyperglycemic mice has been shown to be elevated compared to normoglycemic mice, and VPA supplementation normalized this effect. However, the role of hepatic GSK-3β in athero-protective effect of VPA in aorta is not clear. A direct measurement of aortic GSK-3 will determine the role of GSK-3 at the site of lesion development.

E. Generate a cross between ApoE$^{-/-}$ and GSK-3α$^{-/-}$ mice. Even though the use of small inhibitors is an important tool to establish the role of GSK-3, there are many other intracellular targets affected by the inhibitor that may contribute to the outcome as discussed previously. Therefore, a genetic knock-out animal model can provide a more direct answer. GSK-3α$^{-/-}$ mice are fully viable although GSK-3β$^{-/-}$ mice die due to liver degeneration during the embryonic stage (MacAulay et al. 2007; Hoeflich et al. 2000). Therefore, a cross between GSK-3α$^{-/-}$ and ApoE$^{-/-}$ mice will provide a valuable means to evaluate the effect of GSK-3α in accelerated atherosclerosis.

10 REFERENCES

Alam, S.E., Nasser, S.S., Fernainy, K.E., Habib, A.A., Badr, K.F. (2004) Cytokine imbalance in acute coronary syndrome. Curr. Opin. Pharmacol. 4(2):166-170.

Ali, A., Hoeflich, K.P., Woodgett, J.R. (2001) Glycogen synthase kinase-3: properties, functions, and regulation. Chem. Rev. 101:2527-2540.

Anand, S.S., Islam, S., Rosengren, A., Franzosi, M.G., Steyn, K., Yusufali, A.H., Keltai, M., Diaz, R., Rangarajan, S., Yusuf, S. (2008) INTERHEART Investigators. Risk factors for myocardial infarction in women and men: insights from the INTERHEART study. Eur. Heart. J. 29(7):932-940.

Arias, E.B., Kim, J., Cartee, G.D. (2004) Prolonged incubation in PUGNAc results in increased protein O-Linked glycosylation and insulin resistance in rat skeletal muscle. Diabetes. 53(4):921-30.

Azab, A.N., Mehta, D.V., Chesebro, J.E., Greenberg, M.L. (2009) Ethylbutyrate, a valproate-like compound, exhibits inositol-depleting effects--a potential mood-stabilizing drug. Life Sci. 84(1-2):38-44.

Baltzis, D., Pluquet, O., Papadakis, A.I., Kazemi, S., Qu, L.K., Koromilas, A.E. (2007) The eIF2alpha kinases PERK and PKR activate glycogen synthase kinase 3 to promote the proteasomal degradation of p53. J. Biol. Chem. 282(43):31675-87.

Bell, G.I., Polonsky, K.S. (2001) Diabetes mellitus and genetically programmed defects in beta-cell function. Nature. 414(6865):788-91.

Bengoechea-Alonso, M.T., Ericsson, J. (2009) A phosphorylation cascade controls the degradation of active SREBP1. J. Biol. Chem. 284(9):5885-95.

Bickel, P.E., Freeman, M.W. (1992) Rabbit aortic smooth muscle cells express inducible macrophage scavenger receptor messenger RNA that is absent from endothelial cells. J. Clin. Invest. 90: 1450–1457.

Bijur,G.N., Jope,R.S. (2001) Proapoptotic stimuli induce nuclear accumulation of glycogen synthase kinase-3 beta. J. Biol. Chem. 276:37436-37442.

Bouche, C., Serdy, S., Kahn, C.R., Goldfine, A.B. (2004) The cellular fate of glucose and its relevance in type 2 diabetes. Endocr. Rev. 25:807-830.

Bowden, C.L., Brugger, A.M., Swann, A.C., Calabrese, J.R., Janicak, P.G., Petty, F., Dilsaver, S.C., Davis, J.M., Rush, A.J., Small, J.G., Garza-Trevino, E.S., Risch, S.C., Goodnick, P.J., Morris, D.D. (1994) Efficacy of divalproex vs lithium and placebo in the treatment of mania. The Depakote Mania Study Group. J. Am. Med. Assoc. 271:918-924.

Bowes, A.J., Khan, M.I., Shi, Y., Robertson, L., Werstuck, G.H. (2009) Valproate attenuates accelerated atherosclerosis in hyperglycemic ApoE-deficient mice. Am. J. Path. 174:330-342.

Bown, C.D., Wang, J.F., Young, L. T. (2000) Increased expression of endoplasmic reticulum stress proteins following chronic valproate treatment of rat C6 glioma cells. Neuropharmacology. 39:2162-9.

Bown, C.D., Wang, J.F., Chen, B., Young, L.T. (2002) Regulation of ER stress proteins by valproate: therapeutic implications. Bipolar. Disord. 4(2):145-51.

Brand, K., Page, S., Rogler, G., Bartsch, A., Brandl, R., Knuechel, R., Page, M., Kaltschmidt, C., Baeuerle, P.A., Neumeier, D. (1996) Activated transcription factor nuclear factor-kappa B is present in the atherosclerotic lesion. J. Clin. Invest. 97(7):1715-22.

Brewster, J.L., Linseman, D.A., Bouchard, R.J., Loucks, F.A., Precht, T.A., Esch, E.A., Heidenreich, K.A. (2006) Endoplasmic reticulum stress and trophic factor withdrawal activate distinct signaling cascades that induce glycogen synthase kinase-3 beta and a caspase-9-dependent apoptosis in cerebellar granule neurons. Mol. Cell. Neurosci. 32:242-253.

Brown, M.S., Goldstein, J.L. (1997) The SREBP pathway: regulation of cholesterol metabolism by proteolysis of a membrane-bound transcription factor. Cell. 89(3):331-40.

Brown, M.S., Goldstein, J.L. (1999) A proteolytic pathway that controls the cholesterol content of membranes, cells, and blood. PNAS. 96(20):11041-8.

Brownlee, M. (2001) Biochemistry and molecular cell biology of diabetic complications. Nature. 414:813-820.

Brownlee, M. (2005) The pathobiology of diabetic complications: a unifying mechanism. Diabetes. 54(6):1615-1625.

Chait, A., Bornfeldt, K.E. (2008) Diabetes and atherosclerosis: is there a role for hyperglycemia? J. Lipid. Res. 50:S335-S339.

Chen, G., Huang, L-D., Jiang, Y-M., Manji, H.K. (1999a) The mood-stabilizing agent valproate inhibits the activity of glycogen synthase kinase-3. J. Neurochemistry. 72:1327-1330.

Chen, G., Yuan, P.S., Jiang, Y.M., Huang, L.D., Manji, H.K. (1999b) Valproate robustly enhances AP-1 mediated gene expression. Brain Res. Mol. Brain Res. 64:52-8.

Chen, B., Wang, J.F., Young, L.T. (2000) Chronic valproate treatment increases expression of endoplasmic reticulum stress proteins in the rat cerebral cortex and hippocampus. Biol. Psychiatry. 48(7):658-664.

Choi, J.H., Nam, K.H., Kim, J., Baek, M.W., Park, J.E., Park, H.Y., Kwon, H.J., Kwon, O.S., Kim, D.Y., Oh, G.T. (2005) Trichostatin A exacerbates atherosclerosis in low density lipoprotein receptor-deficient mice. Arterioscler. Thromb. Vasc. Biol. 25:2404-2409.

Chung, S.S., Ho, E.C., Lam, K.S., Chung, S.K. (2003) Contribution of polyol pathway to diabetes-induced oxidative stress. J. Am. Soc. Nephrol. 14(8 Suppl 3):S233-6.

Ciaraldi, T.P., Oh, D.K., Christiansen, L., Nikoulina, S.E., Kong, A.P., Baxi, S., Mudaliar, S., Henry, R.R. (2006) Tissue-specific expression and regulation of GSK-3 in human skeletal muscle and adipose tissue. Am. J. Physiol. Endocrinol. Metab. 291(5):E891-8.

Cohen, P. Frame, S. (2001) The renaissance of GSK3. Nat. Rev. Mol. Cell Biol. 2:769-776.

Cohen, P., Goedert, M. (2004) GSK3 inhibitors: development and therapeutic potential. Nat. Rev. Drug. Discov. 3(6):479-87.

Cohen, P. (2006) The twentieth centry struggle to decipher insulin signalling. Nat. Rev. Mol. Cell. Bio. 7(11):867-873.

Colgan, S.M., Tang, D., Werstuck, G.H., Austin, R.C. (2007) Endoplasmic reticulum stress causes the activation of sterol regulatory element binding protein-2. Int. J. Biochem. Cell. Biol. 39(10):1843-51.

Cooksey, R.C., Hebert, L.F. Jr, Zhu, J.H., Wofford, P., Garvey, W.T., McClain, D.A.

(1999) Mechanism of hexosamine-induced insulin resistance in transgenic mice overexpressing glutamine:fructose-6-phosphate amidotransferase: decreased glucose transporter GLUT4 translocation and reversal by treatment with thiazolidinedione. Endocrinology. 140(3):1151-7.

Cozzone, D., Fröjdö, S., Disse, E., Debard, C., Laville, M., Pirola, L., Vidal, H. (2008) Isoform-specific defects of insulin stimulation of Akt/protein kinase B (PKB) in skeletal muscle cells from type 2 diabetic patients. Diabetologia. 51(3):512-21.

Cui, J., Shao, L., Young, L.T., Wang, J.F. (2007) Role of glutathione in neuroprotective effects of mood stabilizing drugs lithium and valproate. Neuroscience. 144(4):1447-53.

Cusi, K. (2009) Nonalcoholic fatty liver disease in type 2 diabetes mellitus.Curr Opin Endocrinol. Diabetes. Obes. 2009 Mar 2. [Epub ahead of print]

D'Alessandris, C., Andreozzi, F., Federici, M., Cardellini, M., Brunetti, A., Ranalli, M., Del Guerra, S., Lauro, D., Del Prato, S., Marchetti, P., Lauro, R., Sesti, G. (2004) Increased O-glycosylation of insulin signaling proteins results in their impaired activation and enhanced susceptibility to apoptosis in pancreatic beta-cells. FASEB. J. 18(9):959-61.

De Sarno, P., Li, X. Jope, R.S. (2002) Regulation of Akt and glycogen synthase kinase-3 beta phosphorylation by sodium valproate and lithium. Neuropharmacology. 43:1158-64.

Degenhardt, T.P., Fu, M.X., Voss, E., Reiff, K., Neidlein, R., Strein, K., Thorpe, S.R., Baynes, J.W., Reiter, R. (1999) Aminoguanidine inhibits albuminuria, but not the formation of advanced glycation end-products in skin collagen of diabetic rats. Diabetes. Res. Clin. Pract. 43(2):81-9.

Deng, X., Yellaturu, C., Cagen, L., Wilcox, H.G., Park, E.A., Raghow, R., Elam, M.B. (2007) Expression of the rat sterol regulatory element-binding protein-1c gene in response to insulin is mediated by increased transactivating capacity of specificity protein 1 (Sp1). J. Biol. Chem. 282(24):17517-29.

Doble, B.W., Woodgett, J.R. (2003) GSK-3: tricks of the trade for a multi-tasking kinase. J. Cell. Sci. 116(Pt 7):1175-86.

Doble, B.W., Patel, S., Wood, G.A., Kockeritz, L.K., Woodgett, J.R. (2007) Functional redundancy of GSK-3alpha and GSK-3beta in Wnt/beta-catenin signaling shown by using an allelic series of embryonic stem cell lines. Dev. Cell. 12(6):957-71.

Dong, D.L., Hart, G.W. (1994) Purification and characterization of an O-GlcNAc selective N-acetyl-beta-D-glucosaminidase from rat spleen cytosol. J. Biol. Chem. 269(30):19321-30.

Du, X.L., Edelstein, D., Dimmeler, S., Ju, Q., Sui, C., Brownlee, M. (2001) Hyperglycemia inhibits nitric oxide synthase activity by posttranslational modification at the Akt site. J. Clin. Invest. 108:1341-8.

Dzau, V.J., Braun-Dullaeus, R.C., Sedding, D.G. (2002) Vascular proliferation and atherosclerosis: new perspectives and therapeutic strategies. Nat. Med. 8(11):1249-56.

Eldar-Finkelman, H., Krebs, E.G. (1997) Phosphorylation of insulin receptor substrate 1 by glycogen synthase kinase 3 impairs insulin action. PNAS. 94(18):9660-4.

Eldar-Finkelman, H. (2002) Glycogen synthase kinase 3: an emerging therapeutic target. Trends. Mol. Med. 8(3):126-32.

Embi, N., Rylatt, D.B., Cohen, P. (1980) Glycogen synthase kinase-3 from rabbit skeletal muscle. Separation from cyclic-AMP-dependent protein kinase and phosphorylase kinase. Eur. J. Biochem. 107:519-527.

Feng, H.L., Leng, Y., Ma, C.H., Zhang, J., Ren, M., Chuang, D.M. (2008) Combined lithium and valproate treatment delays disease onset, reduces neurological deficits and prolongs survival in an amyotrophic lateral sclerosis mouse model. Neuroscience. 155(3):567-72.

Frame, S. Cohen, P. (2001) GSK3 takes centre stage more than 20 years after its discovery. Biochem. J. 359:1-16.

Frame, S., Cohen, P., Biondi, R.M. (2001) A common phosphate binding site explains the unique substrate specificity of GSK-3 and its inactivation by phosphorylation. Mol. Cell. 7:1321-7.

Freidenberg, G.R., Henry, R.R., Klein, H.H., Reichart, D.R., and Olefsky, J.M. (1987) Decresed kinase activity of insulin receptors from adipocytes of non-insulin-dependent diabetic subjects. J.Clin. Invest. 79:240-250.

Fröjdö, S., Vidal, H., Pirola, L. (2009) Alterations of insulin signaling in type 2 diabetes: A review of the current evidence from humans. Biochim. Biophys. Acta. 1792(2):83-92.

Glass, C.K., Witztum, J.L. (2001) Atherosclerosis - the road ahead. Cell. 104(4):503-516.

Gleissner, C.A., Galkina, E., Nadler, J.L., Ley, K. (2007) Mechanisms by which diabetes increases cardiovascular disease. Drug. Discov. Today. Dis. Mech. 4(3):131-140.

Goldberg, H.J., Scholey, J., Fantus, I.G. (2000) Glucosamine activates the plasminogen activator inhibitor 1 gene promoter through Sp1 DNA binding sites in glomerular mesangial cells. Diabetes. 49(5):863-71.

Goldberg, I.J. (2004) Why does diabetes increase atherosclerosis? I don't know! J. Clin. Invest. 114:613-615.

Goldin, A., Beckman, J.A., Schmidt, A.M., Creager, M.A. (2006) Advanced glycation end products sparking the development of diabetic vascular injury. Circulation. 114:597-605.

Gottlicher, M., Minucci, S., Zhu, P., Kramer, O.H., Schimpf, A., Giavara, S., Sleeman, J.P., Lo Coco, F., Nervi, C., Pelicci, P.G., Heinzel, T. (2001) Valproic acid defines a novel class of HDAC inhibitors inducing differentiation of transformed cells. EMBO. J. 20:6969–6978.

Gould, T.D., Quiroz, J.A., Singh, J., Zarate, C.A., Manji, H.K. (2004) Emerging experimental therapeutics for bipolar disorder: insights from the molecular and cellular actions of current mood stabilizers. Mol. Psychiatry. 9(8):734-55.

Grimes, C.A. Jope, R.S. (2001) The multifaceted roles of glycogen synthase kinase 3beta in cellular signaling. Prog. Neurobiol. 65:391-426.

Haberland, M., Montgomery, R.L., Olson, E.N. (2009) The many roles of histone deacetylases in development and physiology: implications for disease and therapy. Nat. Rev. Genet. 10(1):32-42.

Haffner, S.M., Lehto, S., Ronnemaa, T., Pyorala, K., Laakso, M. (1998) Mortality from coronary heart disease in subjects with type2 diabetes and in nondiabetic subjects with and without prior myocardial infarction. N. Engl. J. Med. 339:229-234.

Hajra, L., Evans, A.I., Chen, M., Hyduk, S.J., Collins, T., Cybulsky, M.I. (2000) The NF-kappa B signal transduction pathway in aortic endothelial cells is primed for activation in regions predisposed to atherosclerotic lesion formation. PNAS.

97(16):9052-7.

Hall, A.C., Brennan,A., Goold, R.G., Cleverley, K., Lucas, F.R., Gordon-Weeks, P.R. Salinas, P.C. (2002) Valproate regulates GSK-3-mediated axonal remodeling and synapsin I clustering in developing neurons. Mol. Cell. Neurosci. 20:257-270.

Han, I., Oh, E.S., Kudlow, J.E. (2000) Responsiveness of the state of O-linked N-acetylglucosamine modification of nuclear pore protein p62 to the extracellular glucose concentration. Biochem. J. 350 Pt 1:109-14.

Hansson, G.K. (2005) Inflammation, atherosclerosis, and coronary artery disease. N. Engl. J. Med. 352(16):1685-95.

Hansson, G.K., Libby, P. (2006) The immune response in atherosclerosis: a double-edged sword. Na.t Rev. Immunol. 6(7):508-19.

Hoeflich, K.P., Luo, J., Rubie, E.A., Tsao, M.S., Jin, O. Woodgett, J.R. (2000) Requirement for glycogen synthase kinase-3beta in cell survival and NF-kappaB activation. Nature. 406:86-90.

't Hoen, P.A., Van der Lans, C.A., Van Eck, M., Bijsterbosch, M.K., Van Berkel, T.J., Twisk, J. (2003) Aorta of ApoE-deficient mice responds to atherogenic stimuli by a prelesional increase and subsequent decrease in the expression of antioxidant enzymes. Circ. Res. 93(3):262-9.

Hofmann, M.A., Lalla, E., Lu, Y., Gleason, M.R., Wolf, B.M., Tanji, N., Ferran, L.J. Jr, Kohl, B., Rao, V., Kisiel, W., Stern, D.M., Schmidt, A.M. (2001) Hyperhomocysteinemia enhances vascular inflammation and accelerates atherosclerosis in a murine model. J. Clin. Invest. 107(6):675-83.

Holmes, T., O'Brien, T.A., Knight, R., Lindeman, R., Symonds, G., Dolnikov, A. (2008) The role of glycogen synthase kinase-3beta in normal haematopoiesis, angiogenesis and leukaemia. Curr. Med. Chem. 15(15):1493-9.

Hoshi, M., Takashima, A., Noguchi, K., Murayama, M., Sato, M., Kondo, S., Saitoh, Y., Ishiguro, K., Hoshino, T., Imahori, K. (1996) Regulation of mitochondrial pyruvate dehydrogenase activity by tau protein kinase I/glycogen synthase kinase 3beta in brain. PNAS. 93(7):2719-23.

Hossain, P., Kawar, B., El Nahas, M. (2007) Obesity and diabetes in the developing world--a growing challenge. N. Engl. J. Med. 356(3):213-5.

Hotamisligil, G.S., Erbay, E. (2008) Nutrient sensing and inflammation in metabolic diseases. Nat. Rev. Immunol. 8(12):923-34.

Hsueh, W., Abel, E.D., Breslow, J.L., Maeda, N., Davis, R.C., Fisher, E.A., Dansky, H., McClain, D.A., McIndoe, R., Wassef, M.K., Rabadan-Diehl, C., Goldberg, I.J. (2007) Recipes for creating animal models of diabetic cardiovascular disease. Cir. Res. 100(10):1415-27.

Huang, S., Czech, M.P. (2007) The GLUT4 glucose transporter. Cell. Metab. 5(4):237-52.

Huang, W.C., Lin, Y.S., Chen, C.L., Wang, C.Y., Chiu, W.H., Lin, C.F. (2009) Glycogen synthase kinase-3{beta} mediates endoplasmic reticulum stress-induced lysosomal apoptosis in leukemia. J. Pharmacol. Exp. Ther. [Epub ahead of print]

Hurel, S.J., Rochford, J.J., Borthwick, A.C., Wells, A.M., Vandenheede, J.R., Turnbull, D.M., Yeaman, S.J. (1996) Insulin action in cultured human myoblasts: contribution of different signaling pathways to regulation of glycogen synthesis. Biochem. J. 320(Pt 3):871-877.

James, L.R., Tang, D., Ingram, A., Ly, H., Thai, K., Cai, L., Scholey, J.W. (2002) Flux through the hexosamine pathway is a determinant of nuclear factor kappaB- dependent promoter activation. Diabetes. 51(4):1146-56.

Jope, R.S., Johnson, G.V. (2004) The glamour and gloom of glycogen synthase kinase-3. Trends. Biochem. Sci. 29(2):95-102.

Jope, R.S., Yuskaitis, C.J., Beurel, E. (2007) Glycogen synthase kinase-3 (GSK3). inflammation, diseases, and therapeutics. Neurochem. Res. 32:577-595.

Kaneko, M., Bucciarelli, L., Hwang, Y.C., Lee, L., Yan, S.F., Schmidt, A.M., Ramasamy, R. (2005) Aldose reductase and AGE-RAGE pathways: key players in myocardial ischemic injury. Ann. N. Y. Acad. Sci. 1043:702-9.

Kasuga, M., Fujita-Yamaguchi, Y., Blithe, D.L., Kahn, C.R. (1983) Tyrosine-specific protein kinase activity is associated with the purified insulin receptor. PNAS. 80(8):2137-41.

Keane, P.E., Simiand, J., Mendes, E., Santucci, V., Morre, M. (1983) The effects of analogues of valproic acid on seizures induced by pentylenetetrazol and GABA content in brain of mice. Neuropharmacology. 22(7):875-9.

Kher, N. Marsh, J.D. (2004) Pathobiology of atherosclerosis--a brief review. Semin. Thromb. Hemost. 30:665-672.

Kim, H.K., Davidson, L.M., Kritchevsky, D. (1976) Quantitative recovery of lipids from aortas stained with sudan IV. Atherosclerosis. 23(3):559-62.

Kim, A.J., Shi, Y., Austin, R.C. and Werstuck, G.H. (2005) Valproate protects cells from ER stress-induced lipid accumulation and apoptosis by inhibiting glycogen synthase kinase-3. J. Cell. Sci. 118:89-99.

Klein, P.S., Melton, D.A. (1996) A molecular mechanism for the effect of lithium on development. PNAS. 93:8455-8459.

Kockeritz L, Doble B, Patel S, Woodgett JR. (2006) Glycogen synthase kinase-3--an overview of an over-achieving protein kinase. Curr. Drug. Targets. 7:1377-1388.

Koya, D., King, G.L. (1998) Protein kinase C activation and the development of diabetic complications. Diabetes. 47(6):859-66.

Krook, A., Björnholm, M., Galuska, D., Jiang, X.J., Fahlman, R., Myers, M.G. Jr, Wallberg-Henriksson, H., Zierath, J.R. (2000) Characterization of signal transduction and glucose transport in skeletal muscle from type 2 diabetic patients. Diabetes. 49(2):284-92.

Kruth, H.S (1984) Histochemical detection of esterified cholesterol within human atherosclerotic lesions using the fluorescent probe filipin. Atherosclerosis. 51:281-292..

Kruth, H.S., Fry, D.L. (1984) Histochemical detection and differentiation of free and esterified cholesterol in swine atherosclerosis using filipin. Exp. Mol. Pathol. 40(3):288-94

Kuboki, K., Jiang, Z.Y., Takahara, N., Ha, S.W., Igarashi, M., Yamauchi, T., Feener, E.P., Herbert, T.P., Rhodes, C.J., King, G.L. (2000) Regulation of endothelial constitutive nitric oxide synthase gene expression in endothelial cells and in vivo : a specific vascular action of insulin. Circulation. 101(6):676-81.

Kunjathoor, V.V., Wilson, D.L. and LeBoeuf, R.C. (1996) Increased atherosclerosis in streptozotocin-induced diabetic mice. J. Clin. Invest. 97:1767-1773.

Lagace, D.C., Nachtigal, M.W. (2004) Inhibition of histone deacetylase activity by valproic acid blocks adipogenesis. J. Biol. Chem. 279(18):18851-60.

Lajoie, C., Calderone, A., Trudeau, F., Lavoie, N., Massicotte, G., Gagnon, S. Beliveau, L. (2004) Exercise training attenuated the PKB and GSK-3 dephosphorylation in the myocardium of ZDF rats. J. Appl. Physiol. 96:1606-1612.

Lander, H.M., Tauras, J.M., Ogiste, J.S., Hori, O., Moss, R.A., Schmidt, A.M. (1997) Activation of the receptor for advanced glycation end products triggers a p21(ras)-dependent mitogen-activated protein kinase pathway regulated by oxidant stress. J. Biol. Chem. 272(28):17810-4.

Laviola, L., Belsanti, G., Davalli, A.M., Napoli, R., Perrini, S., Weir, G.C., Giorgino, R., Giorgino, F. (2001) Effects of streptozocin diabetes and diabetes treatment by islet transplantation on in vivo insulin signaling in rat heart. Diabetes. 50(12):2709-20.

Lawlor, M.A., and Alessi, D.R. (2001) PKB/Akt: a key mediator of cell proliferation, survival and insulin responses? J. Cell. Sci. 114(16):2903-10.

Lee, S.L. (2001) The glucose-regulated proteins: stress induction and clinical applications. Trends Biol. Sci. 26:504-10.

Lee, J.N., Ye, J. (2004) Proteolytic activation of SREBP induced by cellular stress through the depletion of Insig-1. J. Biol. Chem. 279:45257-45265.

Levi, Z., Shaish, A., Yacov, N., Levkovitz, H., Trestman, S., Gerber, Y., Cohen, H., Dvir, A., Rhachmani, R., Ravid, M., Harats, D. (2003) Rosiglitazone (PPARγ-agonist) attenuates atherogenesis with no effect on hyperglycaemia in a combined diabetes-atherosclerosis mouse model. Diabetes. Obes. Metab. 5:45–50.

Li, Y.M., Mitsuhashi, T., Wojciechowicz, D., Shimizu, N., Li, J., Stitt, A., He, C., Banerjee, D., Vlassara, H. (1996) Molecular identity and cellular distribution of advanced glycation endproduct receptors: relationship of p60 to OST-48 and p90 to 80K-H membrane proteins. PNAS. 93(20):11047-52.

Li, Q., Verma, I.M. (2002) NF-kappaB regulation in the immune system. Nat. Rev. Immunol. 2:725-734.

Li, L., Sawamura, T., Renier, G. (2004) Glucose enhances human macrophage LOX-1 expression: role for LOX-1 in glucose-induced macrophage foam cell formation. Circ. Res. 94(7):892-901.

Li, Y., Schwabe, R.F., Devries-Seimon, T., Yao, P.M., Gerbod-Giannone, M.C., Tall, A.R., Davis, R.J., Flavell, R., Brenner, D.A., Tabas, I. (2005) Free cholesterol-loaded

macrophages are an abundant source of TNF-alpha and IL-6. Model of NF-kappa B- and MAP kinase-dependent inflammation in advanced atherosclerosis. J. Biol. Chem. 280:21763-21772.

Libby, P. (2008) The molecular mechanisms of the thrombotic complications of atherosclerosis. J. Intern. Med. 263:517-527.

Lim, H.J., Lee, S., Lee, K.S., Park, J.H., Jang, Y., Lee, E.J., Park, H.Y. (2006) PPARgamma activation induces CD36 expression and stimulates foam cell like changes in rVSMCs. Prostaglandins Other Lipid Mediat. 80: 165–174.

Lin, H.Y., Masso-Welch, P., Di, Y.P., Cai, J.W., Shen, J.W., Subjeck, J.R. (1993) The 170-kDa glucose-regulated stress protein is an endoplasmic reticulum protein that binds immunoglobulin. Mol. Biol. Cell. 4(11):1109-19.

Liu, H., Miller, E., van de Water, B., Stevens, J.L. (1998) Endoplasmic reticulum stress proteins block oxidant-induced Ca2+ increases and cell death. J. Biol. Chem. 273:12858-12862.

Liu, Z., Tanabe, K., Bernal-Mizrachi, E., Permutt, M.A. (2008) Mice with beta cell overexpression of glycogen synthase kinase-3beta have reduced beta cell mass and proliferation. Diabetologia. 51:623-631.

Lonn, E.M., Yusuf, S., Dzavik, V., Doris, C.I., Yi, Q., Smith, S., Moore-Cox, A., Bosch, J., Riley, W.A., Teo, K.K., for the SECURE Investigators. (2001) Effects of Ramipril and vitamin E on atherosclerosis: the study to evaluate cartotid ultrasound changes in patients treated with ramipril and vitamin E (SECURE). Circulation. 103:919-25.

Lonn, E., Yusuf, S., Hoogwerf, B., Pogue, J., Yi, Q., Zinman, B., Bosch, J., Dagenais, G., Mann, J.F. Gerstein, H.C. (2002) Effects of vitamin E on cardiovascular and microvascular outcomes in high-risk patients with diabetes: results of the HOPE study and MICRO-HOPE substudy. Diabetes. Care. 25:1919-1927.

Lonn, E., Bosch, J., Yusuf, S., Sheridan, P., Pogue, J., Arnold, J.M., Ross, C., Arnold, A., Sleight, P., Probstfield, J., Dagenais, G.R., HOPE and HOPE-TOO Trial Investigators. (2005) Effects of long-term vitamin E supplementation on cardiovascular events and cancer: a randomized controlled trial. JAMA. 293:1338-47.

Lusis, A.J. (2000) Atherosclerosis. Nature. 407:233-241.

MacAulay, K., Doble, B.W., Patel, S., Hansotia, T., Sinclair, E.M., Drucker, D.J., Nagy, A., Woodgett, J.R. (2007) Glycogen synthase kinase 3alpha-specific regulation of murine hepatic glycogen metabolism. Cell Metab. 6(4):329-37.

MacDonald, R.L. Bergey, G.K. (1979) Valproic acid augments GABA-mediated postsynaptic inhibition in cultured mammalian neurons. Brain. Res. 170:558-562.

Maeda, N., Johnson, L., Kim, S., Hagaman, J., Friedman, M., Reddick, R. (2007) Anatomical differences and atherosclerosis in apolipoprotein E-deficient mice with 129/SvEv and C57BL/6 genetic backgrounds. Atherosclerosis. 195(1):75-82.

Marciniak, S.J., Ron, D. (2006) Endoplasmic reticulum stress signaling in disease. Physiol. Rev. 86:1133-49.

Marshall, S., Bacote, V., Traxinger, R.R. (1991) Discovery of a metabolic pathway mediating glucose-induced desensitization of the glucose transport system. Role of hexosamine biosynthesis in the induction of insulin resistance. J. Biol. Chem. 266:4706–4712.

Martinez, A., Perez, D.I. (2008) GSK-3 inhibitors: a ray of hope for the treatment of Alzheimer's disease? J. Alzheimers. Dis. 15(2):181-91.

Matsumoto, K., Hirano, K., Nozaki, S., Takamoto, A., Nishida, M., Nakagawa-Toyama, Y., Janabi, M.Y., Ohya, T., Yamashita, S., Matsuzawa, Y. (2000) Expression of macrophage (Mphi) scavenger receptor, CD36, in cultured human aortic smooth muscle cells in association with expression of peroxisome proliferator activated receptor-gamma, which regulates gain of Mphi-like phenotype in vitro, and its implication in atherogenesis. Arterioscler. Thromb. Vasc. Biol. 20:1027–1032.

Matsumoto, M., Han, S., Kitamura, T., Accili, D. (2006) Dual role of transcription factor FoxO1 in controlling hepatic insulin sensitivity and lipid metabolism. J. Clin. Invest. 116(9):2464-72.

Matthews, J.A., Belof, J.L., Acevedo-Duncan, M., Potter, R.L. (2007) Glucosamine-induced increase in Akt phosphorylation corresponds to increased endoplasmic reticulum stress in astroglial cells. Mol. Cell. Biochem. 298(1-2):109-23.

McKnight, G.L., Mudri, S.L., Mathewes, S.L., Traxinger, R.R., Marshall, S., Sheppard, P.O., O'Hara, P.J. (1992) Molecular cloning, cDNA sequence, and bacterial expression of human glutamine:fructose-6-phosphate amidotransferase. J. Biol. Chem. 267:25208-12.

McQuillan, B.M., Hung, J., Beilby, J.P., Nidorf, M., Thompson, P.L. (2001) Antioxidant vitamins and the risk of carotid atherosclerosis. The Perth Carotid Ultrasound Disease Assessment study (CUDAS). J. Am. Coll. Cardiol. 38(7):1788-94.

Meares, G.P., Jope, R.S. (2007) Resolution of the nuclear localization mechanism of glycogen synthase kinase-3: functional effects in apoptosis. J. Biol. Chem. 282:16989-17001.

Melchionda, N., Forlani, G., Marchesini, G., Baraldi, L., Natale, S. (2002) WHO and ADA criteria for the diagnosis of diabetes mellitus in relation to body mass index. Insulin sensitivity and secretion in resulting subcategories of glucose tolerance. Int. J. Obes. Relat. Metab. Disord. 26(1):90-96

Miwa, H., Yamamoto, M. (1990) Liquid chromatographic determination of free and total fatty acids in milk and milk products as their 2-nitrophenylhydrazides. J. Chromatogr. 523:235-46.

Monaco, C., Andreakos, E., Kiriakidis, S., Mauri, C., Bicknell, C., Foxwell, B., Cheshire, N., Paleolog, E., Feldmann, M. (2004) Canonical pathway of nuclear factor kappa B activation selectively regulates proinflammatory and prothrombotic responses in human atherosclerosis. PNAS. 101(15):5634-9.

Monauni, T., Zenti, M.G., Cretti, A., Daniels, M.C., Targher, G., Caruso, B., Caputo, M., McClain, D., Del Prato, S., Giaccari, A., Muggeo, M., Bonora, E., Bonadonna, R.C. (2000) Effects of glucosamine infusion on insulin secretion and insulin action in humans. Diabetes. 49(6):926-35.

Montminy, M., Koo, S.H. (2004) Diabetes: outfoxing insulin resistance? Nature. 432(7020):958-9.

Mora, A., González-Polo, R.A., Fuentes, J.M., Soler, G., Centeno, F. (1999) Different mechanisms of protection against apoptosis by valproate and Li+. Eur. J. Biochem. 266(3):886-91.

Moreno, P.R., Fuster, V. (2004) New aspects in the pathogenesis of diabetic atherothrombosis. J. Am. Coll. Cardiol. 44(12):2293-300.

Morris, J.A., Dorner, A.J., Edwards, C.A., Hendershot, L.M., Kaufman, R.J. (1997) Immunoglobulin Binding Protein (BiP) Function Is Required to Protect Cells from Endoplasmic Reticulum Stress but Is Not Required for the Secretion of Selective Proteins. J. Biol. Chem. 272:4327-4334.

Muoio, D.M., Newgard, C.B. (2008) Mechanisms of disease: molecular and metabolic mechanisms of insulin resistance and beta-cell failure in type 2 diabetes. Nat. Rev. Mol. Cell. Biol. 9(3):193-205.

Neeper, M., Schmidt, A.M., Brett, J., Yan, S.D., Wang, F., Pan, Y.C., Elliston, K., Stern, D., Shaw, A. (1992) Cloning and expression of a cell surface receptor for advanced glycosylation end products of proteins. J. Biol. Chem. 267(21):14998-5004.

Nikoulina, S.E., Ciaraldi, T.P., Mudaliar, S., Mohideen, P., Carter, L., Henry, R.R. (2000) Potential role of glycogen synthase kinase-3 in skeletal muscle insulin resistance of type 2 diabetes. Diabetes. 49:263-271.

Nikoulina, S.E., Ciaraldi, T.P., Mudaliar, S., Carter, L., Johnson, K., Henry, R.R. (2002) Inhibition of glycogen synthase kinase 3 improves insulin action and glucose metabolism in human skeletal muscle. Diabetes. 51(7):2190-8.

Ohinmaa, A., Schopflocher, D., Jacobs, P., Demeter, S., Chuck, A., Golmohammadi, K., Klarenbach, S.W. (2006) A population-based analysis of health behaviours, chronic diseases and associated costs. Chronic. Dis. Can. 27(1):17-24.

Ohno, T., Horio, F., Tanaka, S., Terada, M., Namikawa, T., Kitoh, J. (2000) Fatty liver and hyperlipidemia in IDDM (insulin-dependent diabetes mellitus) of streptozotocin-treated shrews. Life Sci. 66:125-131.

Okamoto, H., Fujioka, Y., Takahashi, A., Takahashi, T., Taniguchi, T., Ishikawa, Y., Yokoyama, M. (2006) Trichostatin A, an inhibitor of histone deacetylase, inhibits smooth muscle cell proliferation via induction of p21(WAF1). J. Atheroscler. Thromb. 13:183-191.

Özcan, U., Cao, Q., Yilmaz, E., Lee, A-H., Iwakoshi, N.N., Özdelen, E., Tuncman, G., Görgun, C., Glimcher, L.H., Hotamisligil, G.S. (2004) Endoplasmic reticulum stress links obesity, insulin action, and type 2 diabetes. Science. 306:457-461.

Pahl, H.L. (1999) Signal transduction from the endoplasmic reticulum to the cell nucleus. Physiol. Rev. 79:683-701.

Paigen, B., Morrow, A., Holmes, P.A., Mitchell, D., Williams, R.A. (1987) Quantitative assessment of atherosclerotic lesions in mice. Atherosclerosis. 68:231-240.

Park, L., Raman, K.G., Lee, K.J., Lu, Y., Ferran, L.J. Jr., Chow, W.S., Stern, D., Schmidt, A.M. (1998) Suppression of accelerated diabetic atherosclerosis by the

soluble receptor for advanced glycation endproducts. Nat. Med. 4(9):1025-31.

Penry, J.K., Dean, J.C. (1989) The scope and use of valproate in epilepsy. J. Clin. Psych. 50:17-22

Phiel, C.J., Zhang, F., Huang, E.Y., Guenther, M.G., Lazar, M.A., Klein, P.S. (2001) Histone deacetylase is a direct target of valproic acid, a potent anticonvulsant, mood stabilizer, and teratogen. J. Biol. Chem. 276:36734-36741.

Phiel, C.J., Wilson, C.A., Lee, V.M., Klein, P.S. (2003) GSK-3alpha regulates production of Alzheimer's disease amyloid-beta peptides. Nature. 423(6938):435-9.

Pick, A., Clark, J., Kubstrup, C., Levisetti, M., Pugh, W., Bonner-Weir, S., Polonsky, K.S. (1998) Role of apoptosis in failure of beta-cell mass compensation for insulin resistance and beta-cell defects in the male Zucker diabetic fatty rat. Diabetes. 47(3):358-64.

Pilcher, H.R. (2003) Drug research: the ups and downs of lithium. Nature. 425(6954):118-20.

Pluquet, O., Qu, L.K., Baltzis, D., Koromilas, A.E. (2005) Endoplasmic reticulum stress accelerates p53 degradation by the cooperative actions of Hdm2 and glycogen synthase kinase 3beta. Mol. Cell. Biol. 25(21):9392-405.

Punga, T., Bengoechea-Alonso, M.T., Ericsson, J. (2006) Phosphorylation and ubiquitination of the transcription factor sterol regulatory element-binding protein-1 in response to DNA binding. J. Biol. Chem. 281(35):25278-86.

Qu, L., Huang, S., Baltzis, D., Rivas-Estilla, A.M., Pluquet, O., Hatzoglou, M., Koumenis, C., Taya, Y., Yoshimura, A., Koromilas, A.E. (2004) Endoplasmic reticulum stress induces p53 cytoplasmic localization and prevents p53-dependent apoptosis by a pathway involving glycogen synthase kinase-3beta. Genes. Dev. 18(3):261-77.

Raghow, R., Yellaturu, C., Deng, X., Park, E.A., Elam, M.B. (2008) SREBPs: the crossroads of physiological and pathological lipid homeostasis. Trends. Endocrinol. Metab. 19(2):65-73.

Rawson, R.B. (2003) The SREBP pathway--insights from Insigs and insects. Nat. Rev. Mol. Cell. Biol. 4(8):631-40.

Reddy, R.K., Mao, C., Baumeister, P., Austin, R.C., Kaufman, R.J., Lee, A.S. (2003) Endoplasmic reticulum chaperone protein GRP78 protects cells from apoptosis induced by topoisomerase inhibitors: role of ATP binding site in suppression of caspase-7 activation. J. Biol. Chem. 278(23):20915-24.

Robertson, L.A., Kim, A.J., Werstuck, G.H. (2006) Mechanisms linking diabetes mellitus to the development of atherosclerosis: a role for endoplasmic reticulum stress and glycogen synthase kinase-3. Can. J. Physiol. Pharmacol. 84(1):39-48.

Ron, D., Walter, P. (2007) Signal integration in the endoplasmic reticulum unfolded protein response. Nat. Rev. Mol. Cell. Biol. 8(7):519-29.

Ross, R. (1999) Atherosclerosis is an inflammatory disease. Am. Heart. J. 138:S419-S420.

Ruan, X.Z., Moorhead, J.F., Tao, J.L., Ma, K.L., Wheeler, D.C., Powis, S.H., Varghese, Z. (2006) Mechanisms of dysregulation of low-density lipoprotein receptor expression in vascular smooth muscle cells by inflammatory cytokines. Arterioscler. Thromb. Vasc. Biol. 26: 1150–1155.

Schroder, M., Kaufman, R.J. (2005) ER stress and the unfolded protein response. Mut. Res. 569:29-63.

Shao, L., Sun, X., Xu, L., Young, T.,Wang, J-F. (2006) Mood stabilizing drug lithium increases expression of endoplasmic reticulum stress proteins in primary cultured rat cerebral cortical cells. Life. Sci. 78(12):1317-23.

Shi, Y., Gerritsma, D., Bowes, A.J., Capretta, A., Werstuck, G.H. (2007) Induction of GRP78 by valproic acid is dependent upon histone deacetylase inhibition. Bioorg. Med. Chem. Lett. 17(16):4491-4.

Singh, L.P., Crook, E.D. (2000) The effects of glucose and the hexosamine biosynthesis pathway on glycogen synthase kinase-3 and other protein kinases that regulate glycogen synthase activity. J. Investig. Med. 48(4):251-8.

Small, D.M., Bond, M.G., Waugh, D., Prack, M., Sawyer, J.K. (1984) Physicochemical and histological changes in the arterial wall of nonhuman primates during progression and regression of atherosclerosis. J. Clin. Invest. 73(6):1590-605.

Song, L., De Sarno, P., Jope, R.S. (2002) Central role of glycogen synthase kinase-3beta in endoplasmic reticulum stress-induced caspase-3 activation. J. Biol. Chem.

277:44701-44708.

Srinivasan, S., Ohsugi, M., Liu, Z., Fatrai, S., Bernal-Mirachi, E., Permutt, M.A. (2005) Endoplasmic reticulum stress-induced apoptosis is partly mediated by reduced insulin signaling through phosphatidylinositol 3-kinase/Akt and increased glycogen synthase kinase-3beta in mouse insulinoma cells. Diabetes. 54:968-975.

Srivastava, S., Watowich, S.J., Petrash, J.M., Srivastava, S.K., Bhatnagar, A. (1999) Structural and kinetic determinants of aldehyde reduction by aldose reductase. Biochemistry. 38(1):42-54.

Sundqvist, A., Ericsson, J. (2003) Transcription-dependent degradation controls the stability of the SREBP family of transcription factors. PNAS. 100(24):13833-8.

Tabas, I. (2000) Cholesterol and phospholipid metabolism in macrophages. Biochem. Biophys. Acta. 1529(1-3):164-74.

Takadera, T., Fujibayahi, M., Kaniyu, H., Sakota, N., Ohyashiki, T. (2007) Caspase-dependent apoptosis induced by thapsigargin was prevented by glycogen synthase kinase-3 inhibitors in cultured rat cortical neurons. Neurochem. Res. 32:1336-1342.

Taniguchi, C.M., Kondo, T., Sajan, M., Luo, J., Bronson, R., Asano, T., Farese, R., Cantley, L.C., Kahn, C.R. (2006) Divergent regulation of hepatic glucose and lipid metabolism by phosphoinositide 3-kinase via Akt and PKClambda/zeta. Cell. Metab. 3(5):343-53.

Tannock, L.R., Kirk, E.A., King, V.L., LeBoeuf, R., Wight, T.N., Chait, A. (2006) Glucosamine supplementation accelerates early but not late atherosclerosis in LDL receptor-deficient mice. J. Nutr. 136:2856-2861.

Thallas-Bonke, V., Lindschau, C., Rizkalla, B., Bach, L.A., Boner, G., Meier, M., Haller, H., Cooper, M.E., Forbes, J.M. (2004) Attenuation of extracellular matrix accumulation in diabetic nephropathy by the advanced glycation end product cross-link breaker ALT-711 via a protein kinase C-alpha-dependent pathway. Diabetes. 53(11):2921-30.

Thomson, M.J., Puntmann, V., Kaski, J.C. (2007) Atherosclerosis and oxidant stress: the end of the road for antioxidant vitamin treatment? Cardiovasc. Drugs. Ther. 21:195-210.

Trowbridge, J.J., Xenocostas, A., Moon, R.T., Bhatia, M. (2006) Glycogen synthase

kinase-3 is an in vivo regulator of hematopoietic stem cell repopulation. Nat. Med. 12(1):89-98.

Underwood, K.W., Andemariam, B., McWilliams, G.L., Liscum, L. (1996) Quantitative analysis of hydrophobic amine inhibition of intracellular cholesterol transport. J. Lipid. Res. 37:1556-1568.

Veerababu, G., Tang, J., Hoffman, R.T., Daniels, M.C., Hebert, L.F. Jr, Crook, E.D., Cooksey, R.C., McClain, D.A. (2000) Overexpression of glutamine: fructose-6-phosphate amidotransferase in the liver of transgenic mice results in enhanced glycogen storage, hyperlipidemia, obesity, and impaired glucose tolerance. Diabetes. 49(12):2070-8.

Vosseller, K., Wells, L., Lane, M.D., Hart, G.W. (2002) Elevated nucleoplasmic glycosylation by O-GlcNAc results in insulin resistance associated with defects in Akt activation in 3T3-L1 adipocytes. PNAS. 99:5313-8.

Walker, R.M., Smith, G.S., Barsoum, N.J., Macallum, G.E. (1990) Preclinical toxicology of the anticonvulsant calcium valproate. Toxicology. 63:137-155.

Wang, J-F., Bown, C., Young, L.T. (1999) Differential display PCR reveals novel targets for the mood-stabilizing drug valproate including the molecular chaperone GRP78. Mol. Pharm. 55:521-527.

Wang, J.F., Azzam, J.E., Young, L.T. (2003) Valproate inhibits oxidative damage to lipid and protein in primary cultured rat cerebrocortical cells. Neuroscience. 116(2):485-489.

Wells-Knecht, K.J., Zyzak, D.V., Litchfield, J.E., Thorpe, S.R., Baynes, J.W. (1995) Mechanism of autoxidative glycosylation: identification of glyoxal and arabinose as intermediates in the autoxidative modification of proteins by glucose. Biochemistry. 34(11):3702-9.

Welsh, G.I., Miyamoto, S., Price, N.T., Safer, B., Proud, C.G. (1996) T-cell activation leads to rapid stimulation of translation initiation factor eIF2B and inactivation of glycogen synthase kinase-3. J. Biol. Chem. 271(19):11410-3.

Werstuck, G.H., Lentz, S.R., Dayal, S., Hossain, G.S., Sood, S.K., Shi, Y.Y., Zhou, J., Maeda, N., Krisans, S.K., Malinow, M.R. and Austin, R.C. (2001) Homocysteine-induced endoplasmic reticulum stress causes dysregulation of the cholesterol and triglyceride biosynthetic pathways. J. Clin. Invest. 107:1263-1273.

Werstuck, G.H., Kim, A.J., Brenstrum, T., Ohnmacht, S.A., Panna, E., Capretta, A. (2004) Examining the correlations between GSK-3 inhibitory properties and anti-convulsant efficacy of valproate and valproate-related compounds. Bioorg. Med. Chem. Lett. 14:5465-5467.

Werstuck, G.H., Khan, M.I., Femia, G., Kim, A.J., Sood, S.K., Zhou,J., Halford, C., Tedesco, V., Austin, R.C., Trigatti, B., Shi, Y. (2006) Identification of a mechanism linking glucosamine-induced ER dysfunction to accelerated atherosclerosis in a hyperglycemic mouse model. Diabetes. 55(1):93-101.

Williams, R.S.B., Cheng, L., Mudge, A.W., Harwood, A.J. (2002) A common mechanism of action for three mood-stabilizing drugs. Nature. 417:292-295.

Wilson, S.H., Caplice, N.M., Simari, R.D., Holmes, D.R. Jr, Carlson, P.J., Lerman, A. (2000) Activated nuclear factor-kappaB is present in the coronary vasculature in experimental hypercholesterolemia. Atherosclerosis. 148(1):23-30.

Xanthoulea, S., Curfs, D.M., Hofker, M.H., de Winther, M.P. (2005) Nuclear factor kappa B signaling in macrophage function and atherogenesis. Curr. Opin. Lipidol. 16(5):536-42.

Yang, T., Espenshade, P.J., Wright, M.E., Yabe, D., Gong, Y., Aebersold, R., Goldstein, J.L., Brown, M.S. (2002) Crucial step in cholesterol homeostasis: sterols promote binding of SCAP to INSIG-1, a membrane protein that facilitates retention of SREBPs in ER. Cell. 110(4):489-500.

Ye, J., Rawson, R.B., Komuro, R., Chen, X., Davé, U.P., Prywes, R., Brown, M.S., Goldstein, J.L. (2000) ER stress induces cleavage of membrane-bound ATF6 by the same proteases that process SREBPs. Mol. Cell. 6(6):1355-64.

Yusuf, S., Dagenais, G., Pogue, J., Bosch, J., Sleight, P. (2000) Vitamin E supplementation and cardiovascular events in high-risk patients. The Heart Outcomes Prevention Evaluation Study Investigators. N. Engl. J Med. 342:154-160.

Zhang, Z., Zhang, Z.Y., Fauser, U., Schluesener, H.J. (2008) Valproic acid attenuates inflammation in experimental autoimmune neuritis. Cell. Mol. Life Sci. 65(24):4055-65.

Zhou, J., Werstuck, G.H., Lhotak, S., deKoning, A.B.L., Hossain, G.S., Sood, S.K., Shi, Y.Y., Moller, J., Ritskes-Hoitinga, M., Falk, E., Austin, R.C. (2004) Association of multiple cellular stress pathways with accelerated atherosclerosis in hyperhomocysteinemic ApoE-deficient mice. Circulation. 110:207-213.